**UNIVERSITY FOR DEVELOPMENT STUDIES, GHANA**

UNIVERSITY FOR DEVELOPMENT STUDIES

**TOPP-LEONE ZUBAIR GENERATED FAMILY OF**

**DISTRIBUTIONS WITH APPLICATIONS TO LIFETIME DATA**

**RICHARD NKRUMAH**

**2021**

**UNIVERSITY FOR DEVELOPMENT STUDIES, GHANA**

**TOPP-LEONE ZUBAIR GENERATED FAMILY OF**

**DISTRIBUTIONS WITH APPLICATIONS TO LIFETIME DATA**

**BY**

**RICHARD NKRUMAH (BSc. Statistics, MSc. Statistics)**

**UDS/DAS/0001/17**

**THESIS SUBMITTED TO THE DEPARTMENT OF STATISTICS,**

**FACULTY OF MATHEMATICAL SCIENCES, UNIVERSITY FOR**

**DEVELOPMENT STUDIES, IN PARTIAL FULFILLMENT OF**

**THE REQUIREMENTS FOR THE   AWARD OF DOCTOR OF**

**PHILOSOPHY DEGREE IN APPLIED STATISTICS**

**JULY, 2021**

# DECLARATION

Student

I hereby declare that the research is an original work and that all borrowed materials are duly cited.

Signature :…………………..                    Date:………………….

Richard Nkrumah

(Candidate)

Supervisors

We hereby declare that the preparation and presentation of the research thesis was supervised in accordance with the guidelines on supervision of dissertation/thesis laid down by the University for Development Studies.

Signature: ……………                    Date:……………….

Dr. Suleman Nasiru

(Principal Supervisor)

Signature:……………………                    Date: ……………….

Dr. Abukari Alhassan

(Co-Supervisor)

i

**DEDICATION**

To my lovely wife,  Mrs. Angela Nkrumah

(Senior Midwife, Greater Accra Regional Hospital, Ridge).

UNIVERSITY FOR DEVELOPMENT STUDIES

## ACKNOWLEDGEMENTS

# ABSTRACT

The Topp-Leone Zubair family of distribution was developed in this study to model life time data. This family of distributions is an improvement of the Topp-Leone and the Zubair families which lacked scale parameter and shape parameters respectively. The statistical properties of the generator were obtained , thus; mixture representation, moments, moment generating function, incomplete moments, inequality measures, mean deviation, median deviation, mean residual life, stochastic ordering, Stress-strength, order statistics and the $r^{th}$ non-central moment. The method of estimations for the parameters of the generator was Maximum Likelihood estimation. Five new distributions have been developed from the family. These are: Topp-Leone Zubair Nadarajah Haghighi, Topp-Leone Zubair Lomax, Topp-Leone Zubair Weibull, Topp-Leone Zubair Kumaraswamy and Topp-Leone Zubair Inverse Weibull. Further, the Topp-Leone Zubair Lomax regression model was developed and applied to censored data with independent factors. The simulation results showed that the average bias and the root mean square error of the estimators decrease as the sample size increases. Thus, the estimators passed the consistency test. The new models were also subjected to real life data and they were better than their competing models as per Kolmogorov-Smirnov test, Bayesian Information criteria, Cramér-Von Mises, Akaike Information Criteria and that of Corrected Akaike Information Criteria. Histogram plots demonstrated a better fit of the new models on the respective data applied.It is recommended that the Topp-Leone Zubair family should be used to enhance the modeling performances of existing distributions that lack either shape or scale parameters.

iv

# TABLE OF CONTENTS

UNIVERSITY FOR DEVELOPMENT STUDIES

UNIVERSITY FOR DEVELOPMENT STUDIES

UNIVERSITY FOR DEVELOPMENT STUDIES

ix

# LIST OF TABLES

# LIST OF FIGURES

UNIVERSITY FOR DEVELOPMENT STUDIES

**ACRONYMS**

| | |
|---|---|
| **AIC** | Akaike Information Criterion |
| **AICc** | Corrected Akaike Information Criterion |
| **BIC** | Bayesian Information Criterion |
| **CDF** | Cumulative Distribution Function |
| **CM** | Cramér-von Misses |
| **EDF** | empirical distribution function |
| **IM** | Incomplete Moment |
| **K-S** | Kolmogorov-Smirnov |
| **MGF** | Moment Generating Function |
| **MLE** | maximum likelihood estimation |
| **MRL** | Mean Residual Life |
| **NH** | Nadarajah Haghighi |
| **PDF** | Probability Density Function |
| **TL** | Topp-Leone |
| **TLZ** | Topp-Leone Zubair |
| **TLZW** | Topp-Leone Zubair Weibull |
| **TLZNH** | Topp-Leone Zubair Nadarajah Haghighi |
| **TLZLx** | Topp-Leone Zubair Lomax |
| **TLZLx_R** | Topp-Leone Zubair Lomax Regression |
| **TLZKw** | Topp-Leone Zubair Kumaraswamy |
| **TLZIW** | Topp-Leone Zubair Inverse Weibull |
| **TTT** | Total Time on Test |
| **T-X** | Transformed-Transformer |

# CHAPTER ONE

# INTRODUCTION

## 1.0 Background of Study

Many fields in practice apply several computational techniques in their operational activities. These fields are, for example; public health, medicine, management, biological and engineering. In their daily activities they use lifetime data to model stress, machine failure, aerodynamic events and many more. In these applications, statistical methods are well used. The most dominating one is the use of statistical distributions, especially where lifetime data is the sourced information. In real life situations, statistical distributions are used in many parametric analyses. They form the basis of many parametric models. Practically, technical problems are addressed using these models. In going forward, these applications have motivated researchers to develop several prospective distribution techniques to solve different dimensions of practical real life problems. In these developments, however, the ability of the distributions to exhibit better modeling properties become also of a great concern. This is because, flexible distribution models ensure better conclusions and decisions to be made on specific problem cases (Nasiru et al., 2018).

Users of these statistical techniques prefer working with most current, flexible and generalized forms of distributions. For this, they see as more convenient and reliable. Interestingly, generalizations of statistical distribution techniques have taken researchers to different dimensions. A critical review (Cordeiro et al., 2013; Vatto et

1

al., 2016)    reveals some generalized methods which have been used to generate

distribution that have desirable properties. Generalization can be traced back before

1980 where new distributions were developed from quantiles, transformation functions

and differential equations (Freimer et al., 1988; Lee et al., 2013). Improvements in these

techniques have created a paradigm shift in generating new distributions. These new

distributions permit for additional parameters. Recently, some new distributions have

been developed   from generators and have demonstrated improvements in goodness of

fit and tail properties (Vatto et al., 2016; Zohdy et al., 2017, Nasiru et al., 2018).

Furthermore, the Topp-Leone distribution (TL) proposed by Topp and Leone (1955) has

been very attractive as a generator due to its desirable properties, and this has been

applied in many fields. The distribution did not get much attention initially though, this

was because; the important statistical properties were not studied by the initial authors.

By means of improvement, some of the properties like the moment function, central

moments and the characteristic function were developed by Nadarajah and Kotz (2003).

Further to that, a number of researchers became motivated to do further studies on the

TL. Ghitany et al. (2005) provided the reliability measures. Kurtosis were studied and

reported by Kotz et al. (2007), a two-sided generalized TL distribution by Vicaria et al.

(2008), goodness-of-fit by Al-Zahrani (2012). The various studies presented TL distribution more appropriate for lifetime data analysis.

More recently, Sangsanit and Bodhisuwan (2016) studied the TL distribution and came up with a generator known as Topp-Leone G family of distributions. They proposed that if $X$ is being a TL-G random variable with parameter $\lambda$ and dependency vector $\phi$ , then the cumulative distribution function (CDF) of TL-G follow as;

$$F_{TL}(x) = [G_1(x;\phi)]^\lambda [2 - G_1(x;\phi)]^\lambda, \ \lambda > 0, \phi > 0, x \in \mathbb{R} \ , \qquad (1.1)$$

where $G_1(x;\phi)$ is the density CDF.

Despite some attempts in improving upon the TL distribution, the TL-G family of distributions still has some problems that need to be addressed to improve upon lifetime data modeling.

## 1.1 Problem Statement

The TL-G family, proposed by Sanganit and Bodhisuwan (2016) lacks a scale parameter. This means that any new distribution that would be generated from the TL-G may also lack a scale parameter, unless that distribution comes with its own scale parameter during the generating stage. The methodological issue arising from the

3

underlining problem is that; the family is inefficient in terms of variability control which scale parameters give.

To overcome this drawback, there was the need to introduce an additional scale parameter into the TL-G family. In this case, we have combined the TL-G and Zubair-G families into a single family called Topp-Leone Zubair generated (TLZ-G) family of distributions. This addresses the problem of lack of scale and shape parameters in the TL-G and Zubair-G families respectively. The TLZ-G family of distributions therefore has the ability to introduce both scale and shape parameters to an existing statistical distribution to make it more flexible.

## 1.2 General Objectives

In a broader perspective the study develops, assesses the statistical properties and illustrates the applications of Topp-Leone Zubair generated (TLZ-G) family of distributions.

## 1.3 Specific Objectives

  i.   To develop the TLZ-G family of distributions.

 ii.   Derive the statistical properties of the TLZ-G family of distributions.

iii.   Develop estimators for the parameters of the family.

 iv.   Investigates the behavior of the estimators through simulations.

  v.   Illustrates the applications of some special distributions from the TLZ-G family.

## 1.4 Significance of Study

The TLZ-G family has the capacity to generate many distributions with sound modeling properties than the TL and Zubair generators. In this case, offspring distributions can be used efficiently to model in the area of health, engineering, agriculture and aerodynamics. Thus, for example; modeling stress levels, cancer conditions, machine failure times, crop diseases and many more. The new distribution arising from the TLZ-G can be used to develop new parametric regression models.

## 1.5 Organisation of the study

This study is grouped into six chapters. Chapter one presents the introduction of the study, where in that case, general areas of applications of some probability distributions, the TL-G family is presented. In the same chapter, the problem statement, general objectives, specific objectives and the significance of the study are also presented.

In chapter two, literature of probability distributions and some generator families of distributions have been reviewed. The gaps in these literatures are well presented. This is where the problem of the lack of scale parameter and shape parameters are established.

The chapter three is the methodology which presents the key properties of the Topp-Leone and the Zubair generator family of distributions. In the same chapter, the maximum likelihood estimator, the Kaplan Meier estimator, goodness of fit test, Cramér-Von Mises Test, Komogorov-Smirnov test, Akaike information criterion, Bayesian information criterion and the total time on test transform are defined.

Chapter four presents the theoretical results of the TLZ-G. It also presents the statistical properties of the new generator and the six new distributions that are developed.

Chapter five presents on the simulation studies and the empirical results. In this case the applications of the six new models are studied and conclusions on their flexibility to model life time are drawn.

Chapter six presents the summary of the five objectives, conclusion and recommendations.

# CHAPTER TWO

# LITERATURE REVIEW

## 2.1 Introduction

This chapter presents review of literature on some probability distribution generators. In this case, especially, the generators which have been used over the years to modify existing distributions with the aim of making them flexible in modeling real life data are reviewed. Further to this review, the drawbacks of these generators, by virtue of possessing only scale parameters or shape parameters respectively controlling variability, skewness and kurtosis have been discussed. The chapter ends with the stating need for a generator to possess both scale parameter and shape parameter and hence the combination of TL and Zubair generators to form TLZ-G family.

## 2.2 The Kumaraswamy Generator Family of Distribution

The Kumaraswamy generated family of distributions (Kumaraswamy , 1980) has received commendable attention from authors. Some distributions that have been developed from it are , Kumaraswamy Weibull(KwW), by Cordeiro et al. (2010), Kumaraswamy Gumbel (KwGu), by Cordeiro et al. (2011), inverted Kumaraswamy by Al-Fattah et al. (2017) and Kumaraswamy odd Burr-G family by Nasir et al. (2018). Despite the good contribution of this distribution to modifyng existing distributions, it does not have a scale parameter. It only has two shape parameters. In an attempt to develop new distributions like Kumaraswamy TL, and the kumaraswamy exponetiated exponential, the new distributions based on the Kumaraswamy generated family would

not yield much of flexibily in terms of variabilty control, this is because the baseline distributions themselves have only shape parameters without scale parameters.

## 2.3 Marshall Olkin generated family

Marshall and Olkin (1997) introduced the Marshall Olkin generated (MO-G) family for adding a parameter to distributions. This has given birth to the Kumaraswamy Marshall-Olkin-G (KwMO-G) and beta Marshall-Olkin-G (BMO-G) by Alizadeh et al. (2015b), Marshall-Olkin generalized-G family by Yousof et al. (2018) and among others. The MO-G has a single scale parameter to enrich new distributions that do not have such parameter. The MO-G is not better in using for modifying distributions which have shape parameter deficiencies, more specifically if the objective is to improve upon kurtosis and skewness characteristics.

## 2.4 Exponentiated Distribution Family

The exponentiated distribution with a single shape parameter was developed by Gupta et al. (1998). The shape parameter enables the distribution to control kurtosis and skewness. Unfortunately, this family does not have a scale parameter to control the variability which are mostly characterized with many of real life data. Consequently, new distributions that may be developed from this generator automatically inherit such limitation, except for those baseline distributions that come along with their own scale parameters. The exponentiated distribution family has been used to introduce exponentiated Kumaraswamy, exponentiated Lomax and many more (Lemonte, 2013). However, these families of distributions suffer the lack of scale parameters. Effectively, they are not flexible enough for the lack of variability control (Fernando et al. 2017).

## 2.5 The Beta-Generated Family

The beta distribution served as a generator in the work of Eugene et al. (2002), to propose the beta-generated family of distributions. The family could be described as a generalization of order statistics (Jones, 2004). Also were other proposed distributions, for example: beta-extended Weibull (Cordeiro et al., 2012); beta-Weibull (Famoye et al., 2005); beta-exponentiated Pareto (Zea et al., 2012); beta-Gumbel (Nadarajah and Kotz, 2004); beta-generalized logistic (Morais et al., 2013); beta-normal (Eugene et al., 2002); beta-exponential (Nadarajah and Kotz, 2005); beta-Fréchet (Nadarajah and Gupta, 2004); beta-Cauchy (Alshawarbeh et al., 2012). The Beta generated family has two shape parameters. The limitation here is that, the distribution lacks a scale parameter to enrich its family of distributions. Apart from the generator being able to control skewness and kurtosis, is has no control over variability that may exist in data of real life applications ( Nadarajah et al., 2014).

## 2.6 Odd Log Logistics Family of Distribution

The odd log logistics generated (OLL-G) family was introduced by Gleaton and Lynch (2006) to provide flexibility in modeling data having high skewness. Further to that, recently, several authors have modified existing distributions using the OLL-G. This can be seen in the work of Da Cruz et al. (2016), they came up with the log-odd log-logistic Weibull regression model for survival analysis, Braga et al. (2017) also investigated the odd log-logistic Student t distribution, Cordeiro et al. (2017) also came

up with the generalized odd log-logistic family and most recently, Da Cruz et al. (2017) looked at the bivariate odd-log-logistic-Weibull regression model, They used the new regression to model oral health-related quality of life. Furthermore, the heteroscedastic odd log-logistic generalized gamma regression model for censored data was developed by Prataviera et al. (2018). The OLL-G has drawn a lot of attention from authors. Notwithstanding its diverse applications, the distribution has only a single shape parameter which takes control of skewness and kurtosis. It lacks a scale parameter. This implies that it may not be appropriate for baseline distributions that lack scale parameters to be modified by the OLL-G for the lack of variability control.

## 2.7 Quadratic Rank Transmuted Map

In the work of Shaw and Buckley (2009) they came up with the quadratic rank transmuted map (QRTM) family of distribution by using the rank transmuted map as a tool for constructing non-Gaussian family of distributions. The QRTM has one scale parameter to control variability. There is no shape parameter to control kurtosis and skewness which life time data exhibits. In effect, new distributions giving birth from this family may lack this key property, for example, the distribution derived from the QRTM known as cubic transmuted distribution in Kareema and Maysaa (2017) lacks a shape parameter. New distributions may lack shape parameter from this family, unless such baseline distributions have embedded shape properties in order to demonstrate more flexibility in modeling.

10

## 2.8 Exponentiated Generalized Class of Distributions

Cordeiro et al. (2013) introduced the Exponentiated Generalized (EG) Class of distributions. Out of this distribution, some distributions like the exponentiated generalized Weibull (EPGW) in Fernando et al. (2017), exponentiated generalized exponential (EGE) in Cordeiro et al. (2013) have been developed. The EG family distribution has two shape parameters. The parameters give greater flexibility by controlling tail weights and also enhancing the entropy at the center of its density function. However, the drawback in this generator is that it is not able to control variability in data applications due to the lack of a scale parameter. This means that, in an attempt to modifying existing distributions with the EG generator, if the baseline distributions do not have scale parameters then the modification will suffer variability control.

## 2.9 The Logistics-X family

The logistic-X is developed by Tahir et al. (2016). It has one shape parameter, exhibiting left-skewed, symmetrical, reversed-J shaped and right-skewed, increasing, decreasing, upside-down bathtub, bathtub hazard rates shapes. The authors used the generator to develop several distributions, for example, the logistic-weibull(LW), logistics-Frechet (LF), logistics-Pareto (LP), logistic-uniform (LU) and logistic-Bur XII ( LBXII). Despite the great applications of the logistic family, it has not been able to contribute in enriching baseline distributions with the control of variability.

## 2.10 Topp-Leone Generated Family

The TL-G family, proposed by Sanganit and Bodhisuwan (2016) has given birth to many distributions, for example the TL generalized exponential (TLGE), TL Weibull Lomax (TLWLx) in Farrukh et al. (2019), TL Lomax (TLLx) in Sangsanit et al. (2016). The drawback of the TL-G is that it has a shape parameter but with no scale parameter. This means that any new distribution that would be generated from the TL-G may also lack a scale parameter, unless that distribution comes with its own scale parameter during the generating stage. The issue arising from this limitation is that; the family is inefficient in terms of variability which scale parameters give.

## 2.11 Alpha Power Transformation

Mahdavi and Kundu (2017) came up with a new method for improving statistical distributions. The method has given birth to a lot of distributions, for example, the alpha power exponential Weibull, by Rahman and El-Bassiouny (2017), alpha power transformed Lindley by Dey et al. (2018), alpha power inverted exponential by Unal et al. (2018), alpha power inverse Weibull by Ramadan and Walaa (2018), alpha power transformed Frechet by Nasiru et al. (2019), alpha power transformed inverse Lindley by Dey et al. (2019) and alpha power transformed power Lindley by Hassan et al. (2019). The drawback in the alpha power transformation is the lack of shape parameter making it unable to exhibit power over the skewness and kurtosis in data modeling.

12

Notwithstanding this deficiency, the baseline distributions that have shape parameters will complement it.

## 2.12 Zubair Generated Family of Distributions

The Zubair-G family of distributions was developed by Zubair (2018). Distributions such as the Weibull, exponential, Kumaraswamy , Lomax, inverse Weibul have been modified by this generator. These modifications take forms such as Zubair Kumaraswamy (ZKw), Zubair Lomax (ZLx), Zubair Inverse Weibull (ZIW) and Zubair Weibull (ZW). The generator has scale parameter but lacks a shape parameter. In effect, because the Zubair family has no shape parameter, combing with any distribution which also has no shape parameter is not appropriate. The Zubair generator has not received much attention in literature, so it has been well   consideration in this study for improvement.

## 2.13 Summary of Literature Review

In the literature reviewed, it shows that some generators that have scale parameters do not have shape parameters, and those that have shape parameters do not have scale parameters. The lack of shape parameters limit the generator in controlling kurtosis and skewness and the lack of scale parameter limits the generator in controlling variability. More importantly, if baseline distributions have no scale or shape parameters they may not inherit from the generator, because the generator itself does not have. In this case, it is imperative to develop a generator that has both shape and scale parameters to control variability, kurtosis and skewness, so that the baselines that do not have such properties may inherit it from the parent. In doing this, the study combined most current

generators, thus, TL-G generated family which has a shape parameter,      to Zubair

generated family which has a scale parameter in order to form TLZ-G family of

distributions.  In this case, the common distribution would have both scale and shape

parameters to allow for more flexibility in data modeling.

## CHAPTER THREE

## METHODOLOGY

### 3.0 Introduction

This chapter explains the various methods which were used to achieve the study objectives. The key concepts discussed here are the Zubair-G family, Topp-Leone-G family, the maximum likelihood estimation methods, model selection criteria, goodness of fit test, Cox-Snell residual, total time on test transform and source of data.

### 3.1 Zubair-G Family

Supposing $X$ is a random variable of the Zubair-G family (Zubair, 2018), then the CDF, Probability Density Function (PDF), hazard and the quantile functions are given respectively as:

$$G_1(x) = \frac{e^{\alpha G(x;\phi)^2} - 1}{e^{\alpha} - 1}, \alpha, \phi > 0, x \in \mathbb{R},$$ (3.1)

$$f_1(x) = \frac{2\alpha g(x;\phi)G(x;\phi)e^{\alpha G(x;\phi)^2}}{e^{\alpha} - 1}, \alpha, \phi > 0, x \in \mathbb{R},$$ (3.2)

$$h_1(x) = \frac{2\alpha g(x;\phi)G(x;\phi)e^{\alpha G(x;\phi)^2}}{e^{\alpha} - e^{\alpha G(x;\phi)^2}}, \alpha, \phi > 0, x \in \mathbb{R},$$ (3.3)

and

$$Q_1(u) = G_1^{-1}\left( \frac{\log((u(e^{\alpha} - 1)) + 1)}{\alpha} \right)^{\frac{1}{2}}, \alpha, \phi > 0, x \in \mathbb{R},$$ (3.4)

15

where $G(x;\phi)$ is the baseline CDF of the existing distribution, $\alpha$ is a scale parameter and $\phi$ is a $p \times 1$ vector of parameters.

## 3.2 Topp-Leone G Family

Sanganit and Bodhisuwan (2016) proposed the TL-G family of distributions. In that case, supposing a random variable $X$ follows TL-G distribution, then the CDF, PDF, Hazard and the Quantile functions are given respectively as;

$$F_{TL}(x) = [G_1(x;\phi)]^\lambda [2 - G_1(x;\phi)]^\lambda$$

$$= [1 - (1 - G_1(x;\phi))^2]^\lambda \quad, \lambda > 0, \phi > 0, x \in \mathbb{R} \, , \tag{3.5}$$

$$f_{TL}(x) = 2\lambda g(x;\phi) G_1(x;\phi)^{\lambda-1} (1 - G_1(x;\phi))(2 - G_1(x;\phi))^{\lambda-1}, \lambda > 0, \phi > 0, x \in \mathbb{R} \, , \tag{3.6}$$

$$h_{TL}(x) = \frac{2\lambda g(x;\phi) G_1(x;\phi)^{\lambda-1}(1 - G_1(x;\phi))(2 - G_1(x;\phi))^{\lambda-1}}{1 - [1 - (1 - G_1(x;\phi))^2]^\lambda}, \lambda > 0, \phi > 0, x \in \mathbb{R}, \tag{3.7}$$

$$Q_{TL}(x) = G_1^{-1}\left(1 - \sqrt{(1 - u^{\frac{1}{\alpha}})}\right), \lambda > 0, \phi > 0, x \in \mathbb{R} \, , \tag{3.8}$$

where $G(x;\phi)$ is the baseline CDF of the existing distribution, $\lambda$ is a shape parameter and $\phi$ is a $p \times 1$ vector of parameters.

The TL distribution has some good properties which encourages its use for generating other distributions.

16

**3.3 Maximum Likelihood Estimation**

The maximum likelihood estimation (MLE) method has been used extensively over other methods like the maximum product estimation method, methods of moment estimation, graphical method, ordinary least squares estimates, Bayesian method and also the Kernel estimation methods to estimate parameters of probability distributions. The method is centered on the likelihood function (Beno, 2018). Choosing a method for estimating parameters requires by practically selecting the one which produces the minimal error (Ahmed et al., 2010). MLE demonstrates well in minimizing error in parameter estimation. It has endowed properties such as consistency, asymptotic normality, asymptotic efficiency and invariance. Hence, the MLE was adopted to estimate the parameters of the TLZ-G families of distributions.

Supposing we have $n$ size of independently and identically distributed random sample

$X_1, X_2, ..., X_n$ with joint PDF $g(x|\phi) = \prod_{i=1}^{n} g(x_i; \phi)$ and a vector parameters

$\phi = (\phi_1, \phi_2...\phi_k)^{'}, k < n$, which characterizes the PDF. Then, the joint PDF follows as;

$$g(x|\phi) = \prod_{i=1}^{n} g(x_i; \phi). \tag{3.9}$$

If the random values of $X$ are known, we determine the likelihood function to make way for estimating the parameters. In that case, $\phi$ becomes the focus property in the conditioned function, where the PDF is now the likelihood functions and written as;

17

$$L(\phi \mid x) = \prod_{i=1}^{n} g(x_i; \phi). \qquad (3.10)$$

It is more convenient to apply logarithm to the likelihood function in order to make it friendlier to work with. The logarithm reduces the complexities of the functional powers. Here, we have log-likelihood function as;

$$\ell(\phi \mid x_1, x_1, ..., x_n) = \prod_{i=1}^{n} \log g(x_i; \phi) \ . \qquad (3.11)$$

The log-likelihood function is monotonic in nature and implies that any maximization responsively maximizes the likelihood function and vice versa. Maximization of the likelihood function is realized when the estimates $\hat{\phi}$ are values of $\phi$. Taking the first partial derivative of the likelihood function in respective of $\phi_1, \phi_2, ..., \phi_k$ and setting it to zero, we obtain the score function as;

$$\frac{\partial \ell(\phi \mid x_1, x_2, ..., x_n)}{\partial \phi_i} = 0, i = 1, 2, ..., k \qquad (3.12)$$

Producing the solution for the equation in respective of $\phi_1, \phi_2, ..., \phi_k$ gives the parameter estimates.

18

### 3.4 Goodness of Fit Test

Supposing we decide to take random sample $X_1, X_2,..., X_n$ , where sample is believed to come from a specific distribution. In order to be sure of this, we conduct goodness-of-fit test to ascertain if indeed the random sample come from the specific distribution. Three popular tests have been considered in this case, these include: Cramér-Von Mises Test, and Kolmogorov-Smirnov Test (K-S) and Anderson Darling Test.

### 3.4.1 Cramér-von Mises Test

Cramér-von and Mises (1928) proposes the test to judge the goodness of fit of a theoretical CDF compared to an empirical CDF or for comparing two empirical CDFs. In other applications like transportation analysis, the Cramér-von and Mises theory supports algorithm for estimating minimum possible distance.

Given $W^*$ as Cramér-von Mises test statistic: $G(x_i; \vartheta)$ as CDF with a known $G$ and unknown $k$ -dimensional parameter vector $\vartheta$ . The test for computing the test statistic $W^*$ is as follows:

1.  Order the $x_i$ 's in ascending form and estimate $G(x_i; \hat{\vartheta}) = u_i$ .

2.  Taking $\Phi(\cdot)$ as the CDF of standard normal distribution and $\Phi^{-1}(\cdot)$ as its quantile, estimate $z_i = \Phi^{-1}(u_i)$ .

3. Compute $W^2 = \sum_{i=1}^{n} \left( z_i - \frac{(2i-1)}{2n} \right)^2 + \frac{1}{12n}$, hence, represent $W^2$ as

$W^* = W^2 \left( 1 + \frac{0.5}{n} \right)$ then obtain test statistic.

We select the model with the smallest $W^*$ as the best between when comparing two

or more models.

### 3.4.2 Kolmogorov-Smirnov Test

In a specific distribution, we use Kolmogorov-Smirnov ($K-S$) test to verify if some

selected random sample $X_1, X_2, ..., X_n$ coming from a population can be linked to a

specific distribution. In this case, the K-S test measures the distance between the

empirical sample distribution and that of the estimated CDF of the competing

distributions. The null hypothesis is stated as $H_0$: The sample come from the specific

distribution. The alternative hypothesis is $H_1$: The sample does not come from the

specific distribution. If $G(x_i)$ is the value of the CDF of the competing distribution at

$x_i$ and $\hat{G}(x_i)$ is the value of the empirical distribution at $x_i$, then we write the K-S test

statistic as;

$$K - S = Max\left\{ |G(x_i) - \hat{G}(x_i)|, |G(x_i) - \hat{G}(x_{i-1})| \right\}, i = 1, 2, ..., n \qquad (3.13)$$

$$\hat{G}(x_i) = \frac{\#\{x_j : x_j \le x_i\}}{n}, \qquad (3.14)$$

where $\#\{\cdot\}$ is the number of points less than or equal to $x_i$, thus when $x_i$ values are grouped from the smallest value to the highest. Further, given a significance level and a tabulated K-S value, we then can compare between standard values to the computed test static value. Here, if we have more than one distribution under study, we pick the distribution with the smallest K-S value as the best fit.

### 3.4.3 Anderson Darling Test

The Anderson Darling $(A^*)$ test technique assigns weights to tails compared with $K-S$ test. It enable sensitive test to be carried out based on specific distributions. The $A^*$ test is given by:

$$A^* = -M - \Lambda \; , \tag{3.15}$$

where

$$\Lambda = \sum_{i=1}^{M} \frac{(2i-1)}{M} \left[ \ln F(\Psi_i) + \ln(1 - F(\Psi_M + 1 - i)) \right] ,$$

and $F$ is the CDF of the specified distribution. $\Psi_i$, the ordered data sets. The $A^*$ is the test statistic , $m(i)$ is the number of points less than $\Psi_i$. The test decision criteria is that when the test statistic value is greater than the critical value provided from in the table, then the hypothesis is rejected (Stephens, 1974).

21

### 3.5 Model Selection Criteria

In a distribution, if more parameters are added, they practically enhance the model fitness. It does not matter the primary importance of the addition. The most important thing is increase in likelihood of a model over the other. In comparing models, one main issue is whether the models are nested. Non nested models are best compared using information criteria frameworks than likelihood ratio test. This study makes use of the following information criteria: the Bayesian Information Criterion (BIC), Akaike Information Criterion (AIC) and Corrected Akaike Information Criterion (AICc).

### 3.5.1 Akaike Information Criterion

The AIC has been outstanding among several model selection tools. It was initiated by Akaike (1973) and improved by Akaike (1974) respectively. The method is applied by assuming some optional models and using them as proper models for certain data. Test statistic is hereby given as;

$$AIC = -2logL(\hat{\phi}) + 2k \ . \hspace{3cm} (3.16)$$

In that case, $k$ defines the number of model estimated parameters. $L(\hat{\phi})$ is the likelihood of the model. In determining the best model for dataset, the model with the smallest value of AIC is picked.

As an added advantage, for models that have several parameters, the AIC has the capacity to penalize them. It is also good for selecting models of large sample. Despite the advantages, the criterion produces some biasness. Further, in overcoming this

22

problem, Sugiura (1978) introduced the AICc. In the work of Hurvich and Tsai (1989), they demonstrated the ability of the AICc to select models well with small samples and many parameters. The AICc test statistic with the sample size $n$ considered is given by;

$$AICc = AIC + \frac{2k(k+1)}{n-k-1}. \qquad (3.17)$$

### 3.5.2 Bayesian Information Criterion

In literature, the BIC is also referred to as Schwarz Information Criterion (SIC). It was first used by Schwarz (1978). The assumption here is; data should be independent and identically distributed in order to permit for approximating the bayes factor in the data. The BIC test statistic is given by;

$$BIC = -2logL(\hat{\phi}) + k\log(n) . \qquad (3.18)$$

The BIC has better functionality over the AIC. It is capable of penalizing models of small or large samples and also with several parameters. The model with the smallest BIC value is chosen, and this tells the model is better compared to others. It is more appropriate to use the BIC along with AIC to achieve better model selection.

### 3.6 Cox-Snell Residual

The Cox-Snell residual was proposed by Cox and Snell (1968). It has been used extensively in survival analysis, where censored data is more of concern. The Cox-Snell residual is defined as $\eta_{c_i} = -\log(\hat{S}(t_i))$ , where $\hat{S}(t_i)$ is the estimated survival function and $t_i$, $i = 1, 2, 3...n$ represent the event times. The special Cox-Snell property

is that: $\eta_{c_i}$ follows standard exponential distribution when a model well fits a given data. The Cox-Snell is adopted in this study to assess the regression model developed.

## 3.7 Total Time on Test Transform

The shape of the hazard rate function of a given dataset is key in stochastic studies. It tells if a random sample comes from a known life distribution. Drawing conclusion on the shape was a challenge, until Barlow and Doksum (1972) came up with the total time on test (TTT)-transform method. The main idea of the method, though, was to solve problem of statistical inference in order restrictions. TTT-transform enables a graphical view of the bathtub shape of the hazard rate by researchers (Aarset, 1987; Barlow, 1972). Given the distribution's CDF as $G$ and survival function as $S(u) = 1 - G(u)$ , then TTT-Transform is given by;

$$H^{-1}(p) = \int_0^{G^{-1}(P)} S(u)du, \; p \in [0,1] \quad . \tag{3.19}$$

Hence the scaled TTT-transform is computed from;

$$\varphi G(p) = \frac{H^{-1}(p)}{H^{-1}(1)}. \tag{3.20}$$

The curve of $\varphi G(p)$ against $0 \le p \le 1$ is the scaled TTT-transform curve.

Barlow and Doksum (1972) demonstrated how the scaled TTT-transform curve is used to explain the behavior of the hazard rate function. They indicated that;

1.  When the scaled TTT-transform curve appears concave above the $45^0$ line, then it indicates an increasing hazard rate function.

2.  When the scaled TTT-transform curve appears convex below the $45^0$ line, then it indicates a decreasing hazard rate function.

3.  When the scaled TTT-transform curve begins as convex below and then concaves above the $45^0$ line, it shows the hazard rate function as having a bathtub shape.

4.  When the scaled TTT-transform curve begins with concave above and convex below the $45^0$ line, it means that, hazard rate function depicts upside down bathtub or unimodal shape.

With a specified ordered sample $X_{1:n}, X_{2:n}, ..., X_{n:n}$, the TTT can be computed using

$$TTT_i = \sum_{j=1}^{i} (n - j + 1)(x_{j:n} - x_{j-1:n}), i = 1, 2..., n \qquad (3.21)$$

The empirical scaled TTT-transform is given by;

$$TTT_i^* = \frac{TTT_i}{TTT_n}, \qquad (3.22)$$

where $0 \leq TTT_n \leq 1$. The empirical scaled TTT-transform curve by plotting $\frac{i}{n}$ against

$TTT_i^*$ .

25

### 3.8 Bowley's Skewness and Moors Kurtosis

The Bowley's skewness (Keeping and Kenney, 1962) and the Moors Kurtosis (Moors, 1987) use the quantile function $Q$ of the PDF to compute the numerical skewness and kurtosis. The Bowley's skewness ( $B$ ) and the Moors Kurtosis ( $M$ ) used in this work are given respectively below:

$$B = \frac{Q(3/4) - 2Q(1/2) + Q(1/4)}{Q(3/4) - Q(1/4)} , \tag{3.23}$$

$$\text{and} \quad M = \frac{Q(7/8) - Q(5/8) - Q(3/8) + Q(1/8)}{Q(6/8) - Q(2/8)} . \tag{3.24}$$

### 3.9 Average Bias and Root Mean Square Error

The average bias ( $AB$ ) and the root mean square error ( $RMSE$ ) in this work are used to measure the errors of the estimated parameter values in the simulation processes. Given $\hat{\phi}$ as the parameter estimate of $\phi$ and sample size $k$ . The $AB$ and $RMSE$ measures are given respectively as:

$$\text{Average Bias} = \frac{1}{k} \sum_{i=1}^{k} \left( \phi_i - \hat{\phi}_i \right), \tag{3.25}$$

$$\text{and} \quad RMSE = \sqrt{\frac{\sum_{i=1}^{k} \left( \phi_i - \hat{\phi}_i \right)}{k}}. \tag{3.26}$$

### 3.10 Data and Source

This study used nine secondary data sets to show the applications of the special distributions developed. The data sets are Failure times of device components, Maximum stress per 31,000psi, Survival times of guinea pigs, Breaking stress,

26

Windshield Service Times, Waiting Times of blowhole eruption, Milk Production , Cost of cybercrimes to GDP and Transformer Turn Data.

The first data set represents failure times of device component.  The data constitutes 50 random samples of device components which have failure times. The data set, as shown in Appendix B1 can be seen in Aarset (1987) and Hadeel,  (2019).

The second data set is the maximum stress data,   in Appendix B2. The data  is seen in Birnbaum and Saunders (1969) and Sangsanit (2016). This consists of 101 observations with maximum stress per 31,000 psi.

The third dataset in Appendix B3 is the survival times (in days) of 72 guinea pigs which were infected with virulent tubercle bacilli. The data was observed and reported in Bjerkedal (1960) and also   used by Farrukh et al. (2019).

The fourth data set constitutes breaking stress of carbon fibres. It is found in Appendix B4. The data contains 100 observations on breaking stress of carbon fibers in Gigapascals (GPa). This was studied by Nichols and Padgett (2006). The data was also used by Amal et al.(2019).

The fifth data set are service times of 63 aircraft windshield from Tahir et al. (2015). The data, shown in Appendix B5   was also used by Farrukh et al. (2019).

The sixth data set is the Waiting times of consecutive Blowhole Eruptions Data. The data was discussed by Pinho et al. (2015). This is a sample of 64 waiting times per second within 65 successive eruptions, of a blowhole also called the Kiama Blowhole. This data is given in Appendix B6, and has also been used by Hadeel (2019).

27

The seventh data set is the milk production data. The data set was the total milk produced by 107 cows who for the first time gave birth at Carnaúba farms of Agropecuária Manoel Dantas Ltd (AMDA) in Paraíba (Brazil). The data is showed in Appendix B7.  The original data was transformed into bounds [0,1]  and used by De Brito et al. (2017) and   Haitham and Mustafa (2017).

The eighth data set is the Cost of Cybercrimes to Gross Domestic Product data. The dataset was first reported by McAfee Incorporation (2014), and to the best of knowledge, this is the first time the ratio form of the dataset based on 23 randomly selected countries is used in such stochastic modeling. The dataset is shown in Appendix B8.

The ninth data set is the transformer turn data   which can be found in the book of (Nelson and Wayne, 2004) and also used by Farrukh et al., (2019). The data in Appendix B9 presents the life of a transformer testing, done    under three levels of voltages: thus, 35.40Kv, 42.4kv and 46.7kv where (+) indicates censored data. In each of the levels, 10 samples were tested of which a total of 13% of the data set were censored. The variables of importance for this study are  $x_i$  =times of failure of the transformer in hours , $i$  =1,…30. With three voltage levels defined by associated dummy  variables  35.4Kv: $(\psi_{i1} = 1, \psi_{i2} = 0)$, 42.4Kv: $((\psi_{i1} = 0, \psi_{i2} = 1)$  and  46.7Kv:( $(\psi_{i1} = 0, \psi_{i2} = 0)$ .

**3.11 Summary of Methodology**

This chapter presented definitions of the Zubair-G family and the TL-G family. Methods of parameter estimations, for example the maximum likelihood are explained. Goodness of fit tests, thus, Cramér-Von Mises test and Kolmogorov-Smirnov test are presented. Model selection criteria like the AIC, AICc and the BIC are also defined.

**CHAPTER FOUR**

**THEORETICAL RESULTS**

**4.1 Introduction**

In this chapter, the first three objectives of the study are presented. These include; the derivation of TLZ-G family of distributions, statistical properties and methods of estimation. Five new distributions generated from the TLZ-G are also presented. These new distributions are, TLZ Weibull, TLZ Inverse Weibull, TLZ Lomax, TLZ Kumaraswamy and TLZ Nadarajah Haghighi.

**4.2 Topp-Leone Zubair Family**

The TLZ family was developed by substituting the CDF of Zubair $G_1(x) = (e^{\alpha G(x;\phi)2} - 1)(e^{\alpha} - 1)^{-1}, \alpha, \phi > 0, x \in \mathbb{R}$ into the CDF of TL-G $F_{TL}(x) = [1 - (1 - G_1(x:\phi))^2]^{\lambda}$ , $\lambda > 0, \phi > 0, x \in \mathbb{R}$ . Hence, If a random variable $X$ follows the TLZ-G distribution, then the CDF of TLZ-G is,

$$F(x) = \left[1 - \left(\frac{e^{\alpha} - e^{\alpha G(x;\phi)^2}}{e^{\alpha} - 1}\right)^2\right]^{\lambda}, \ \alpha > 0, \phi > 0, x \in \mathbb{R} , \qquad (4.1)$$

and $G(x;\phi)$ assigned as CDF of a baseline distribution. Hence, probability density function is also obtained by differentiating the CDF of TLZ-G. In that case, the PDF is,

.

$$f(x) = \frac{4\lambda \alpha g(x;\phi)G(x;\phi)(e^{\alpha} - e^{\alpha G(x;\phi)^2})(e^{\alpha G(x;\phi)^2})}{(e^{\alpha} - 1)^2}\left[1 - \left(\frac{e^{\alpha} - e^{\alpha G(x;\phi)^2}}{e^{\alpha} - 1}\right)^2\right]^{\lambda - 1}, \lambda > 0, \phi > 0, x \in \mathbb{R} . \quad (4.2)$$

30

The hazard function $\tau(x)$ measures the rate of failure occurring within a given period $(t, t+dt)$. The hazard function for TLZ-G exists as,

$$\tau(x) = \frac{4\lambda\alpha g(x;\phi)G(x;\phi)(e^{\alpha} - e^{\alpha G(x;\phi)^2})(e^{\alpha G(x;\phi)^2})\left[1 - \left(\frac{e^{\alpha} - e^{\alpha G(x;\phi)^2}}{e^{\alpha} - 1}\right)^2\right]^{\lambda-1}}{(e^{\alpha}-1)^2\left[1 - \left[1 - \left(\frac{e^{\alpha} - e^{\alpha G(x;\phi)^2}}{e^{\alpha} - 1}\right)^2\right]^{\lambda}\right]} , \lambda > 0, \phi > 0, x \in \mathbb{R} . \quad (4.3)$$

## 4.3 The Mixture Representation

The mixture representation makes it easier to study the statistical properties of the distribution. This is derived based on the PDF of the TLZ-G family to simplify the computation processes of deriving the statistical properties. For instance, in this work, the moments, moment generating functions, incomplete moments, inequality measures, mean and median deviations mean residual life, stress reliability and the order statics are achieved in an easier way, by employing the mixture representation.

**Lemma 4.1.** The mixture representation of the TLZ-G family is;

$$f(x) = 4\lambda\alpha\sum_{i=0}^{\infty}\sum_{j=0}^{2i}\sum_{k=0}^{j}\sum_{m=0}^{\infty} w_{ijkm} g(x;\phi)G(x;\phi)^{2m+1} , \quad (4.4)$$

where

$$w_{ijkm} = \frac{(-1)^{i+j+k}\alpha^m\left[e^{\alpha}(1+j-k)^m - (2+j-k)^m\right]}{(e^{\alpha}-1)^{2+j}m!}\binom{\lambda-1}{i}\binom{2i}{j}\binom{j}{k}.$$

**Proof.** Expanding the PDF using binomial expansion $(1-Z)^{\eta} = \sum_{i=0}^{\infty}(-1)^i\binom{\eta}{i}Z^i, |Z| < 1$, we get,

$$f(x) = \frac{4\lambda\alpha g(x;\phi)G(x;\phi)(e^{\alpha G(x;\phi)^2})(e^{\alpha} - e^{\alpha G(x;\phi)^2})}{(e^{\alpha}-1)^2} \sum_{i=0}^{\infty}(-1)^i \binom{\lambda-1}{i}\left[1-\left(\frac{e^{\alpha} - e^{\alpha G(x;\phi)^2}}{e^{\alpha}-1}\right)^2\right]^{2i}$$

$$= 4\lambda\alpha g(x;\phi)G(x;\phi)(e^{\alpha G(x;\phi)^2})(e^{\alpha} - e^{\alpha G(x;\phi)^2})\sum_{i=0}^{\infty}\sum_{j=0}^{2i}\frac{(-1)^{i+j}}{(e^{\alpha}-1)^{2+j}}\binom{\lambda-1}{i}\binom{2i}{j}(e^{\alpha G(x;\phi)^2}-1)^j \ .$$

Hence, applying Taylor series expansion, $e^Z = \sum_{m=0}^{\infty}\frac{Z^m}{m!}$, the mixture representation becomes,

$$f(x) = 4\lambda\alpha\sum_{i=0}^{\infty}\sum_{j=0}^{2i}\sum_{k=0}^{j}\sum_{m=0}^{\infty}w_{ijkm}g(x:\phi)G(x:\phi)^{2m+1} \ ,$$

$$w_{ijkm} = \frac{(-1)^{i+j+k}\alpha^m\left[e^{\alpha}(1+j-k)^m - (2+j-k)^m\right]}{(e^{\alpha}-1)^{2+j}m!}\binom{\lambda-1}{i}\binom{2i}{j}\binom{j}{k} \ .$$

## 4.4 Statistical Properties

This section presents the statistical properties of the TLZ-G family. The properties include; quantile function, moments, moment generating function, incomplete moments, inequality measures, Bonferroni curve, mean deviation, median deviation, mean residual life, stochastic ordering, stress-strength reliability, order statistics and the $r^{th}$ non-central moment of the $p^{th}$ order statistic.

### 4.4.1 The Quantile Function of TLZ-G Family

The quantile function is relevant in the simulation of random numbers and also presents itself as alternative way of describing the shape of a distribution.

**Proposition 4.1**. The quantile function of the TLZ-G family is of the form,

$$Q_X(u) = G^{-1}\sqrt{\frac{1}{\alpha}\log\left[e^\alpha - (e^\alpha - 1)\left(1 - u^{\frac{1}{\lambda}}\right)^{\frac{1}{2}}\right]}, u \in [0,1], \qquad (4.5)$$

where $G^{-1}(.)$ is the quantile function of the baseline distribution .

**Proof.** By definition, the quantile function is given as $x_u = F^{-1}(u)$, so by setting

$x_u = Q_X(u)$ and performing some manipulations, we obtain the Quantile function of

the TLZ-G as,

$$Q_X(u) = G^{-1}\sqrt{\frac{1}{\alpha}\log\left[e^\alpha - (e^\alpha - 1)\left(1 - u^{\frac{1}{\lambda}}\right)^{\frac{1}{2}}\right]}, u \in [0,1] .$$

### 4.4.2 Moments

Moments become very important when finding the mean, variance, skewness and kurtosis of a given probability distribution.

**Proposition 4.2.** The $r^{\text{th}}$ non-central moment of the TLZ-G family is given as;

$$\mu_r^{'} = 4\lambda\alpha\sum_{i=0}^{\infty}\sum_{j=0}^{2i}\sum_{k=0}^{j}\sum_{m=0}^{\infty}w_{ijkm}\int_{-\infty}^{\infty}x^r g(x)G(x)^{2m+1}dx, r = 1, 2, ... . \qquad (4.6)$$

**Proof.** By definition**,** $\mu_r^{'} = E(X^r) = \int_{-\infty}^{\infty}x^r f(x)dx$ . Substituting the mixture representation into the definition and simplifying gives;

33

$$\mu_r^1 = \int_{-\infty}^{\infty} x^r 4\lambda\alpha \sum_{i=0}^{\infty}\sum_{j=0}^{2i}\sum_{k=0}^{j}\sum_{m=0}^{\infty} w_{ijkm} g(x)G(x)^{2m+1}$$

$$= 4\lambda\alpha \sum_{i=0}^{\infty}\sum_{j=0}^{2i}\sum_{k=0}^{j}\sum_{m=0}^{\infty} w_{ijkm} \int_{-\infty}^{\infty} x^r g(x)G(x)^{2m+1} dx, r = 1, 2, \dots .$$

Alternatively the moment can be expressed in terms of the quantile functions of the baseline distribution.

Let $G(x) = u, u \in [0,1]$, $x = G^{-1}(u) = Q_G(u)$, $\dfrac{du}{dx} = g(x)$ and $du = g(x)dx$. By some substitutions and simplifications we get,

$$\mu_r^{'} = 4\lambda\alpha \sum_{i=0}^{\infty}\sum_{j=0}^{2i}\sum_{k=0}^{j}\sum_{m=0}^{\infty} w_{ijkm} \int_0^1 Q_G(u)^r u^{2m+1} du. \tag{4.7}$$

### 4.4.3 Moment Generating Function

The moment generating function (MGF), serves a great purpose in analytical studies. It is used in computing moments of distributions. The MGF of TLZ-G family is given in proposition 4.3.

**Proposition 4.3.** The moment generating function of the TLZ-G family is given as;

$$M_X(t) = 4\lambda\alpha \sum_{i=0}^{\infty}\sum_{j=0}^{2i}\sum_{k=0}^{j}\sum_{m=0}^{\infty}\sum_{r=0}^{\infty} w_{ijkm} \frac{t^r}{r!}\int_{-\infty}^{\infty} x^r g(x)G(x)^{2m+1} dx. \tag{4.8}$$

**Proof:** By definition $M_X(t) = E(e^{tX}) = \int_{-\infty}^{\infty} e^{tx} f(x)dx$. Substituting the mixture representation and expanding with the Taylor series, $e^{tx} = \sum_{x=0}^{\infty} \frac{t^r}{r!} x^r$, we get,

$$M_X(t) = \sum_{r=0}^{\infty} \frac{t^r}{r!}\int_{-\infty}^{\infty} x^r 4\lambda\alpha \sum_{i=0}^{\infty}\sum_{j=0}^{2i}\sum_{k=0}^{j}\sum_{m=0}^{\infty} w_{ijkm} g(x)G(x)^{2m+1}$$

$$= 4\lambda\alpha \sum_{i=0}^{\infty}\sum_{j=0}^{2i}\sum_{k=0}^{j}\sum_{m=0}^{\infty}\sum_{r=0}^{\infty} w_{ijkm} \frac{t^r}{r!}\int_{-\infty}^{\infty} x^r g(x)G(x)^{2m+1} dx.$$

34

Alternatively, the moment generating function in terms of quantile function is;

$$M_X(t) = 4\lambda\alpha \sum_{i=0}^{\infty} \sum_{j=0}^{2i} \sum_{k=0}^{j} \sum_{m=0}^{\infty} \sum_{r=0}^{\infty} w_{ijkm} \frac{t^r}{r!} \int_0^1 Q_G(u)^r u^{2m+1} du. \qquad (4.9)$$

### 4.4.4 Incomplete Moments

The incomplete moments (IM) serve as the basis for arriving at the inequality measures in distribution analyses. For instance the Lorenz (1905) and Bonferroni (1930) curve inequality measures. The IM of TLZ-G family is given in proposition 4.4.

**Proposition 4.4.** The $r^{th}$ incomplete moment of the TLZ-G is,

$$\varphi_r(t) = 4\lambda\alpha \sum_{i=0}^{\infty} \sum_{j=0}^{2i} \sum_{k=0}^{j} \sum_{m=0}^{\infty} w_{ijkm} \int_{-\infty}^{t} x^r g(x) G(x)^{2m+1} dx , \qquad (4.10)$$

where $r = 1, 2, 3...$ .

**Proof.** Using the definition of incomplete moment of a random variable $\varphi_r(t) = \int_{-\infty}^{t} x^r f(x) dx$ and the mixture representation, the incomplete moment of the TLZ-G distribution is,

$$\varphi_r(t) = 4\lambda\alpha \sum_{i=0}^{\infty} \sum_{j=0}^{2i} \sum_{k=0}^{j} \sum_{m=0}^{\infty} w_{ijkm} \int_{-\infty}^{t} x^r g(x) G(x)^{2m+1} dx .$$

Alternatively, in terms the quantile function. Let $G(x) = u$; $x \to -\infty$, $G(x) \to 0$;

$x \to t$; $G(x) \to G(t)$; $x = Q_G(u)$. and $du = dxg(x)$, thus,

$$\varphi_r(t) = 4\lambda\alpha \sum_{i=0}^{\infty} \sum_{j=0}^{2i} \sum_{k=0}^{j} \sum_{m=0}^{\infty} w_{ijkm} \int_0^{G(t)} Q_G(u)^r u^{2m+1} du . \qquad (4.11)$$

### 4.4.5 Inequality Measures

The Inequality measures are very useful in applications, for example in drug dispensaries, stress studies and income analysis. Several inequality measures have been developed with unique properties (Atkinson, 1970). The Lorenz (1905) and Bonferroni (1930) curve properties have been developed for TLZ-G family.

**Proposition 4.5.** The Lorenz curve $Lq(x)$ is,

$$Lq(x) = \frac{4\lambda\alpha}{\mu} \sum_{i=0}^{\infty} \sum_{j=0}^{2i} \sum_{k=0}^{j} \sum_{m=0}^{\infty} w_{ijkm} \int_{-\infty}^{t} xg(x)G(x)^{2m+1} dx \ . \qquad (4.12)$$

**Proof.** By definition,

$$Lq(x) = \frac{1}{\mu} \int_{-\infty}^{t} xf(x)dx$$

$$Lq(x) = \left(\frac{1}{\mu}\right)\left(4\lambda\alpha \sum_{i=0}^{\infty} \sum_{j=0}^{2i} \sum_{k=0}^{j} \sum_{m=0}^{\infty} w_{ijkm} \int_{-\infty}^{t} xg(x)G(x)^{2m+1} dx\right)$$

$$= \frac{4\lambda\alpha}{\mu} \sum_{i=0}^{\infty} \sum_{j=0}^{2i} \sum_{k=0}^{j} \sum_{m=0}^{\infty} w_{ijkm} \int_{-\infty}^{t} xg(x)G(x)^{2m+1} dx \ .$$

In terms of the quantile function we have;

$$Lq(x) = \frac{4\lambda\alpha}{\mu} \sum_{i=0}^{\infty} \sum_{j=0}^{2i} \sum_{k=0}^{j} \sum_{m=0}^{\infty} \sum_{r=0}^{\infty} w_{ijkm} \int_{0}^{G(t)} Q_G(u)u^{2m+1} du \ . \qquad (4.13)$$

**Proposition 4.6.** The Bonferroni curve $Bq(x)$ is,

$$Bq(x) = \frac{4\lambda\alpha}{\mu F(x)} \sum_{i=0}^{\infty} \sum_{j=0}^{2i} \sum_{k=0}^{j} \sum_{m=0}^{\infty} w_{ijkm} \int_{-\infty}^{t} xg(x)G(x)^{2m+1} dx \ . \qquad (4.14)$$

36

**Proof.** By definition,

$$Bq = \frac{Lq(x)}{F(x)}$$

$$= \frac{1}{\mu F(x)} \int_{-\infty}^{t} xf(x)dx$$

$$= \frac{4\lambda\alpha}{\mu F(x)} \sum_{i=0}^{\infty}\sum_{j=0}^{2i}\sum_{k=0}^{j}\sum_{m=0}^{\infty} w_{ijkm} \int_{-\infty}^{t} xg(x)G(x)^{2m+1} dx \,.$$

Alternatively, Bonferroni curve in terms of quantile is,

$$Bq(x) = \frac{4\lambda\alpha}{\mu F(x)} \sum_{i=0}^{\infty}\sum_{j=0}^{2i}\sum_{k=0}^{j}\sum_{m=0}^{\infty} w_{ijkm} \int_{0}^{G(t)} Q_G(u)u^{2m+1}du \,. \qquad (4.15)$$

### 4.4.6 Mean and Median Deviations

The mean and median deviation can measure the totality of variation that exists in a distribution.

**Proposition 4.7**. The mean deviation is,

$$\delta_1 = 2\mu F(x) - 8\lambda\alpha \sum_{i=0}^{\infty}\sum_{j=0}^{2i}\sum_{k=0}^{j}\sum_{m=0}^{\infty} w_{ijkm} \int_{-\infty}^{\mu} xg(x)G(x)^{2m+1}dx \,. \qquad (4.16)$$

**Proof.** By definition,

$$\delta_1 = \int_{-\infty}^{\infty} |x - \mu| f(x)dx$$

$$\delta_1 = \int_{-\infty}^{\mu} (x - \mu)f(x)dx + \int_{\mu}^{\infty} (x - \mu)f(x)dx$$

$$= 2\mu F(x) + 2\int_{-\infty}^{\mu} xf(x)dx$$

$$= 2\mu F(x) - 8\lambda\alpha \sum_{i=0}^{\infty}\sum_{j=0}^{2i}\sum_{k=0}^{j}\sum_{m=0}^{\infty} w_{ijkm} \int_{-\infty}^{\mu} xg(x)G(x)^{2m+1}dx \,.$$

37

**Proposition 4.8.** The median deviation is;

$$\delta_2 = \mu - 8\lambda\alpha \sum_{i=0}^{\infty} \sum_{j=0}^{2i} \sum_{k=0}^{j} \sum_{m=0}^{\infty} w_{ijkm} \int_{-\infty}^{M} xg(x)G(x)^{2m+1}dx \,. \qquad (4.17)$$

**Proof.** By definition,

$$\delta_2 = \int_{-\infty}^{\infty} |x - M| f(x)dx$$

$$\delta_2 = \int_{-\infty}^{M} (M-x) f(x)dx + \int_{M}^{\infty} (x-M) f(x)dx$$

$$= \mu + 2\int_{-\infty}^{M} xf(x)dx$$

$$= \mu - 2\int_{-\infty}^{M} x 4\lambda\alpha \sum_{i=0}^{\infty} \sum_{j=0}^{2i} \sum_{k=0}^{j} \sum_{m=0}^{\infty} w_{ijkm} g(x:\phi)G(x:\phi)^{2m+1} \, dx$$

$$= \mu - 8\lambda\alpha \sum_{i=0}^{\infty} \sum_{j=0}^{2i} \sum_{k=0}^{j} \sum_{m=0}^{\infty} w_{ijkm} \int_{-\infty}^{M} xg(x)G(x)^{2m+1}dx.$$

### 4.4.7 Mean Residual Life

A system has residual life $X_t = X - t \mid X > t$ when it still functions at time $t$ . The mean residual life (MRL) plays a major role in life expectancy analysis and stress testing (Navarro, 2008).

**Proposition 4.9.** The mean residual life is;

$$m(t) = \frac{1}{1-F(t)} \left[ u - 4\lambda\alpha \sum_{i=0}^{\infty} \sum_{j=0}^{2i} \sum_{k=0}^{j} \sum_{m=0}^{\infty} w_{ijkm} \int_{-\infty}^{t} xg(x)G(x)^{2m+1}dx \right] - t. \qquad (4.18)$$

**Proof.** By definition,

$$m(t) = E(X - t \mid X > t) = \frac{\int_{t}^{\infty} (x-t) f(x)dx}{1-F(t)}$$

$$= \frac{\mu - \int_{-\infty}^{t} xf(x)dx}{1-F(t)} - t.$$

Substituting the mixture representation into the definition and simplifying, we get

$$m(t) = \frac{1}{1-F(t)}\left[ \mu - 4\lambda\alpha \sum_{i=0}^{\infty}\sum_{j=0}^{2i}\sum_{k=0}^{j}\sum_{m=0}^{\infty} w_{ijkm}\int_{-\infty}^{t} xg(x)G(x)^{2m+1}dx \right] - t.$$

### 4.4.8 Stochastic Ordering

Stochastic ordering is the common way of showing ordering features in lifetime distribution. In a likelihood ratio order, a random variable $X_1$ becomes greater than $X_2$ if $\frac{f_{X_1}(x)}{f_{X_2}(x)}$ is an increasing function for all $x$.

**Proposition 4.10.** Suppose $X_1 \sim TLZ - G(x;\alpha,\lambda_1,\phi)$ and $X_2 \sim TLZ - G(x;\alpha,\lambda_2,\phi)$, then $X_2$ is greater than $X_1$ in a likelihood ratio order $(X_2 \leq_{lr} X_1)$ if $\lambda_2$ is greater than $\lambda_1$.

**Proof.** The ratio of the density $X_1$ and $X_2$ is,

$$\frac{f_{x_1}(x)}{f_{x_2}(x)} = \left[ 1 - \left( \frac{e^{\alpha} - e^{\alpha G(x:\phi)2}}{e^{\alpha}-1} \right)^2 \right]^{\lambda_1 - \lambda_2} \tag{4.19}$$

Taking the derivative of the ratio of the density with respective to $x$, thus

$$\frac{d}{dx}\frac{f_{x_1}(x)}{f_{x_2}(x)} = \frac{4\lambda_1\alpha g(x:\phi)G(x:\phi)e^{\alpha G(x:\phi)^2}(\lambda_1-\lambda_2)\left(e^{\alpha}-e^{\alpha G(x:\phi)^2}\right)}{\lambda_2(e^{\alpha}-1)^2}\left(1 - \left(\frac{e^{\alpha} - e^{\alpha G(x:\phi)^2}}{e^{\alpha}-1}\right)^2\right)^{\lambda_1-\lambda_2-1}$$

If $\lambda_2 < \lambda_1$, $\frac{d}{dx}\frac{f_{x_1}(x)}{f_{x_2}(x)} < 0$. Thus, likelihood ratio exist for $X_1$ and $X_2$ at where $\lambda_2$ is less than $\lambda_1$. Hence, likelihood ratio order is $(X_2 \leq_{lr} X_1)$.

### 4.4.9 Stress-Strength Reliability

The significance of the stress-strength reliability is seen when a particular study is interested in the extent to which an existing strength of a system or its component can stand a subjected stress before they break out. If the strength of a system is $X_1$ and the subjected stress is $X_2$, the system stands the stress or works satisfactorily if $X_2 < X_1$, hence the stress-strength reliability is $R = P(X_2 < X_1)$.

**Proposition 4.11.** If $X_1 \sim TLZ - G(x; \alpha, \lambda, \phi)$ and $X_2 \sim TLZ - G(x; \alpha, \lambda, \phi)$, then reliability is presented as,

$$R = 4\lambda\alpha \sum_{i=0}^{\infty} \sum_{j=0}^{2i} \sum_{k=0}^{j} \sum_{m=0}^{\infty} \overline{w}_{ijkm} \int_{-\infty}^{\infty} g(x)G(x)^{2m+1} dx .$$ 

(4.20)

**Proof.** The reliability is defined as $R = \int_{-\infty}^{\infty} f(x)F(x)dx$. Substituting the mixture representation and CDF into definition and simplifying, we get,

$$R = \int_{-\infty}^{\infty} 4\lambda\alpha \sum_{i=0}^{\infty} \sum_{j=0}^{2i} \sum_{k=0}^{j} \sum_{m=0}^{\infty} \overline{w}_{ijkm} g(x)G(x)^{2m+1} dx$$

$$= 4\lambda\alpha \sum_{i=0}^{\infty} \sum_{j=0}^{2i} \sum_{k=0}^{j} \sum_{m=0}^{\infty} \overline{w}_{ijkm} \int_{-\infty}^{\infty} g(x)G(x)^{2m+1} dx.$$

### 4.4.10 Order Statistics

The Order statistics serves a great purpose when measuring the minimum, interquartile range and the maximum of set of values (Hogg, 2012).

**Proposition 4.12.** Suppose $X_1, X_2, ..., X_n$ is a random sample of size $n$ from TLZ-G, then the PDF of the $p^{th}$ order statistic $X_{p:n}$ is;

$$f_{p:n}(x) = \frac{n!4\lambda\alpha}{(p-1)!(n-p)!} \sum_{i=0}^{n-p} \sum_{j=0}^{\infty} \sum_{k=0}^{2j} \sum_{m=0}^{k} \sum_{q=0}^{\infty} C_{ijkmq} g(x)G(x)^{2q+1} \ , \quad (4.21)$$

where,

$$C_{ijkmq} = (-1)^{i+j+k} \alpha^q \frac{\left[e^\alpha(1+\alpha(m-k))-(2+(m-k))\right]}{(e^\alpha-1)^{2+k}} \binom{n-p}{i} \binom{\lambda(p+i)-1}{j} \binom{k}{m} \ .$$

**Proof.** The order statistics is defined as;

$$f_{p:n}(x) = \frac{n!}{(p-1)!(n-p)!} \left[F(x)\right]^{p-1} \left[1-F(x)\right]^{n-p} f(x) .$$

Using the binomial expansion on the definition and based on the fact that $0 < F(x) < 1$,

$$f_{p:n}(x) = \frac{n!}{(p-1)!(n-p)!} \sum_{i=0}^{n-p} (-1)^i \binom{n-p}{i} \left[F(x)\right]^{p+i-1} f(x) .$$

Now, Substituting the mixture representation and CDF, then applying the binomial expansion concept thrice and further applying Taylor series; the order statistics is then simplified as;

$$f_{p:n}(x) = \frac{n!4\lambda\alpha}{(p-1)!(n-p)!} \sum_{i=0}^{n-p} \sum_{j=0}^{\infty} \sum_{k=0}^{2j} \sum_{m=0}^{k} \sum_{q=0}^{\infty} C_{ijkmq} g(x)G(x)^{2q+1} ,$$

41

$$C_{ijkmq} = (-1)^{i+j+k} \alpha^q \frac{\left[e^\alpha(1+\alpha(m-k))-(2+(m-k))\right]}{(e^\alpha-1)^{2+k}} \binom{n-p}{i} \binom{\lambda(p+i)-1}{j} \binom{k}{m} .$$

**Proposition 4.13**. The r$^{th}$ non-central moment of the p$^{th}$ order Statistics is

$$\mu_r'^{(p:n)} = \frac{n!4\lambda\alpha}{(p-1)!(n-p)!} \sum_{i=0}^{n-p} \sum_{j=0}^{\infty} \sum_{k=0}^{2j} \sum_{m=0}^{k} \sum_{q=0}^{\infty} C_{ijkmq} \int_{-\infty}^{\infty} x^r g(x)G(x)^{2q+1} dx . \tag{4.22}$$

**Proof.** By definition, $\mu_r'^{(p:n)} = \int_{-\infty}^{\infty} x^r f_{p:n}(x)dx$ . Substituting the $p^{th}$ order statistics into

the definition,

$$\mu_r'^{(p:n)} = \int_{-\infty}^{\infty} x^r \frac{n!4\lambda\alpha}{(p-1)!(n-p)!} \sum_{i=0}^{n-p} \sum_{j=0}^{\infty} \sum_{k=0}^{2j} \sum_{m=0}^{k} \sum_{q=0}^{\infty} C_{ijkmq} g(x)G(x)^{2q+1} dx$$

$$= \frac{n!4\lambda\alpha}{(p-1)!(n-p)!} \sum_{i=0}^{n-p} \sum_{j=0}^{\infty} \sum_{k=0}^{2j} \sum_{m=0}^{k} \sum_{q=0}^{\infty} C_{ijkmq} \int_{-\infty}^{\infty} x^r g(x)G(x)^{2q+1} dx.$$

## 4.5 Parameter Estimation

The maximum likelihood estimation (MLE) method is used to compute the parameters

$\psi = (\alpha, \lambda, \phi)^T$ . Taking $X_1, X_2, ... X_n$ as be a complete random sample of size $n$ , then

the log-likelihood of TLZ-G is,

$$\ell = n \log\left(\frac{4\lambda\alpha}{(e^\alpha-1)^2}\right) + \sum_{i=1}^{n} \log(g(x_i:\phi)) + \sum_{i=1}^{n} \log(G(x_i:\phi)) +$$

$$\sum_{i=1}^{n} \log(e^{\alpha G(x_i:\phi)^2}) + \sum_{i=1}^{n} \log(e^\alpha - e^{\alpha G(x_i:\phi)^2}) + (\lambda-1) \sum_{i=1}^{n} \log\left[1-\left(\frac{e^\alpha-e^{\alpha G(x_i:\phi)^2}}{e^\alpha-1}\right)^2\right] . \tag{4.23}$$

42

Differentiating $\ell$ in respective to $\alpha$ , we get,

$$\frac{\partial \ell}{\partial \alpha} = \frac{n}{\alpha} + \frac{2ne^{\alpha}}{e^{\alpha}-1} + \sum_{i=1}^{n} G(x_i;\phi)^2 e^{\alpha G(x_i;\phi)^2} + \sum_{i=1}^{n} 1 - \left( \frac{e^{\alpha} - G(x_i;\phi)^2 e^{\alpha G(x_i;\phi)^2}}{e^{\alpha} - e^{\alpha G(x_i;\phi)^2}} \right) +$$
$$(\lambda-1) \sum_{i=1}^{n} \frac{e^{\alpha} - G(x_i;\phi)^2 e^{\alpha G(x_i;\phi)^2} + (G(x_i;\phi)^2 - 1)e^{\alpha+\alpha G(x_i;\phi)^2}}{(e^{\alpha}-1)(e^{\alpha G(x_i;\phi)^2}-1)} \qquad (4.24)$$

Differentiating $\ell$ in respective to $\lambda$ , we get,

$$\frac{\partial \ell}{\partial \lambda} = \frac{n}{\lambda} + \sum_{i=1}^{n} \log\left[ 1 - \left( \frac{e^{\alpha} - e^{\alpha G(x_i;\phi)^2}}{e^{\alpha}-1} \right) \right] \qquad (4.25)$$

Differentiating $\ell$ in respective to $\phi$ , we get,

$$\frac{\partial \ell}{\partial \phi} = \sum_{i=1}^{n} \frac{\partial(g(x_i:\phi))/\partial\phi}{g(x_i:\phi)} + \sum_{i=1}^{n} \frac{\partial(G(x_i:\phi))/\partial\phi}{G(x_i:\phi)} + 2\alpha \sum_{i=1}^{n} G(x_i:\phi)\partial(G(x_i:\phi))/\partial\phi -$$
$$2\alpha \sum_{i=1}^{n} \frac{e^{\alpha G(x_i:\phi)^2} G(x_i:\phi)\partial(G(x_i:\phi))/\partial\phi}{e^{\alpha}-e^{\alpha G(x_i:\phi)^2}} + 2\alpha(-1+\lambda)\sum_{i=1}^{n} \frac{e^{\alpha G(x_i:\phi)^2} G(x_i:\phi)\partial(G(x_i:\phi))/\partial\phi}{e^{\alpha G(x_i:\phi)^2}-1} \qquad (4.26)$$

## 4.6  Special Distributions from the Topp-Leone Zubair G Family

Five new distributions have been developed from the TLZ-G   family of distributions. These distributions are TLZ-G   Weibull, TLZ-G   Inverse Weibull, TLZ-G   Lomax, TLZ-G   Kumaraswamy and TLZ-G   Nadarajah Haghighi. The PDF, CDF and quantile functions are derived.

### 4.6.1 Topp-Leone Zubair Nadarajah Haghighi

The CDF and PDF of the Nadarajah Haghighi (NH) are

$$G(x) = 1 - e^{1-(1+\gamma x)^{\beta}}, x > 0, \gamma > 0, \beta > 0 \qquad \text{and} \qquad g(x) = \beta\gamma(1+\gamma x)^{\beta-1}e^{1-(1+\gamma x)^{\beta}}, x > 0$$

43

respectively. Substituting the CDF of the NH into the CDF of the TLZ-G, we get the CDF of TLZNH distribution as,

$$F(x) = \left[ 1 - \left( \frac{e^{\alpha} - e^{\alpha\left(1 - e^{1-(1+\gamma x)^{\beta}}\right)^2}}{e^{\alpha} - 1} \right)^2 \right]^{\lambda} , \quad x > 0, \qquad (4.27)$$

where $\alpha > 0$, $\gamma > 0$ are scale parameters and $\beta > 0$, $\lambda > 0$ are shape parameters.

The density function of the TLZNH is,

$$f(x) = \frac{4\lambda\alpha\beta\gamma\left(1 + \gamma x\right)^{\beta-1} e^{1-(1+\gamma x)^{\beta}} \left(1 - e^{1-(1+\gamma x)^{\beta}}\right)\left(e^{\alpha} - e^{\alpha\left(1 - e^{1-(1+\gamma x)^{\beta}}\right)^2}\right)}{\left(e^{\alpha} - 1\right)^2 \left[ 1 - \left( \frac{e^{\alpha} - e^{\alpha\left(1 - e^{1-(1+\gamma x)^{\beta}}\right)^2}}{e^{\alpha} - 1} \right)^2 \right]^{1-\lambda}}, x > 0 . \qquad (4.28)$$

The plot of the TLZNH PDF for some chosen parameter values are shown in Figure 4.1.

TLZNH PDF shows right skewed, symmetric, unimodal and left skewed shapes.
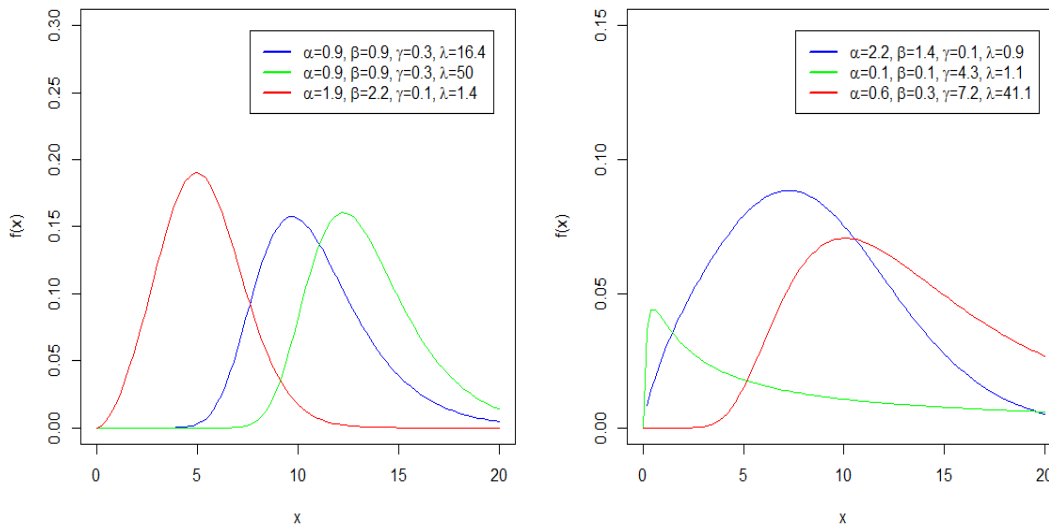
**Figure 4.1: Plot of TLZNH PDF**

The hazard function of the TLZNH is;

$$\tau(x) = \frac{4\lambda\alpha\beta\gamma(1+\gamma x)^{\beta-1}e^{1-(1+\gamma x)^{\beta}}(1-e^{1-(1+\gamma x)^{\beta}})(e^{\alpha}-e^{\alpha(1-e^{1-(1+\gamma x)^{\beta}})2})\left[1-\left(\frac{e^{\alpha}-e^{\alpha(1-e^{1-(1+\gamma x)^{\beta}})^{2}}}{e^{\alpha}-1}\right)^{2}\right]^{\lambda-1}}{(e^{\alpha}-1)^{2}\left[1-\left[1-\left(\frac{e^{\alpha}-e^{\alpha\left(1-e^{1-(1+\gamma x)^{\beta}}\right)^{2}}}{e^{\alpha}-1}\right)^{2}\right]^{\lambda}\right]}, \quad x > 0. \qquad (4.29)$$

The plot of the TLZNH hazard function with some selected parameters is shown in Figure 4.2. The hazard plots show very good shapes, thus upside down bathtub, monotonically increasing and bathtub. These features confirm the TLZNH to be capable of modeling monotonic and non-monotonic failure rates.

45
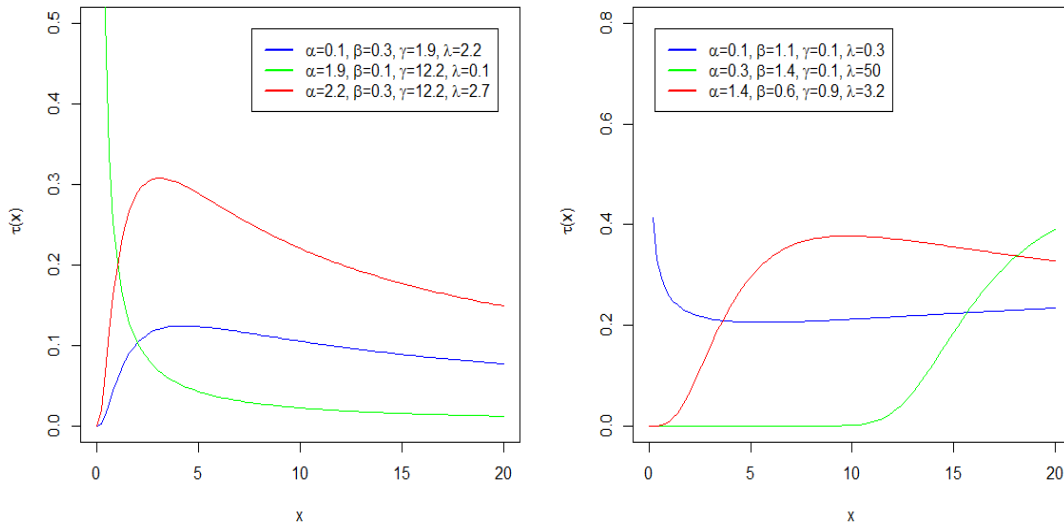
**Figure 4.2: Plot of the TLZNH Hazard function**

The quantile function of the TLZNH distribution is,

$$Q_X(u) = \frac{1}{\gamma}\left\{ \left[ 1 - \log\left( 1 - \sqrt{\frac{1}{\alpha}\log\left( e^\alpha - (e^\alpha - 1)\left(1 - u^{\frac{1}{\lambda}}\right)^{\frac{1}{2}} \right)} \right) \right]^{\frac{1}{\beta}} - 1 \right\}, \ u \in (0,1) \quad (4.30)$$

The quantile function $Q_X(u)$ enables us to compute the Bowley's skewness (Keeping and Kenney, 1962) and the Moors kurtosis (Moors, 1987).

The Bowley's skewness and the Moors kurtosis plots of TLZNH are shown in Figure 4.3. It is seen that TLZNH distribution is sensitive to the parameters $\alpha$ and $\lambda$ with fixed values of $\beta = 0.01$ and $\gamma = 0.04$. There was a responsive flexible change in the skewness and kurtosis. This means that the distribution has the capacity to model varieties of lifetime data.

46
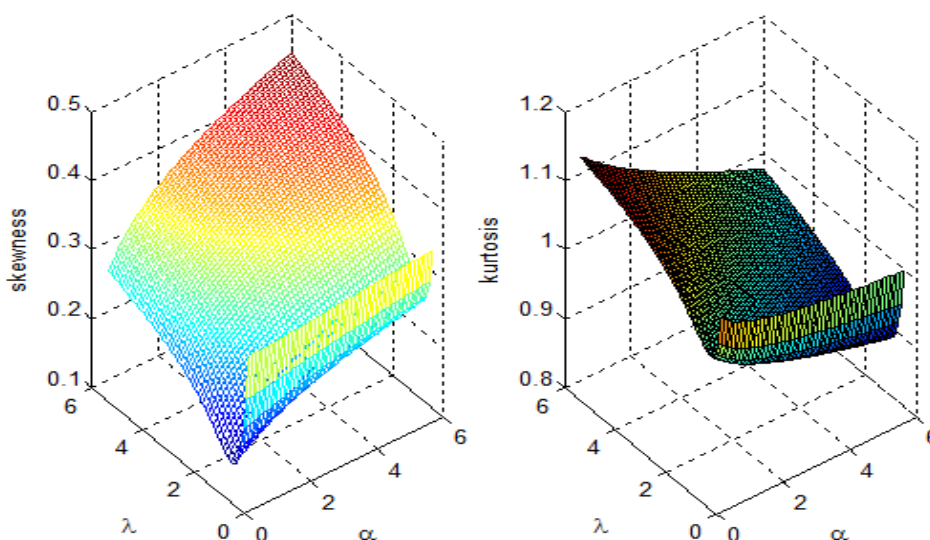
**Figure 4.3: Skewness and Kurtosis Plots of TLZNH**

The moment of TLZNH is derived by inserting the PDF and CDF of NH into the moment of TLZ-G family of distribution. The moment of TLZNH is,

$$\mu_r' = 4\lambda\alpha\beta\gamma \sum_{i=0}^{\infty}\sum_{j=0}^{2i}\sum_{k=0}^{j}\sum_{m=0}^{\infty} w_{ijkm} \int_0^\infty x^r (1+\gamma x)^{\beta-1} e^{1-(1+\gamma x)^\beta} (1-e^{1-(1+\gamma x)^B})^{2m+1} dx, r = 1,2,..., \quad (4.31)$$

$$\text{where, } w_{ijkm} = \frac{(-1)^{i+j+k}\alpha^m \left[ e^\alpha (1+j-k)^m - (2+j-k)^m \right]}{(e^\alpha - 1)^{2+j} m!} \binom{\lambda-1}{i}\binom{2i}{j}\binom{j}{k}.$$

The first six moments for some scenarios have been computed. These are done using R software. Different $\alpha$ and $\lambda$ values are used with fixed values of $\gamma$ **=0.5** and $\beta$ **=1.5** . The computation results indicate integration routines precision. Based on this, it is seen that with fixed $\alpha$ parameter, the addition of $\lambda$ creates a great impact on $\mu_r'$ .In effect, the moment increases whiles $\lambda$ is increasing. The moment also increases whiles $\alpha$ is increasing. Table 4.1 represents the first six moments of the TLZNH distribution.

47

**Table 4. 1: First six moments for some scenarios of $\alpha$ and $\lambda$, with fixed $\gamma$ =0.5 and $\beta$ =1.5 of TLNH**

| $\alpha$ | $\lambda$ | $\mu_1^{'}$ | $\mu_2^{'}$ | $\mu_3^{'}$ | $\mu_4^{'}$ | $\mu_5^{'}$ | $\mu_6^{'}$ |
|------|------|---------|---------|---------|---------|----------|-----------|
| 0.5 | 0.5 | 0.8115 | 1.1037 | 1.9850 | 4.3239 | 10.9086 | 31.0303 |
| | 1.0 | 1.1699 | 1.8452 | 3.5764 | 8.1217 | 20.9964 | 60.6102 |
| | 2.0 | 1.5501 | 2.8593 | 6.0876 | 14.6572 | 39.3251 | 116.2496 |
| | 3.0 | 1.7707 | 3.5686 | 8.0670 | 20.2325 | 55.8139 | 168.1269 |
| | 4.0 | 1.9243 | 4.1175 | 9.7197 | 25.1476 | 70.9256 | 217.0009 |
| 1.0 | 0.5 | 0.9047 | 1.3325 | 2.5424 | 5.7903 | 15.1132 | 44.1271 |
| | 1.0 | 1.2944 | 2.2060 | 4.5384 | 10.7923 | 28.9137 | 85.8028 |
| | 2.0 | 1.6986 | 3.3739 | 7.6238 | 19.2506 | 53.6369 | 163.3420 |
| | 3.0 | 1.9289 | 4.1748 | 10.0103 | 26.3456 | 75.5638 | 234.8120 |
| | 4.0 | 2.0875 | 4.7869 | 11.9774 | 32.5253 | 95.4464 | 301.5430 |
| 2.0 | 0.5 | 1.1079 | 1.8711 | 3.9374 | 9.6472 | 26.6246 | 81.1669 |
| | 1.0 | 1.5529 | 3.0229 | 6.8742 | 17.6547 | 50.2129 | 156.1322 |
| | 2.0 | 1.9912 | 4.4859 | 11.2087 | 30.6751 | 91.1496 | 292.1769 |
| | 3.0 | 2.2318 | 5.4488 | 14.4311 | 41.2153 | 126.3689 | 414.4791 |
| | 4.0 | 2.3944 | 6.1679 | 17.0223 | 50.1792 | 157.6226 | 526.5669 |
| 3.0 | 0.5 | 1.3202 | 2.4857 | 5.6444 | 14.6352 | 42.1900 | 133.0931 |
| | 1.0 | 1.8048 | 3.9051 | 9.6109 | 26.2373 | 78.2904 | 252.8681 |
| | 2.0 | 2.2574 | 5.6153 | 15.1940 | 44.3537 | 138.8849 | 464.5046 |
| | 3.0 | 2.4987 | 6.7014 | 19.1968 | 58.5337 | 189.4966 | 650.0616 |
| | 4.0 | 2.6601 | 7.4983 | 22.3505 | 70.3454 | 233.5396 | 817.1718 |
| 4.0 | 0.5 | 1.5270 | 3.1330 | 7.5535 | 20.4863 | 61.1659 | 198.4151 |
| | 1.0 | 2.0334 | 4.7833 | 12.5387 | 35.9625 | 111.6179 | 372.1090 |
| | 2.0 | 2.4859 | 6.6814 | 19.2597 | 59.2337 | 193.6525 | 671.1329 |
| | 3.0 | 2.7231 | 7.8553 | 23.9392 | 76.9359 | 260.4091 | 927.4040 |
| | 4.0 | 2.8813 | 8.7069 | 27.5710 | 91.4420 | 317.5696 | 1154.7520 |

## 4.6.2 Topp-Leone Zubair Lomax (TLZLx)

The Lomax CDF and PDF respectively defined as $G(x) = 1 - (1 + \gamma x)^{-\beta}$ $x > 0, \gamma > 0, \beta > 0$ and $g(x) = \beta \gamma (1 + \gamma x)^{-\beta - 1}$. Substituting the CDF of Lomax into the CDF of TLZ-G enables us to derive the CDF of TLZLx as,

$$F(x) = \left[ 1 - \left( \frac{e^{\alpha} - e^{\alpha \left( 1 - (1 + \gamma x)^{-\beta} \right)^2}}{e^{\alpha} - 1} \right)^2 \right]^{\lambda}, \quad x > 0, \tag{4.32}$$

where $\alpha > 0$, $\gamma > 0$ are scale parameters and $\beta > 0$, $\lambda > 0$ are shape parameters.

The PDF of the TLZLx is,

$$f(x) = \frac{4 \lambda \alpha (\beta \gamma (1 + \gamma x)^{-\beta - 1})(1 - (1 + \gamma x)^{-\beta})(e^{\alpha} - e^{\alpha (1 - (1 + \gamma x)^{-\beta})^2})}{(e^{\alpha} - 1)^2} \left[ 1 - \left( \frac{e^{\alpha} - e^{\alpha (1 - (1 + \gamma x)^{-\beta})^2}}{e^{\alpha} - 1} \right)^2 \right]^{\lambda - 1}, x > 0. \tag{4.33}$$

The PDF plot of TLZLx is shown in Figure 4.4. The plot shows right skewed and left

skewed shapes of the TLZLx PDF.
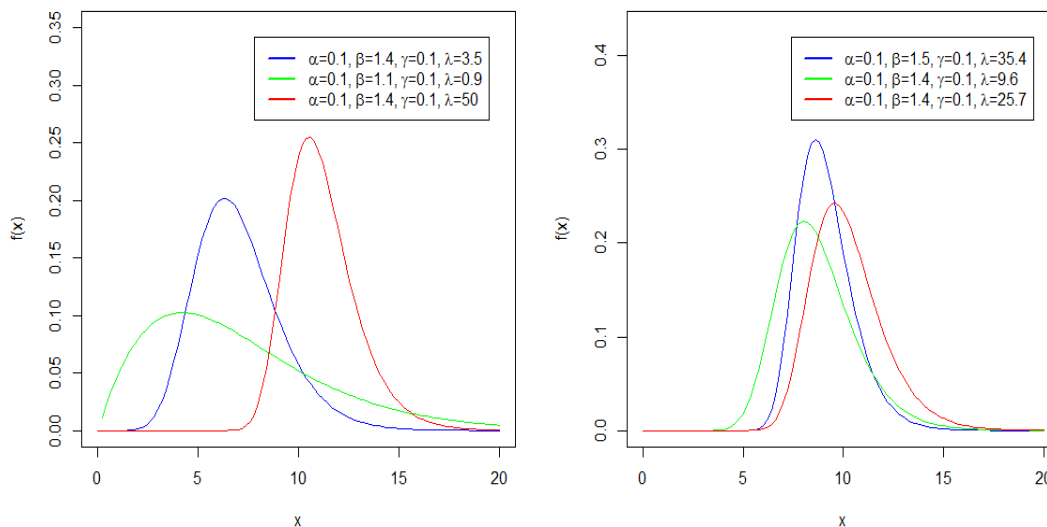


**Figure 4.4:PDF plot of TLZLx**

The hazard function of the TLZLx is;

$$
\tau(x) = \frac{4\lambda\alpha(\beta\gamma(1+\gamma x)^{-\beta-1})(1-(1+\gamma x)^{-\beta})(e^{\alpha}-e^{\alpha(1-(1+\gamma x)^{-\beta})^2})\left[1-\left(\dfrac{e^{\alpha}-e^{\alpha(1-(1+\gamma x)^{-\beta})^2}}{e^{\alpha}-1}\right)^2\right]^{\lambda-1}}{(e^{\alpha}-1)^2\left[1-\left[1-\left(\dfrac{e^{\alpha}-e^{\alpha\left(1-(1+\gamma x)^{-\beta}\right)^2}}{e^{\alpha}-1}\right)^2\right]^{\lambda}\right]}, x>0. \quad (4.34)
$$

50

The hazard function plot of the TLZLx is shown in Figure 4.5. The hazard function of the TLZLx shows a decreasing and upside down bathtub shapes. Also shows bathtub shape.
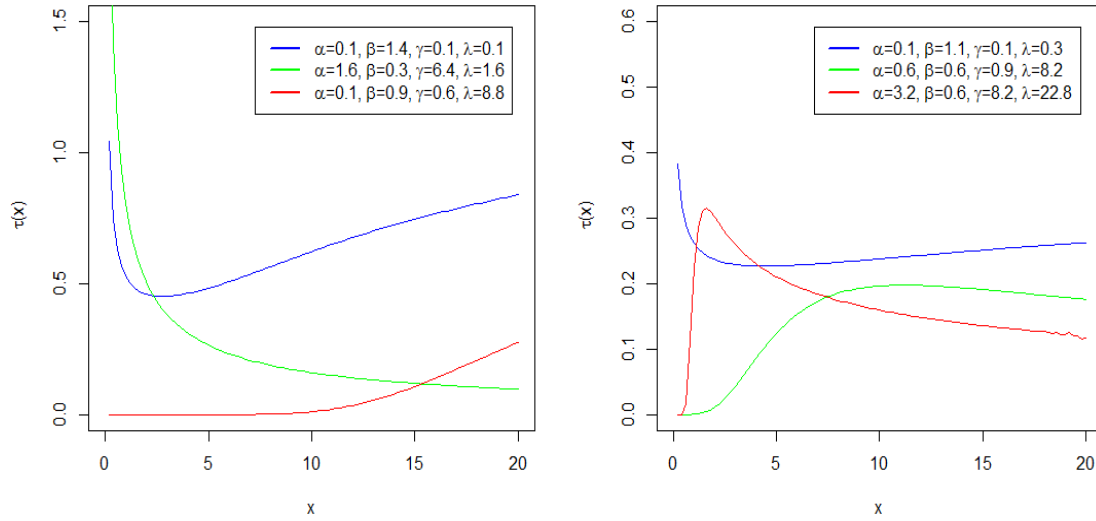


**Figure 4.5: The plot of TLZL Hazard function**

The quantile function of the TLZLx is,

$$
x_u = \frac{1}{\gamma} \left[ \left[ 1 - \sqrt{\frac{1}{\alpha} \log \left( e^\alpha - \left( (e^\alpha - 1)\left( 1 - u^{\frac{1}{\lambda}} \right)^{\frac{1}{2}} \right) \right)} \right]^{\frac{-1}{\beta}} - 1 \right], \ u \in [0,1].
\qquad (4.35)
$$

The Bowley's Skewness and Moors kurtosis of the TLZLx, are shown in Figure 4.6. It shows that $\alpha$ and $\lambda$ have a very sensitive effect on the distribution. For example given fixed values of $\beta = 0.08$ and $\gamma = 0.08$. The distribution is equally better in fitting different data.

51
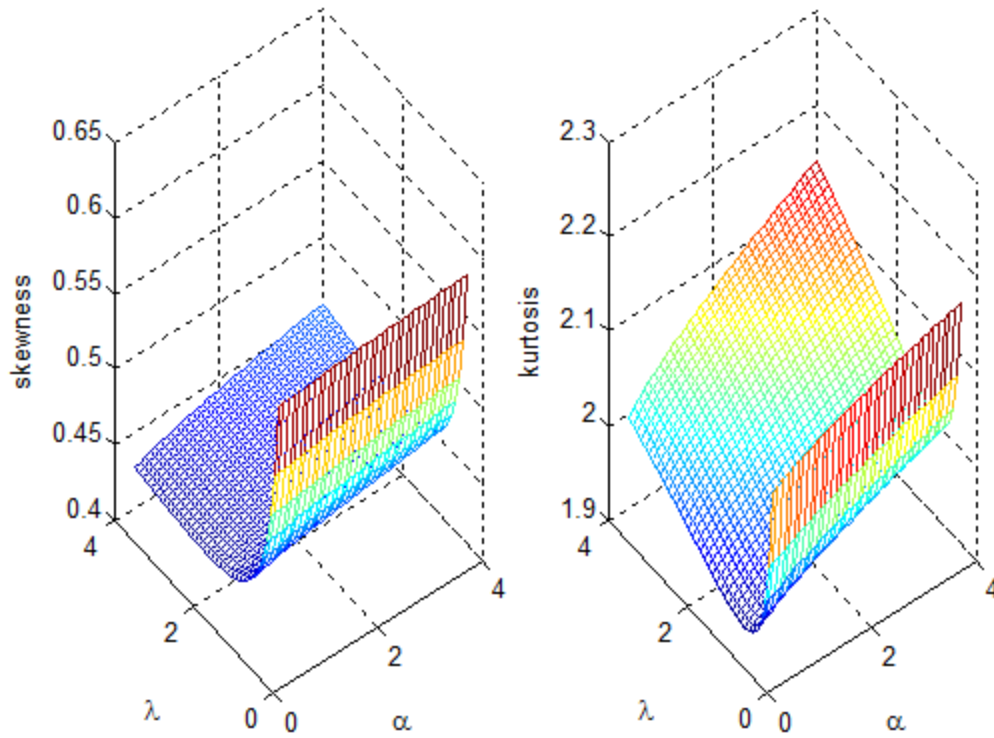
**Figure 4.6: Skewness and Kurtosis Plots**

The moment of TLZLx is derived by inserting the PDF and CDF of Lomax into the moment of TLZ-G family of distribution. The moment of TLZLx is,

$$\mu_r' = \frac{4\lambda\alpha\beta}{\gamma} \sum_{i=0}^{\infty} \sum_{j=0}^{2i} \sum_{k=0}^{j} \sum_{m=0}^{\infty} w_{ijkm} \int_0^{\infty} x^r (1+\tfrac{x}{\gamma})^{-\beta-1} (1-(1+\tfrac{x}{\gamma})^{-\beta})^{2m+1} dx, r=1,2,\ldots,\quad (4.36)$$

$$w_{ijkm} = \frac{(-1)^{i+j+k}\alpha^m \left[ e^{\alpha}(1+j-k)^m - (2+j-k)^m \right]}{(e^{\alpha}-1)^{2+j} m!} \binom{\lambda-1}{i}\binom{2i}{j}\binom{j}{k}.$$

The first six moments for some scenarios have been computed numerically. Different values of $\alpha$ and $\lambda$ are used where values of $\gamma = 1.5$ and $\beta = 3.5$ are fixed. The computation results indicate integration routines precision. This shows that with fixed $\alpha$ parameter, the addition of $\lambda$ creates a great impact on $\mu_r^{'}$. The impact is seen where the moment increases whiles $\lambda$ is increasing. The moment also increases with increasing $\alpha$. Table 4.2 represents first six moments of the TLZLx distribution for parameters.

**Table 4. 2: First six moments for some scenarios of $\alpha$ and $\lambda$, with fixed $\gamma$ =1.5 and $\beta$ =3.5**

| $\alpha$ | $\lambda$ | $\mu_1'$ | $\mu_2'$ | $\mu_3'$ | $\mu_4'$ | $\mu_5'$ | $\mu_6'$ |
|---|---|---|---|---|---|---|---|
| 0.5 | 0.5 | 0.3659 | 0.2941 | 0.4094 | 0.9456 | 3.8671 | 36.3075 |
|  | 1.0 | 0.5553 | 0.5240 | 0.7824 | 1.8625 | 7.7039 | 72.5735 |
|  | 2.0 | 0.7840 | 0.8866 | 1.4555 | 3.6283 | 15.2985 | 144.9909 |
|  | 3.0 | 0.9331 | 1.1767 | 2.0615 | 5.3223 | 22.8018 | 217.2679 |
|  | 4.0 | 1.0449 | 1.4234 | 2.6199 | 6.9592 | 30.2263 | 289.4165 |
| 1.0 | 0.5 | 0.4198 | 0.3759 | 0.5666 | 1.3828 | 5.8530 | 55.9400 |
|  | 1.0 | 0.6344 | 0.6661 | 1.0784 | 2.7176 | 11.6509 | 111.7989 |
|  | 2.0 | 0.8903 | 1.1185 | 1.9938 | 5.2749 | 23.1040 | 223.2939 |
|  | 3.0 | 1.0553 | 1.4765 | 2.8109 | 7.7159 | 34.3949 | 334.5190 |
|  | 4.0 | 1.1783 | 1.7788 | 3.5595 | 10.0655 | 45.5475 | 445.4999 |
| 2.0 | 0.5 | 0.5430 | 0.5841 | 1.0024 | 2.6765 | 12.0014 | 118.3115 |
|  | 1.0 | 0.8089 | 1.0196 | 1.8882 | 5.2318 | 23.8426 | 236.3592 |
|  | 2.0 | 1.1159 | 1.6790 | 3.4402 | 10.0716 | 47.1261 | 471.7477 |
|  | 3.0 | 1.3093 | 2.1891 | 4.8007 | 14.6400 | 69.9682 | 706.2994 |
|  | 4.0 | 1.4519 | 2.6139 | 6.0324 | 19.002 | 92.4437 | 940.1094 |
| 3.0 | 0.5 | 0.6793 | 0.8445 | 1.6023 | 4.5910 | 21.5716 | 218.3198 |
|  | 1.0 | 0.9924 | 1.4477 | 2.9827 | 8.9196 | 42.7577 | 435.9450 |
|  | 2.0 | 1.3420 | 2.3340 | 5.3500 | 17.0188 | 84.2042 | 869.3857 |
|  | 3.0 | 1.5582 | 3.0055 | 7.3903 | 24.5809 | 124.6606 | 1300.7360 |
|  | 4.0 | 1.7164 | 3.5585 | 9.2178 | 31.7471 | 164.3163 | 1730.2750 |
| 4.0 | 0.5 | 0.8195 | 1.1426 | 2.3484 | 7.1252 | 34.8146 | 360.4820 |
|  | 1.0 | 1.1722 | 1.9224 | 4.3187 | 13.7560 | 68.8391 | 719.4373 |
|  | 2.0 | 1.5547 | 3.0380 | 7.6319 | 26.0199 | 135.0658 | 1433.4800 |
|  | 3.0 | 1.7886 | 3.8692 | 10.4465 | 37.3595 | 199.4022 | 2143.1630 |
|  | 4.0 | 1.9593 | 4.5486 | 12.9464 | 48.0374 | 262.2483 | 2849.1430 |

### 4.6.3 Topp-Leone Zubair Weibull (TLZW)

The CDF and PDF of Weibull are defined respectively as: $G(x) = 1 - e^{-\gamma x^\beta}, x > 0, \beta > 0$

and $g(x) = \beta\gamma x^{\beta-1} e^{-\gamma x}, x > 0$. Substituting the Weibull CDF into that of TLZ-G CDF gives,

$$F(x) = \left[ 1 - \left( \frac{e^\alpha - e^{\alpha\left(1 - e^{-\gamma x^\beta}\right)^2}}{e^\alpha - 1} \right)^2 \right]^\lambda, x > 0,$$  (4.37)

where $\alpha > 0$, $\gamma > 0$ are scale parameters and $\beta > 0$, $\lambda > 0$ are shape parameters.

Differentiating the CDF of TLZW gives PDF,

$$f(x) = \frac{4\lambda\alpha\beta\gamma x^{\beta-1} e^{-\gamma x^\beta}(1 - e^{-\gamma x^\beta})(e^\alpha - e^{\alpha(1-e^{-\gamma x^\beta})^2})}{(e^\alpha - 1)^2} \left[ 1 - \left( \frac{e^\alpha - e^{\alpha(1-e^{-\gamma x^\beta})^2})}{e^\alpha - 1} \right)^2 \right]^{\lambda-1}, x > 0$$  (4.38)

The plots of the TLZW PDF with some selected parameters are shown in Figure 4.7. The TLZW PDF shows a right skewed, symmetric and unimodal. Implying that the distribution can model different data.
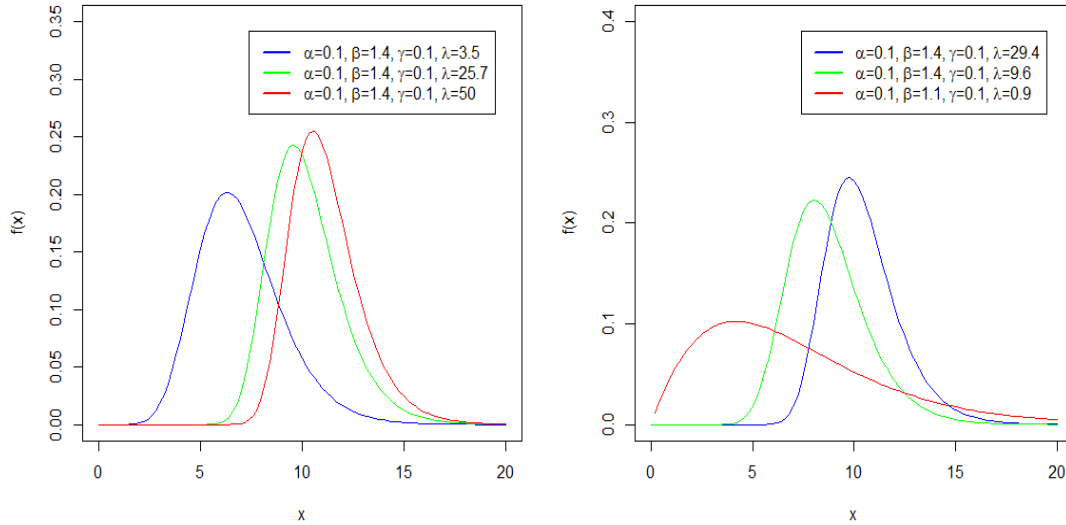


**Figure 4.7: Plot of the TLZW PDF**

The hazard function of the TLZW is given by;

$$\tau(x) = \frac{4\lambda\alpha\beta\gamma x^{\beta-1}e^{-\gamma x^{\beta}}(1-e^{-\gamma x^{\beta}})(e^{\alpha}-e^{\alpha(1-e^{-\gamma x^{\beta}})^2})\left[1-\left(\frac{e^{\alpha}-e^{\alpha(1-e^{-\gamma x^{\beta}})^2}}{e^{\alpha}-1}\right)^2\right]^{\lambda-1}}{(e^{\alpha}-1)^2\left[1-\left[1-\left(\frac{e^{\alpha}-e^{\alpha\left(1-e^{-\gamma x^{\beta}}\right)^2}}{e^{\alpha}-1}\right)^2\right]^{\lambda}\right]}, x>0 \qquad (4.39)$$

56

The plot of the TLZW hazard function with some selected parameters is shown in Figure 4.8. The hazard function is capable of showing both bathtub shape and also upside down bathtub shape. The distribution can model monotonic and non monotonic failure rate realized in lifetime data.
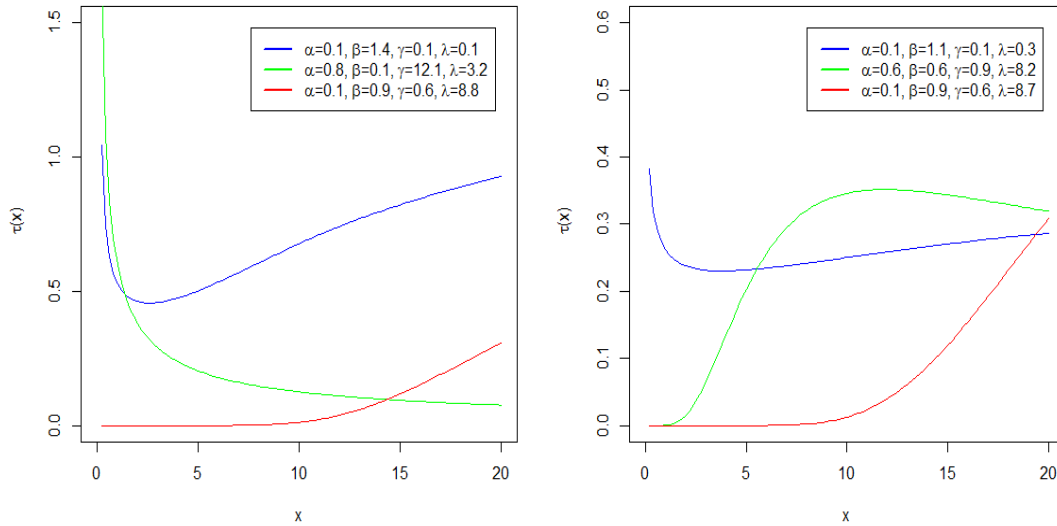


**Figure 4.8: Plot of the TLZW Hazard function**

The quantile function of the TLZW is given as;

$$x_u = \left[ \frac{-1}{\gamma} \log \left[ 1 - \sqrt{ \frac{1}{\alpha} \log \left( e^{\alpha} - (e^{\alpha} - 1)\left(1 - u^{\frac{1}{\lambda}}\right)^{\frac{1}{2}} \right) } \right] \right]^{\frac{1}{\beta}}, \; u \in [0,1]. \qquad (4.40)$$

57

The Bowleys Skewness and Moors Kurtosis plots of TLZW show sensitivity for parameters $\alpha$ and $\lambda$. This is seen below in Figure 4.9, where $\beta = 1.09$ and $\gamma = 0.03$ are fixed. The TLZW has the capacity to model different data.
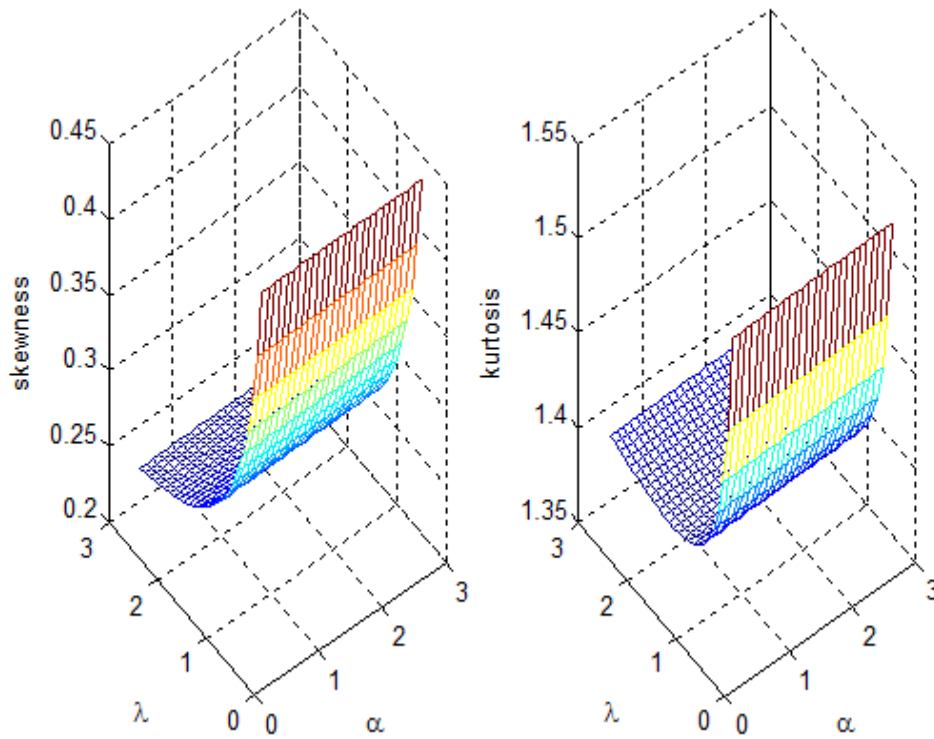


**Figure 4.9: Skewness and Kurtosis of TLZW**

The moment of TLZW is derived by inserting the PDF and CDF of Weibull into the moment of TLZ-G generated family of distribution. The moment of TLZW is,

$$\mu_r^{'} = 4\lambda\alpha\beta\gamma \sum_{i=0}^{\infty}\sum_{j=0}^{2i}\sum_{k=0}^{j}\sum_{m=0}^{\infty} w_{ijkm} \int_0^{\infty} x^{r+\beta-1} e^{-\gamma x}(1-e^{-\gamma x^{\beta}})^{2m+1} dx, r = 1,2,.... \quad (4.41)$$

$$w_{ijkm} = \frac{(-1)^{i+j+k}\alpha^m \left[ e^{\alpha}(1+j-k)^m - (2+j-k)^m \right]}{(e^{\alpha}-1)^{2+j} m!} \binom{\lambda-1}{i}\binom{2i}{j}\binom{j}{k}.$$

The first six moments of TLZW for some scenarios have been computed. In this case, different $\alpha$ and $\lambda$ values are used with fixed values of $\gamma = 0.5$ and $\beta = 1.5$. The computation results indicate integration routines precision. Based on this, it is seen that with fixed $\alpha$ parameter, the addition of $\lambda$ creates a great impact on $\mu_r^{'}$. In effect, the moment increases responsively with increasing $\lambda$ and increasing $\alpha$. Table 4.3 represents the first six moments of TLZW.

**Table 4. 3: First six moments for some scenarios of $\alpha$ and $\lambda$, with fixed $\gamma$ =0.5 and $\beta$ =1.5**

| $\alpha$ | $\lambda$ | $\mu_1'$ | $\mu_2'$ | $\mu_3'$ | $\mu_4'$ | $\mu_5'$ | $\mu_6'$ |
|---|---|---|---|---|---|---|---|
| 0.5 | 0.5 | 0.3964 | 0.7116 | 2.760 | 18.5298 | 192.2205 | 2868.5160 |
| | 1.0 | 8.5569 | 1.3600 | 5.4470 | 36.9108 | 384.0006 | 5735.2180 |
| | 2.0 | 1.0833 | 2.5213 | 10.6282 | 73.2611 | 766.2915 | 11463.2900 |
| | 3.0 | 1.3800 | 3.5530 | 15.5950 | 109.1099 | 1146.9670 | 17184.4100 |
| | 4.0 | 1.6168 | 4.4906 | 20.3822 | 144.5029 | 1526.1070 | 22898.7600 |
| 1.0 | 0.5 | 0.4872 | 0.9771 | 4.0216 | 27.8455 | 293.5058 | 4414.6660 |
| | 1.0 | 0.8263 | 1.8558 | 7.9108 | 55.4028 | 586.1002 | 8825.400 |
| | 2.0 | 1.3045 | 3.4080 | 15.3580 | 109.7302 | 1168.6850 | 17635.3600 |
| | 3.0 | 1.6484 | 4.7680 | 22.4406 | 163.1117 | 1747.9880 | 26430.4300 |
| | 4.0 | 1.9198 | 5.9915 | 29.2230 | 215.6464 | 2324.2040 | 35211.1000 |
| 2.0 | 0.5 | 0.7060 | 1.6977 | 7.7054 | 56.2733 | 610.1946 | 9311.9350 |
| | 1.0 | 1.1713 | 3.1779 | 15.0495 | 111.6344 | 1217.180 | 18608.9100 |
| | 2.0 | 1.7980 | 5.7111 | 28.8757 | 219.9457 | 2422.1730 | 37159.6400 |
| | 3.0 | 2.2323 | 7.8662 | 41.7943 | 325.4543 | 3616.1020 | 55655.2500 |
| | 4.0 | 2.5675 | 9.7656 | 53.9971 | 428.5336 | 4799.8640 | 74098.3500 |
| 3.0 | 0.5 | 0.9626 | 2.6638 | 13.0646 | 99.7115 | 1108.0080 | 17130.5500 |
| | 1.0 | 1.5565 | 4.9047 | 25.3053 | 197.0915 | 2207.0950 | 34216.8300 |
| | 2.0 | 2.3195 | 8.6151 | 47.9250 | 385.9173 | 4380.9260 | 68263.5100 |
| | 3.0 | 2.8310 | 11.683 | 68.6776 | 568.0883 | 6525.5020 | 102152.3000 |
| | 4.0 | 3.2190 | 14.3380 | 88.0192 | 744.6823 | 8643.8540 | 135893.2000 |
| 4.0 | 0.5 | 1.2393 | 3.8338 | 20.0324 | 158.7124 | 1801.997 | 28191.7400 |
| | 1.0 | 1.9519 | 6.9396 | 38.4586 | 312.4472 | 3583.6000 | 56276.8700 |
| | 2.0 | 2.8296 | 11.9247 | 71.8823 | 607.7392 | 7092.6220 | 112149.3000 |
| | 3.0 | 3.4031 | 15.9458 | 102.0254 | 889.8534 | 10538.1700 | 167654.5000 |
| | 4.0 | 3.8331 | 19.3735 | 129.7842 | 1161.269 | 13928.1800 | 222821.8000 |

### 4.6.4 Topp-Leone Zubair Kumaraswamy (TLZKw)

The Kumaraswamy distribution is defined on $0 \le x \le 1$. The PDF and CDF are respectively gives $g(x) = \gamma\beta x^{\gamma-1}(1-x^{\gamma})^{\beta-1}$ , $\gamma > 0, \beta > 0$ and $G(x) = 1-(1-x^{\gamma})^{\beta}$. Substituting the CDF of Kumaraswamy into the CDF of TLZ-G , we obtain the CDF of TLZKw as;

$$F(x) = \left[1 - \left(\frac{e^{\alpha} - e^{\alpha(1-(1-x^{\gamma})^{\beta})^2}}{e^{\alpha}-1}\right)^2\right]^{\lambda}, \ 0 \le x \le 1 \ , \qquad (4.42)$$

where $\beta > 0$, $\gamma > 0$ and $\lambda > 0$ are shape parameters and $\alpha > 0$ is a scale parameter.

The PDF of the TLZKw is;

$$f(x) = \frac{4\lambda\alpha\gamma\beta x^{\gamma-1}(1-x^{\gamma})^{\beta-1}(1-(1-x^{\gamma})^{\beta})(e^{\alpha(1-(1-x^{\gamma})^{\beta})^2})(e^{\alpha} - e^{\alpha(1-(1-x^{\gamma})^{\beta})^2})}{(e^{\alpha}-1)^2\left[1 - \left(\frac{e^{\alpha} - e^{\alpha(1-(1-x^{\gamma})^{\beta})^2}}{e^{\alpha}-1}\right)^2\right]^{1-\lambda}},$$

$$0 \le x \le 1 . \qquad (4.43)$$

The plots of the TLZKw PDF with some selected parameters are shown in Figure 4.10. The TLZKw PDF shows a right skewed, symmetric and unimodal shapes making it suitable for modeling different data.
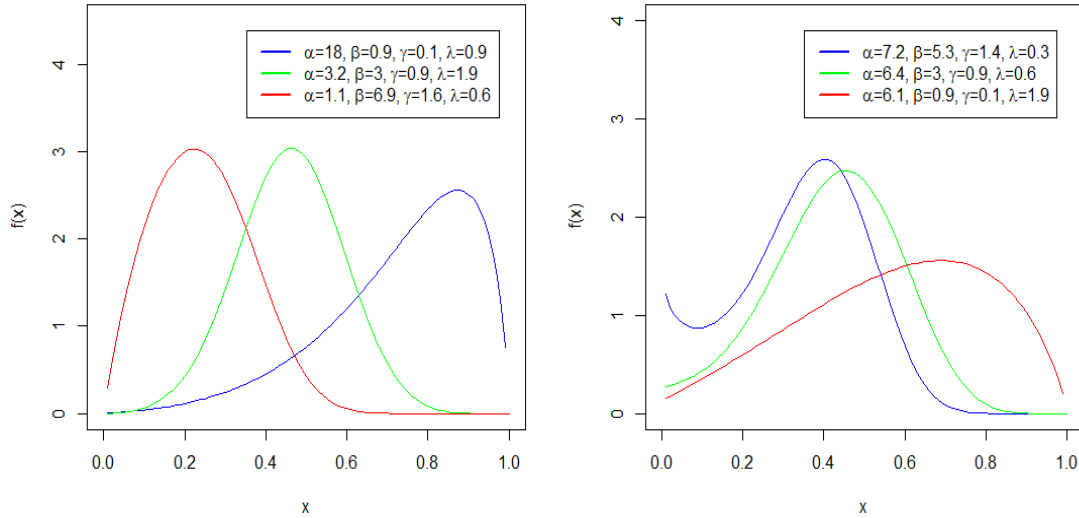
**Figure 4.10: The plot of TLZKw PDF**

The hazard function of the TLZKw is given as,

$$\tau(x) = \frac{4\lambda\alpha\gamma\beta x^{\gamma-1}(1-x^{\gamma})^{\beta-1}(1-(1-x^{\gamma})^{\beta})(e^{\alpha(1-(1-x^{\gamma})^{\beta})^2})(e^{\alpha}-e^{\alpha(1-(1-x^{\gamma})^{\beta})^2})}{(e^{\alpha}-1)^2\left[1-\left(\dfrac{e^{\alpha}-e^{\alpha(1-(1-x^{\gamma})^{\beta})^2})}{e^{\alpha}-1}\right)^2\right]^{1-\lambda}\left(1-\left[1-\left(\dfrac{e^{\alpha}-e^{\alpha(1-(1-x^{\gamma})^{\beta})^2})}{e^{\alpha}-1}\right)^2\right]^{\lambda}\right)},$$

$$0 \le x \le 1. \tag{4.44}$$

The plot of the TLZKw hazard function with some selected parameters is shown in Figure 4.11.

The hazard function shows both bathtub shape and modified upside down bathtub shape.
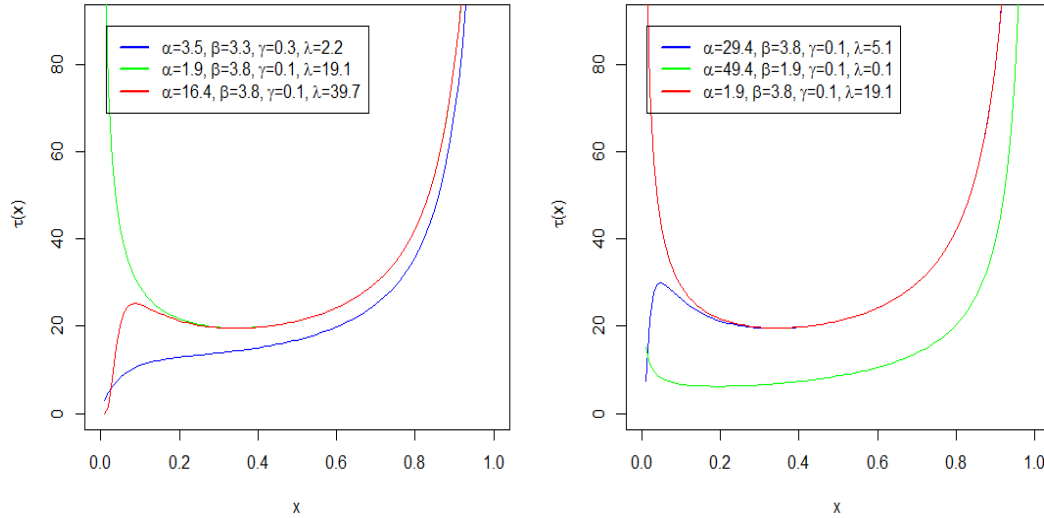


**Figure 4.11: The plot of TLZKw Hazard function**

The quantile function of the TLZKw is,

$$x_u = \left(1 - \left(1 - \sqrt{\left(\frac{1}{\alpha}\ln\left(e^\alpha - (e^\alpha - 1)\left(1 - u^{\frac{1}{\lambda}}\right)^{\frac{1}{2}}\right)\right)}\right)^{\frac{1}{\beta}}\right)^{\frac{1}{\gamma}}, u \in [0,1]. \qquad (4.45)$$

63

The Bowley's Skewness and Moors Kurtosis plots of the TLZKw are shown in Figure 4.12. The plot shows sensitivity of the parameters $\alpha$ and $\lambda$, where $\beta = 1.75$ and $\gamma = 0.03$ are fixed. The new parameters $\alpha$ and $\lambda$ introduced into the Weibull through TLZW makes it better for modeling different data.
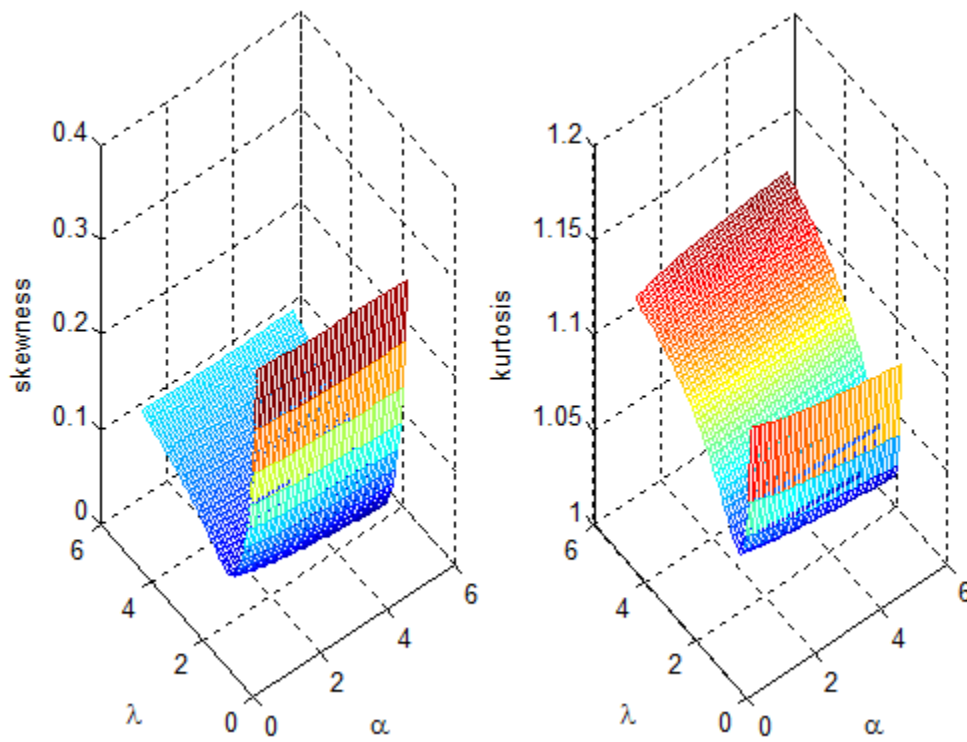


**Figure 4.12: Skewness and Kurtosis plot for TLZKw**

The moment of TLZKw is derived by inserting the PDF and CDF of Lomax into the moment of Topp-Leone Zubair generated family of distribution. The moment of TLZKw is,

$$\mu_r' = 4\lambda\alpha\gamma\beta \sum_{i=0}^{\infty} \sum_{j=0}^{2i} \sum_{k=0}^{j} \sum_{m=0}^{\infty} w_{ijkm} \int_0^{\infty} x^{r+\gamma-1}(1-x^\gamma)^{\beta-1}(1-(1-x^\gamma)^\beta)^{2m+1} dx, r = 1, 2, \dots . \quad (4.46)$$

where, $w_{ijkm} = \dfrac{(-1)^{i+j+k}\alpha^m \left[ e^\alpha(1+j-k)^m - (2+j-k)^m \right]}{(e^\alpha-1)^{2+j}m!} \begin{pmatrix} \lambda-1 \\ i \end{pmatrix} \begin{pmatrix} 2i \\ j \end{pmatrix} \begin{pmatrix} j \\ k \end{pmatrix}.$

Using some scenarios, the first six moments of TLZKw have been arrived at. In doing this, values of $\alpha$ and $\lambda$ are used with fixed values of $\gamma = \mathbf{0.5}$ and $\beta = \mathbf{1.5}$ . The computation results indicate integration routines precision. When $\lambda$ is introduced and increasing, of a fixed $\alpha$, we can see the moment $\mu_r'$ also increasing. In the same way, if $\alpha$ is increasing with fixed $\lambda$, the moment increases. Table 4.4, presents the first six moments of TLZKw.

**Table 4. 4: First six moments for some scenarios of $\alpha$ and $\lambda$, with fixed $\gamma$ =0.5 and $\beta$ =1.5**

| $\alpha$ | $\lambda$ | $\mu_1'$ | $\mu_2'$ | $\mu_3'$ | $\mu_4'$ | $\mu_5'$ | $\mu_6'$ |
|---|---|---|---|---|---|---|---|
| 0.5 | 0.5 | 0.1547 | 0.0545 | 0.0257 | 0.0142 | 0.0087 | 0.0057 |
|  | 1.0 | 0.2446 | 0.0967 | 0.0479 | 0.0271 | 0.0168 | 0.0110 |
|  | 2.0 | 0.3506 | 0.1591 | 0.0844 | 0.0497 | 0.0316 | 0.0212 |
|  | 3.0 | 0.4144 | 0.2048 | 0.1139 | 0.0691 | 0.0447 | 0.0304 |
|  | 4.0 | 0.4585 | 0.2403 | 0.1387 | 0.0862 | 0.0567 | 0.0391 |
| 1.0 | 0.5 | 0.1793 | 0.0682 | 0.0337 | 0.0192 | 0.0119 | 0.0079 |
|  | 1.0 | 0.2793 | 0.1190 | 0.0618 | 0.0362 | 0.0229 | 0.0154 |
|  | 2.0 | 0.3929 | 0.1919 | 0.1070 | 0.0653 | 0.0425 | 0.0292 |
|  | 3.0 | 0.4589 | 0.2433 | 0.1424 | 0.0897 | 0.0597 | 0.0416 |
|  | 4.0 | 0.5035 | 0.2824 | 0.1715 | 0.1107 | 0.0750 | 0.0529 |
| 2.0 | 0.5 | 0.2336 | 0.1006 | 0.0535 | 0.0321 | 0.0208 | 0.0143 |
|  | 1.0 | 0.3518 | 0.1699 | 0.0956 | 0.0592 | 0.0392 | 0.0272 |
|  | 2.0 | 0.4747 | 0.2618 | 0.1587 | 0.1030 | 0.0703 | 0.0500 |
|  | 3.0 | 0.5409 | 0.3217 | 0.2049 | 0.1376 | 0.0962 | 0.0697 |
|  | 4.0 | 0.5839 | 0.3652 | 0.2410 | 0.1660 | 0.1184 | 0.0869 |
| 3.0 | 0.5 | 0.2908 | 0.1379 | 0.0778 | 0.0486 | 0.0324 | 0.0227 |
|  | 1.0 | 0.4215 | 0.2246 | 0.1346 | 0.0872 | 0.0596 | 0.0426 |
|  | 2.0 | 0.5459 | 0.3301 | 0.2139 | 0.1459 | 0.1035 | 0.0759 |
|  | 3.0 | 0.6085 | 0.3943 | 0.2680 | 0.1893 | 0.1379 | 0.1032 |
|  | 4.0 | 0.6478 | 0.4389 | 0.3085 | 0.2235 | 0.1662 | 0.1263 |
| 4.0 | 0.5 | 0.3467 | 0.1772 | 0.1047 | 0.0675 | 0.0462 | 0.0329 |
|  | 1.0 | 0.4837 | 0.2779 | 0.1753 | 0.1178 | 0.0829 | 0.0605 |
|  | 2.0 | 0.6036 | 0.3912 | 0.2669 | 0.1895 | 0.1388 | 0.1044 |
|  | 3.0 | 0.6611 | 0.4563 | 0.3260 | 0.2397 | 0.1805 | 0.1388 |
|  | 4.0 | 0.6963 | 0.5001 | 0.3685 | 0.2777 | 0.2134 | 0.1669 |

### 4.6.5 Topp-Leone Zubair Inverse Weibull (TLZIW)

Inverse Weibull distributions has PDF and CDF, respectively defined as

$g(x) = \frac{\beta\gamma}{x^{\gamma+1}} e^{-\beta/x^{\gamma}}$ $\gamma > 0,\ \beta > 0, x > 0$   and  $G(x) = e^{-\beta/x^{\gamma}}$   $x > 0$ . Combining the CDF of

the Weibull and the CDF of the TLZ-G by means of substitution and then simplifying,

we obtain the CDF of  TLZIW as;

$$F(x) = \left[ 1 - \left( \frac{e^{\alpha} - e^{\alpha(e^{-\beta/x^{\gamma}})^2}}{e^{\alpha} - 1} \right)^2 \right]^{\lambda}, x > 0, \tag{4.47}$$

where $\beta > 0$, $\gamma > 0$ and $\lambda > 0$ are shape parameters and $\alpha > 0$ is a scale parameter.

The PDF  of the TLZIW is;

$$f(x) = 4\lambda\alpha\beta\gamma x^{-(\gamma+1)} (e^{\alpha}-1)^{-2} \left(e^{-\beta/x^{\gamma}}\right)^2 \left(e^{\alpha(e^{-\beta/x^{\gamma}})^2}\right)\left(e^{\alpha} - e^{\alpha(e^{-\beta/x^{\gamma}})^2}\right) \left[ 1 - \left( \frac{e^{\alpha} - e^{\alpha(e^{-\beta/x^{\gamma}})^2}}{e^{\alpha} - 1} \right)^2 \right]^{\lambda-1},\tag{4.48}$$

$$x > 0.$$

The plots of the TLZIW PDF with some selected parameters are shown in Figure 4.13. The TLZIW PDF shows a right skewed, symmetric and unimodal shapes. The distribution can model variaties of data.
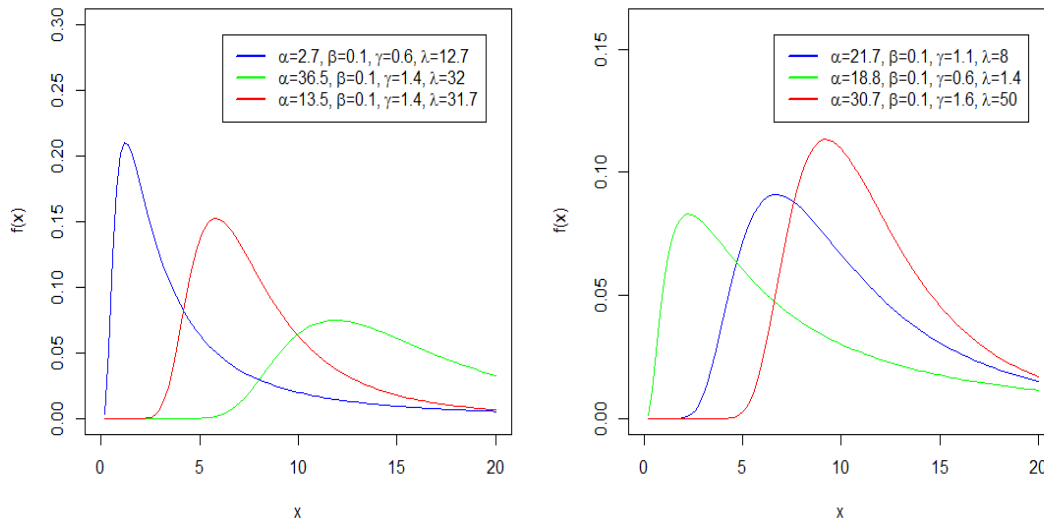
**Figure 4.13: PDF plot of TLZIW**

The hazard function of the TLZIW is,

$$\tau(x,\phi)=\frac{4\lambda\alpha\beta\gamma x^{-(\gamma+1)}(e^{\alpha}-1)^{-2}\left(e^{-\beta/x^{\gamma}}\right)^{2}\left(e^{\alpha(e^{-\beta/x^{\gamma}})^{2}}\right)\left(e^{\alpha}-e^{\alpha(e^{-\beta/x^{\gamma}})^{2}}\right)\left[1-\left(\dfrac{e^{\alpha}-e^{\alpha(e^{-\beta/x^{\gamma}})^{2}}}{e^{\alpha}-1}\right)^{2}\right]^{\lambda-1}}{1-\left[1-\left(\dfrac{e^{\alpha}-e^{\alpha(e^{-\beta/x^{\gamma}})^{2}}}{e^{\alpha}-1}\right)^{2}\right]^{\lambda}},$$

(4.49)

$$x>0.$$

The plot of the TLZIW hazard function with some selected parameters is shown in Figure 4.14. The hazard function depicts both bathtub shape and also upside down bathtub shape.
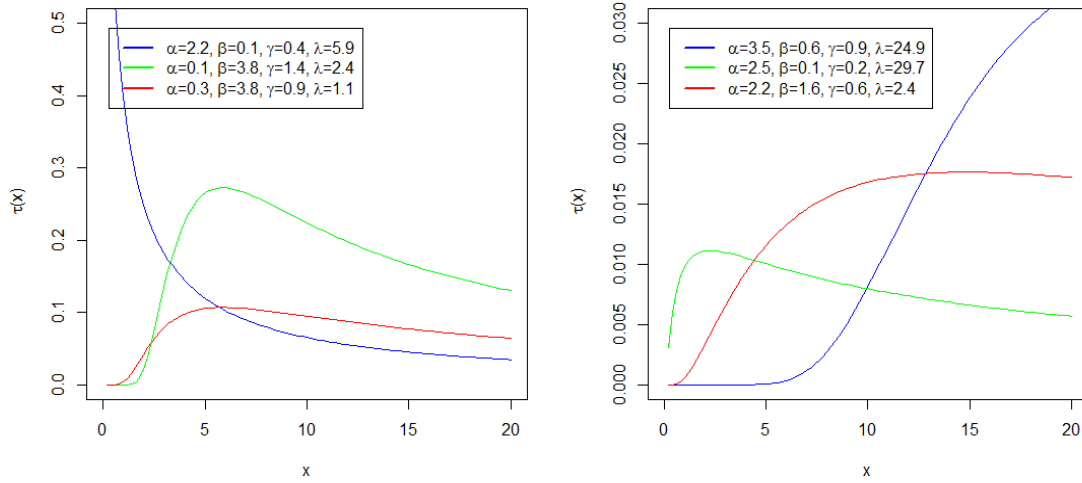


**Figure 4.14: Hazard plot of TLZIW**

The quantile function of the TLZIW is given as;

$$x_u = \left( -\beta \left( \ln \sqrt{ \frac{1}{\alpha} \ln \left( e^\alpha - (e^\alpha - 1) \sqrt{ \left( 1 - u^{\frac{1}{\lambda}} \right) } \right) } \right)^{-1} \right)^{\frac{1}{\gamma}} , \; u \in [0,1].$$

$$(4.50)$$

The Bowley's Skewness and Moor's Kurtosis of TLZIW are shown in Figure 4.15. The plots show that $\alpha$ and $\lambda$ are sensitive parameters of the distribution where the values $\beta = 43.9$ and $\gamma = 10.07$ are fixed. This means that TLZIW is good for modeling different data.
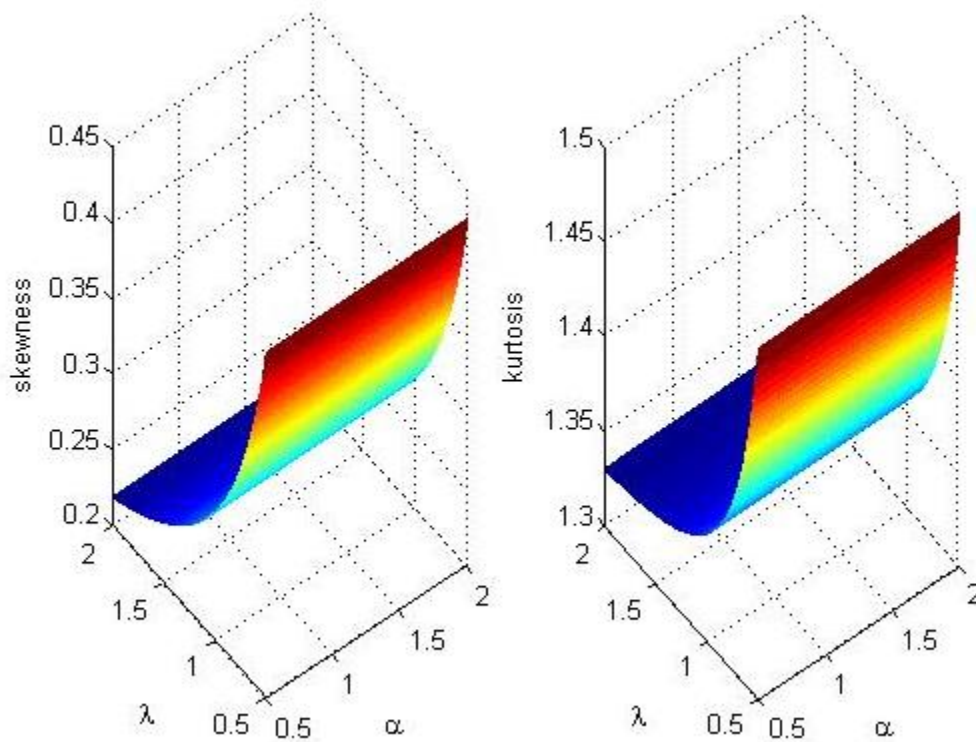


**Figure 4.15: Skewness and kurtosis of TLZIW**

The moment of TLZIW is derived by inserting the PDF and CDF of Inverse Weibull into the moment of TLZ-G family of distribution. The moment of TLZIW is,

$$\mu_r^{'} = 4\lambda\alpha\beta\gamma \sum_{i=0}^{\infty}\sum_{j=0}^{2i}\sum_{k=0}^{j}\sum_{m=0}^{\infty} w_{ijkm} \int_0^{\infty} x^{r-\gamma-1} e^{-\beta/x^{\gamma}} (e^{-\beta/x^{\gamma}})^{2m+1} dx, r = 1, 2, \dots . \quad (4.51)$$

$$w_{ijkm} = \frac{(-1)^{i+j+k}\alpha^m \left[ e^{\alpha}(1+j-k)^m - (2+j-k)^m \right]}{(e^{\alpha}-1)^{2+j} m!} \binom{\lambda-1}{i}\binom{2i}{j}\binom{j}{k}.$$

The first six moments for some scenarios have been computed. In this case, different $\alpha$ and $\lambda$ values are used with fixed values of $\gamma = 3.5$ and $\beta = 2.5$ . The computation results indicate integration routines precision. Based on this, it is seen that with fixed $\alpha$ parameter, the addition of $\lambda$ creates a great impact on $\mu_r^{'}$. In effect, the moment increases with increasing $\lambda$ and increasing $\alpha$ . Table 4.5 presents the first six moments of TLZIW.

**Table 4. 5: First six moments for some scenarios of $\alpha$ and $\lambda$, with fixed $\gamma$ =3.5 and $\beta$ =2.5**

| $\alpha$ | $\lambda$ | $\mu_1'$ | $\mu_2'$ | $\mu_3'$ | $\mu_4'$ | $\mu_5'$ | $\mu_6'$ |
|---|---|---|---|---|---|---|---|
| 1.0 | 1.0 | 1.7318 | 3.2486 | 6.7236 | 15.8383 | 45.2281 | 188.2232 |
| | 1.5 | 1.8813 | 3.8066 | 8.4319 | 21.0771 | 63.2823 | 274.1532 |
| | 2.0 | 1.9903 | 4.2424 | 9.8530 | 25.6911 | 80.0042 | 357.2204 |
| | 2.5 | 2.0766 | 4.6047 | 11.0897 | 29.8783 | 95.7626 | 438.1033 |
| | 3.0 | 2.1482 | 4.9171 | 12.1953 | 33.7486 | 110.7741 | 517.2235 |
| 1.5 | 1.0 | 1.8164 | 3.5882 | 7.8481 | 19.5941 | 59.4401 | 263.2192 |
| | 1.5 | 1.9783 | 4.2206 | 9.8821 | 26.1662 | 83.3678 | 383.8292 |
| | 2.0 | 2.0958 | 4.7137 | 11.5738 | 31.9577 | 105.5469 | 500.4814 |
| | 2.5 | 2.1886 | 5.1231 | 13.0454 | 37.2145 | 126.4563 | 614.1005 |
| | 3.0 | 2.2654 | 5.4757 | 14.3605 | 42.0738 | 146.3796 | 725.2658 |
| 2.0 | 1.0 | 1.9039 | 3.9523 | 9.1015 | 23.9538 | 76.6503 | 358.1094 |
| | 1.5 | 2.0772 | 4.6603 | 11.4875 | 32.0476 | 107.631 | 522.4585 |
| | 2.0 | 2.2025 | 5.2110 | 13.4698 | 39.1778 | 136.3485 | 681.4288 |
| | 2.5 | 2.3011 | 5.6673 | 15.1928 | 45.6478 | 163.4209 | 836.2707 |
| | 3.0 | 2.3825 | 6.0601 | 16.7319 | 51.6273 | 189.2156 | 987.7707 |
| 2.5 | 1.0 | 1.9925 | 4.3342 | 10.4651 | 28.8816 | 96.8837 | 474.2394 |
| | 1.5 | 2.1759 | 5.1168 | 13.2220 | 38.6657 | 136.0838 | 691.9368 |
| | 2.0 | 2.3081 | 5.7240 | 15.5092 | 47.2784 | 172.4064 | 902.4772 |
| | 2.5 | 2.4118 | 6.2264 | 17.4955 | 55.0899 | 206.6395 | 1107.5270 |
| | 3.0 | 2.4974 | 6.6585 | 19.2689 | 62.3069 | 239.251 | 1308.1350 |
| 3.0 | 1.0 | 2.0806 | 4.7269 | 11.9171 | 34.3219 | 120.0552 | 612.2431 |
| | 1.5 | 2.2729 | 5.5818 | 15.0572 | 45.9413 | 168.5887 | 893.1271 |
| | 2.0 | 2.4109 | 6.2437 | 17.6586 | 56.1601 | 213.5345 | 1164.7030 |
| | 2.5 | 2.5191 | 6.7908 | 19.9159 | 65.4236 | 255.8801 | 1429.1510 |
| | 3.0 | 2.6083 | 7.2609 | 21.9303 | 73.9792 | 296.2106 | 1687.8370 |

### 4.6.6 Topp-Leone Zubair Lomax Regression (TLZLx_R)

In survival analysis, there are many ways of coming up with a regression model. For instance, the location-scale frequency type of regression model is widely used in clinical trials.

In this type of presentation, the regression analysis of lifetimes are specified based on the distribution of lifetime, thus: $X$ with vector of covariates, given as $\psi = (\psi_1,...,\psi_P)^T$. The vector of covariates are therefore allowed to depend on the distribution parameters ( Furrukh et al. 2019). In this case the parameter $\gamma$ in TLZLx is allowed to depend on $\psi$, with a link function $\gamma = \exp(\psi_1^T \tau)$, $i = 1,...,n$ where $\tau = (\tau_1,...,\tau_p)^T$ is the regression coefficient vector. The TLZLx regression model has $\psi$ depended on by $\gamma$. This condition is essential in practical studies. Hence, the survival function for $X \mid \psi$ becomes;

$$S(X \mid \psi) = 1 - \left[ 1 - \left( \frac{e^\alpha - e^{\alpha\left(1 - (1+(\exp(\psi^T \tau))x)^{-\beta}\right)^2}}{e^\alpha - 1} \right)^2 \right]^\lambda , \quad x > 0$$

(4.52)

Equation (4.52) is termed as the TLZLx parametric regression model. The regression model can be used to fit several data types.

Taking that $(x_1,\psi_1),...,(x_n,\psi_n)$ is a sample of $n$ independent observations with a response variable $x_i$ making up for the observed lifetime or censoring for the i*th* member.

73

Let lifetime ($F$) and Censoring ($C$) be members of $x_i$. This means that conventional likelihood estimation procedure can be administered here. Thus; $\Theta = (\tau^T, \beta, \alpha, \lambda)^T$ as vector from model (4.52) has the form $l(\Theta) = \sum_{i \in F} l_i(\Theta) + \sum_{i \in C} l_i(\Theta)^{(c)}$ , where,

$l_i(\Theta) = \log(f(x_i \mid \psi_i))$, $l_i^{(c)}(\Theta) = \log(S(x_i \mid \psi_i))$ and $f(x_i \mid w_i)$, $S(x_i \mid \psi_i)$ are the density and survival of $X$ respectively. The log likelihood for $\Theta$ reduces to;

$$l(\Theta) = r\log\left(\frac{4\lambda\alpha}{(e^\alpha - 1)^2}\right) + \sum_{i \in F}^{n} \log(\beta(\exp(\psi_1^T\tau))(1 + (\exp(\psi_1^T\tau))x)^{-\beta-1}) + \sum_{i \in F}^{n} \log(1 - (1 + (\exp(\psi_1^T\tau))x)^{-\beta}) +$$

$$\sum_{i \in F}^{n} \log(e^{\alpha(1-(1+(\exp(\psi_1^T\tau))x)^{-\beta}2)}) + \sum_{i \in F}^{n} \log(e^\alpha - e^{\alpha(1-(1+(\exp(\psi_1^T\tau))x)^{-\beta}2)}) + (\lambda - 1)\sum_{i \in F}^{n}\log\left[1 - \left(\frac{e^\alpha - e^{\alpha(1-(1+(\exp(\psi_1^T\tau))x)^{-\beta}2)}}{e^\alpha - 1}\right)^2\right] +$$

$$\sum_{i \in C}\log\left\{1 - \left[1 - \left(\frac{e^\alpha - e^{\alpha\left(1-(1+(\exp(\psi^T\tau))x)^{-\beta}\right)^2}}{e^\alpha - 1}\right)^2\right]^\lambda\right\}.$$

$$(4.53)$$

## 4.7 Summary of Chapter four

The chapter four presented the theoretical results. In this case, the mixture representation, and other statistical properties of the TLZ generator family were developed. These statistical properties includes the quantile function of TLZ generator, moments, incomplete moments, moment generating function, inequality measures, mean and mean residual life , median deviations, stochastic order statistics and the maximum likelihood estimators. Six distributions were also developed and these include the TLZNH, TLZLx, TLZW, TLZKw , TLZIW and the TLZLx_R.

# CHAPTER FIVE

# SIMULATIONS AND APPLICATIONS

## 5.0 Introduction

This chapter presents results of objective four and five. These are results on Monte Carlo simulations and applications of the developed models to lifetime data.

## 5.1 Monte Carlo Simulation

Monte Carlo simulation is done to study the behavior of the estimators of the parameters under MLE.

In this case, all the five new distributions were studied. The R software was used in the process to enable the Average Bias (AB) and the Root Means Square Error (RMSE) to be computed.

First of all, simulation study was done on TLZNH using sample sizes as n= 25, 50, 75 and 100. In each case of sample size, the experiment was replicated 1000 times. Four different sets of parameter values were used, these are I: $\alpha = 0.1, \beta = 0.2,$ $\gamma = 0.1, \lambda = 0.2$ ,II: $\alpha = 0.2, \beta = 0.1, \gamma = 0.1, \lambda = 0.2$ III: $\alpha = 0.2, \beta = 0.1, \gamma = 5.4, \lambda = 0.3$ and IV: $\alpha = 0.4, \beta = 0.2, \gamma = 0.2, \lambda = 1.0$ . The set of parameters was to generate random samples from TLZNH. The result as displayed in Table 5.1 shows AB and the RMSE to be decreasing when sample size is increasing.

**Table 5. 1: Monte Carlo Simulation Result of TLZNH**

| | Actual Parameter | | | | | AB | | | | RMSE | | | |
|---|---|---|---|---|---|---|---|---|---|---|---|---|---|
| | $\alpha$ | $\beta$ | $\gamma$ | $\lambda$ | $n$ | $\hat{\alpha}$ | $\hat{\beta}$ | $\hat{\gamma}$ | $\hat{\lambda}$ | $\hat{\alpha}$ | $\hat{\beta}$ | $\hat{\gamma}$ | $\hat{\lambda}$ |
| I | 0.1 | 0.2 | 0.1 | 0.2 | 25 | 1.074 | 0.120 | 0.112 | 7.279 | 1.629 | 0.081 | 0.253 | 6.231 |
| | | | | | 50 | 0.292 | 0.060 | -0.036 | 5.399 | 0.854 | 0.060 | 0.133 | 5.367 |
| | | | | | 75 | 0.092 | 0.030 | -0.067 | 1.210 | 0.431 | 0.051 | 0.103 | 5.237 |
| | | | | | 100 | 0.038 | 0.031 | -0.078 | 0.496 | 0.232 | 0.045 | 0.082 | 3.896 |
| II | 0.2 | 0.1 | 0.1 | 0.2 | 25 | 1.269 | 0.012 | 0.328 | 2.844 | 1.667 | 0.034 | 0.399 | 9.641 |
| | | | | | 50 | 1.026 | 0.007 | 0.298 | 2.866 | 1.359 | 0.022 | 0.383 | 5.943 |
| | | | | | 75 | 0.854 | 0.004 | 0.270 | 2.817 | 1.151 | 0.017 | 0.366 | 5.800 |
| | | | | | 100 | 0.725 | 0.002 | 0.254 | 1.604 | 0.987 | 0.013 | 0.343 | 5.640 |
| III | 0.2 | 0.1 | 5.4 | 0.3 | 25 | 3.171 | 0.042 | 5.027 | 2.335 | 7.757 | 0.063 | 4.603 | 3.727 |
| | | | | | 50 | 2.571 | 0.017 | 4.891 | 2.374 | 5.863 | 0.042 | 3.169 | 3.321 |
| | | | | | 75 | 2.560 | 0.001 | 4.315 | 5.653 | 4.208 | 0.032 | 4.496 | 2.968 |
| | | | | | 100 | 2.135 | -0.003 | 0.529 | 3.946 | 3.552 | 0.029 | 3.486 | 1.880 |
| IV | 0.4 | 0.2 | 0.2 | 1.0 | 25 | 1.416 | 0.026 | 1.606 | 0.145 | 1.907 | 0.075 | 2.870 | 0.250 |
| | | | | | 50 | 0.773 | 0.002 | 4.784 | 0.044 | 2.421 | 0.065 | 9.286 | 0.203 |
| | | | | | 75 | 0.302 | -0.015 | 0.041 | -0.037 | 0.918 | 0.052 | 4.836 | 0.137 |
| | | | | | 100 | 0.062 | -0.023 | 1.412 | -0.070 | 0.400 | 0.042 | 2.311 | 0.097 |

Similarly, in the simulation study of TLZLx, sample sizes n= 25, 50, 75 and 100 were used alongside with four sets of parameter values such as **I**: $\alpha = 7.3, \beta = 1.2, \gamma = 1.4, \lambda = 1.1$ **II:** $\alpha = 4.3, \beta = 1.2, \gamma = 1.1, \lambda = 1.1$, **III**: $\alpha = 4.3, \beta = 1.2, \lambda = 3.1, \lambda = 1.1$ and **IV:** $\alpha = 7.2, \beta = 1.2, \gamma = 1.4, \lambda = 1.1$ . In each case of sample size and set of parameter values, the experiment was replicated 1000 times. The result show in Table 5.2 that both AB and RMSE decrease with increasing sample size.

**Table 5. 2: Monte Carlo Simulation Result of TLZLx**

| | Actual Parameter | | | | | AB | | | | RMSE | | | |
|---|---|---|---|---|---|---|---|---|---|---|---|---|---|
| | $\alpha$ | $\beta$ | $\gamma$ | $\lambda$ | $n$ | $\hat{\alpha}$ | $\hat{\beta}$ | $\hat{\gamma}$ | $\hat{\lambda}$ | $\hat{\alpha}$ | $\hat{\beta}$ | $\hat{\gamma}$ | $\hat{\lambda}$ |
| **I** | **7.3** | **1.2** | **1.4** | **1.1** | **25** | 6.080 | 0.104 | 2.490 | 9.579 | 10.768 | 1.145 | 7.13( | 7.681 |
| | | | | | **50** | 9.852 | -0.154 | 4.648 | 3.309 | 8.512 | 0.429 | 6.51 | 8.164 |
| | | | | | **75** | 6.721 | -0.235 | 4.860 | 1.514 | 7.767 | 0.349 | 5.80 | 7.283 |
| | | | | | **100** | 2.932 | -0.278 | 0.765 | 0.440 | 4.207 | 0.345 | 5.61( | 2.999 |
| **II** | **4.3** | **1.2** | **1.1** | **1.1** | **25** | 5.572 | 0.718 | 1.222 | 4.620 | 6.093 | 7.730 | 6.58 | 7.681 |
| | | | | | **50** | 8.590 | 0.005 | 0.750 | 6.652 | 9.816 | 1.388 | 2.48 | 4.464 |
| | | | | | **75** | 9.403 | -0.126 | 0.755 | 3.572 | 7.352 | 0.353 | 2.15 | 7.491 |
| | | | | | **100** | 1.575 | -0.158 | 0.645 | 2.931 | 1.172 | 0.299 | 1.93 | 2.151 |
| **III** | **4.3** | **1.2** | **3.1** | **1.1** | **25** | 7.530 | 0.613 | -0.791 | 3.674 | 6.823 | 7.188 | 7.36( | 5.578 |
| | | | | | **50** | 7.406 | -0.012 | -1.303 | 7.188 | 3.765 | 0.774 | 3.74 | 3.225 |
| | | | | | **75** | 3.172 | -0.100 | -1.411 | 1.916 | 8.235 | 0.329 | 3.92 | 3.412 |
| | | | | | **100** | 4.829 | -0.118 | -1.672 | 0.848 | 3.723 | 0.262 | 2.47 | 1.839 |
| **IV** | **7.2** | **1.2** | **1.4** | **1.1** | **25** | 6.444 | 0.096 | 2.332 | 9.497 | 8.915 | 0.798 | 5.01 | 6.342 |
| | | | | | **50** | 1.756 | -0.145 | 3.469 | 4.012 | 5.091 | 0.741 | 0.26 | 3.841 |
| | | | | | **75** | 1.885 | -0.253 | 1.518 | 3.104 | 5.004 | 0.337 | 1.52 | 4.932 |
| | | | | | **100** | 0.084 | -0.295 | 1.051 | 0.976 | 1.585 | 0.355 | 0.04 | 1.064 |

77

Simulation study was done for TLZW using sample sizes n= 25, 50, 75 and 100. The experiments, on each of the samples were replicated 1000 times. In such case, four parameter values were used, these are  **I**: $\alpha = 0.5,\ \beta = 0.3,\ \gamma = 2.2,\ \lambda = 0.3$ , **II**:  $\alpha = 0.1,$ $\beta = 0.11,$ $\gamma = 0.1,$ $\lambda = 0.6$ ,  **III**: $\alpha = 0.1,\ \beta = 0.5,\ \gamma = 0.3,\ \lambda = 0.1$ and  **IV**: $\alpha = 0.1, \beta = 0.5,\ \gamma = 0.4,\ \lambda = 0.4$ . Hence, random values were obtained from TLZW. The results in Table 5.3 shows AB and RMSE consistently decrease for some parameter values whiles others fluctuate with increasing sample size.

**Table 5. 3: Monte Carlo Simulation Result of TLZW**

| | Actual Parameter | | | | | AB | | | | RMSE | | | |
|---|---|---|---|---|---|---|---|---|---|---|---|---|---|
| | $\alpha$ | $\beta$ | $\gamma$ | $\lambda$ | $n$ | $\hat{\alpha}$ | $\hat{\beta}$ | $\hat{\gamma}$ | $\hat{\lambda}$ | $\hat{\alpha}$ | $\hat{\beta}$ | $\hat{\gamma}$ | $\hat{\lambda}$ |
| I | 0.5 | 0.3 | 2.2 | 0.3 | 25 | 2.512 | -0.084 | -1.623 | 0.640 | 3.689 | 3.689 | 1.721 | 0.813 |
| | | | | | 50 | 2.244 | -0.087 | -1.703 | 0.594 | 3.272 | 3.272 | 2.723 | 0.770 |
| | | | | | 75 | 2.246 | -0.091 | -1.725 | 0.600 | 3.259 | 3.959 | 1.235 | 0.773 |
| | | | | | 100 | 1.999 | -0.096 | -1.744 | 0.543 | 2.830 | 2.830 | 0.750 | 0.709 |
| II | 0.1 | 0.11 | 0.1 | 0.6 | 25 | 0.935 | -0.021 | -0.165 | 0.384 | 1.227 | 0.059 | 0.312 | 0.902 |
| | | | | | 50 | 0.517 | -0.046 | -0.250 | 0.615 | 1.226 | 0.058 | 0.305 | 0.676 |
| | | | | | 75 | 0.211 | -0.058 | -0.283 | 0.881 | 1.162 | 0.041 | 0.299 | 0.628 |
| | | | | | 100 | 0.123 | -0.087 | -0.297 | 0.963 | 1.131 | 0.013 | 0.127 | 0.365 |
| III | 0.1 | 0.5 | 0.3 | 0.1 | 25 | 0.718 | -0.282 | 0.238 | 0.764 | 0.910 | 0.299 | 0.461 | 0.858 |
| | | | | | 50 | 0.741 | -0.275 | 0.136 | 0.693 | 0.909 | 0.291 | 0.277 | 0.779 |
| | | | | | 75 | 0.691 | -0.249 | 0.058 | 0.599 | 0.888 | 0.270 | 0.196 | 0.704 |
| | | | | | 100 | 0.606 | -0.229 | 0.018 | 0.525 | 0.834 | 0.253 | 0.173 | 0.646 |
| IV | 0.1 | 0.5 | 0.4 | 0.4 | 25 | 0.786 | -0.011 | 0.196 | 0.236 | 1.024 | 0.194 | 0.454 | 0.397 |
| | | | | | 50 | 0.742 | -0.037 | 0.138 | 0.214 | 0.907 | 0.140 | 0.288 | 0.332 |
| | | | | | 75 | 0.782 | -0.044 | 0.125 | 0.216 | 0.933 | 0.127 | 0.248 | 0.315 |
| | | | | | 100 | 0.750 | -0.044 | 0.108 | 0.204 | 0.887 | 0.115 | 0.219 | 0.296 |

Simulation results for TLZKw is shown in Table 5.4, the parameter values **I:** $\alpha = 0.2, \beta = 0.3,\ \gamma = 0.2, \lambda = 0.5,$ **II:** $\alpha = 0.1, \beta = 0.3,\ \gamma = 0.2, \lambda = 0.5$ **III:** $\alpha = 0.2,$ $\beta = 0.3,\ \ \gamma = 0.2, \lambda = 0.1$, and **IV:** $\alpha = 0.1,\ \beta = 0.2, \gamma = 0.4, \lambda = 0.3$ were used with samples sizes n= 25, 50, 75 and 100. In each case of sample size, the experiment was replicated 1000 times to obtain random samples from TLZKw. The results indicate AB and RMSE to be consistently decreasing when sample size is increasing.

**Table 5. 4: Monte Carlo Simulation Result of TLZKw**

| | **Actual Parameter** | | | | | **AB** | | | | **RMSE** | | | |
|---|---|---|---|---|---|---|---|---|---|---|---|---|---|
| | $\alpha$ | $\beta$ | $\gamma$ | $\lambda$ | $n$ | $\hat{\alpha}$ | $\hat{\beta}$ | $\hat{\gamma}$ | $\hat{\lambda}$ | $\hat{\alpha}$ | $\hat{\beta}$ | $\hat{\gamma}$ | $\hat{\lambda}$ |
| **I** | 0.2 | 0.3 | 0.2 | 0.5 | 25 | 2.349 | 0.181 | 0.367 | -0.203 | 2.877 | 0.242 | 0.787 | 0.287 |
| | | | | | 50 | 1.805 | 0.132 | 0.326 | -0.217 | 2.203 | 0.174 | 0.577 | 0.270 |
| | | | | | 75 | 1.502 | 0.106 | 0.310 | -0.229 | 1.851 | 0.137 | 0.518 | 0.268 |
| | | | | | 100 | 1.220 | 0.087 | 0.319 | -0.237 | 1.532 | 0.116 | 0.509 | 0.271 |
| **II** | 0.1 | 0.3 | 0.2 | 0.5 | 25 | 2.476 | 0.194 | 0.328 | -0.199 | 3.003 | 0.259 | 0.650 | 0.286 |
| | | | | | 50 | 1.827 | 0.137 | 0.335 | -0.216 | 2.173 | 0.176 | 0.657 | 0.270 |
| | | | | | 75 | 1.461 | 0.107 | 0.310 | -0.223 | 1.788 | 0.139 | 0.533 | 0.265 |
| | | | | | 100 | 1.297 | 0.093 | 0.297 | -0.229 | 1.585 | 0.119 | 0.506 | 0.262 |
| **III** | 0.2 | 0.3 | 0.2 | 0.1 | 25 | 2.002 | 0.335 | 0.095 | -0.009 | 2.475 | 0.429 | 0.217 | 0.041 |
| | | | | | 50 | 1.325 | 0.245 | 0.061 | -0.001 | 1.689 | 0.305 | 0.152 | 0.038 |
| | | | | | 75 | 1.047 | 0.203 | 0.032 | 0.007 | 1.388 | 0.252 | 0.102 | 0.035 |
| | | | | | 100 | 0.853 | 0.166 | 0.013 | 0.015 | 1.185 | 0.210 | 0.079 | 0.036 |
| **IV** | 0.1 | 0.2 | 0.4 | 0.3 | 25 | 2.267 | 0.149 | 0.075 | 0.038 | 2.772 | 0.195 | 0.636 | 0.229 |
| | | | | | 50 | 1.480 | 0.099 | 0.064 | 0.015 | 1.824 | 0.126 | 0.539 | 0.177 |
| | | | | | 75 | 1.249 | 0.083 | 0.029 | 0.017 | 1.529 | 0.104 | 0.372 | 0.149 |
| | | | | | 100 | 1.084 | 0.073 | 0.010 | 0.018 | 1.354 | 0.090 | 0.232 | 0.135 |

In the simulation study of TLZIW, just like the earlier ones, sample sizes n= 25, 50, 75 and 100 were used, where in each case of sample size, the experiment was replicated 1000 times. Four parameter values were also used in the study, these are **I**: $\alpha = 0.1$, $\beta = 0.2$, $\gamma = 0.4$, $\lambda = 0.3$ **II:** $\alpha = 0.4$, $\beta = 0.4$, $\gamma = 0.2$, $\lambda = 0.3$ **III**: $\alpha = 0.2$, $\beta = 0.4$, $\gamma = 0.2$, $\lambda = 0.3$ **IV**: $\alpha = 0.2$, $\beta = 0.1$, $\gamma = 0.2$, $\lambda = 0.2$ to obtain random samples from TLZIW. In Table 5.5 the AB and RMSE decrease with increasing sample size.

**Table 5. 5: Monte Carlo Simulation Result of TLZIW**

| | True Parameter Value | | | | | ABIASS | | | | RMSE | | | |
|---|---|---|---|---|---|---|---|---|---|---|---|---|---|
| | $\alpha$ | $\beta$ | $\gamma$ | $\lambda$ | $n$ | $\hat{\alpha}$ | $\hat{\beta}$ | $\hat{\gamma}$ | $\hat{\lambda}$ | $\hat{\alpha}$ | $\hat{\beta}$ | $\hat{\gamma}$ | $\hat{\lambda}$ |
| **I** | **0.1** | **0.2** | **0.4** | **0.3** | 25 | 3.569 | -0.135 | 0.017 | 0.255 | 3.986 | 0.143 | 1.440 | 0.279 |
| | | | | | 50 | 2.936 | -0.130 | 0.016 | 0.223 | 4.852 | 0.136 | 0.378 | 0.239 |
| | | | | | 75 | 2.441 | -0.153 | 0.011 | 0.201 | 2.722 | 0.129 | 0.722 | 0.240 |
| | | | | | 100 | 2.240 | -0.221 | 0.001 | 0.194 | 2.484 | 0.126 | 0.190 | 0.205 |
| **II** | **0.4** | **0.4** | **0.2** | **0.3** | 25 | 4.302 | -0.225 | 0.029 | 0.021 | 4.758 | 0.254 | 0.096 | 0.060 |
| | | | | | 50 | 3.507 | -0.209 | 0.007 | 0.033 | 3.811 | 0.232 | 0.082 | 0.042 |
| | | | | | 75 | 3.200 | -0.201 | 0.036 | 0.012 | 3.472 | 0.221 | 0.154 | 0.037 |
| | | | | | 100 | 2.892 | -0.188 | 0.034 | 0.004 | 3.116 | 0.208 | 0.033 | 0.068 |
| **III** | **0.2** | **0.4** | **0.1** | **0.1** | 25 | 0.061 | -0.013 | 0.039 | 0.001 | 0.337 | 0.059 | 0.256 | 0.003 |
| | | | | | 50 | 0.021 | -0.011 | 0.025 | 0.001 | 0.167 | 0.045 | 0.089 | 0.003 |
| | | | | | 75 | 0.012 | -0.008 | 0.020 | 0.000 | 0.088 | 0.036 | 0.031 | 0.002 |
| | | | | | 100 | 0.006 | -0.010 | 0.021 | 0.000 | 0.066 | 0.039 | 0.074 | 0.002 |
| **IV** | **0.2** | **0.1** | **0.2** | **0.2** | 25 | 3.002 | -0.052 | 0.078 | 0.031 | 3.853 | 0.067 | 0.443 | 0.054 |
| | | | | | 50 | 1.277 | -0.026 | 0.181 | 0.012 | 2.205 | 0.048 | 2.312 | 0.033 |
| | | | | | 75 | 0.697 | -0.015 | 0.035 | 0.006 | 1.549 | 0.036 | 0.116 | 0.023 |
| | | | | | 100 | 0.336 | -0.088 | 0.027 | 0.002 | 1.028 | 0.026 | 0.127 | 0.016 |

## 5.2 Applications of the special distributions

This section presents the applications of the five new models to lifetime data. Results on the descriptive statistics of data, TTT test, maximum likelihood estimators, the goodness-of-fit test and histogram plots are presented.

## 5.2.1 Applications of TLZNH

In the case of TLZNH, two different data sets were used, these are the failure times and maximum stress data sets.

First of all, the failure times data is applied on the TLZNH. The summary statistics in Table 5.6 shows an average failure time of 45.666, negatively skewed, thus -0.1319 with kurtosis of -1.6425.

**Table 5. 6: Descriptive statistics of failure times data**

| Dataset | Min | Max | Mean | Std. Dev. | Skewness | Kurtosis |
|---|---|---|---|---|---|---|
| Failure times | 0.1000 | 86.000 | 45.6660 | 32.8353 | -0.1319 | -1.6425 |

The failure times data exhibits a bathtub failure rate. This is seen in Figure 5.1 where the TTT transform plot is first convex below the 45 degrees line and then followed by a concave shape above the line.
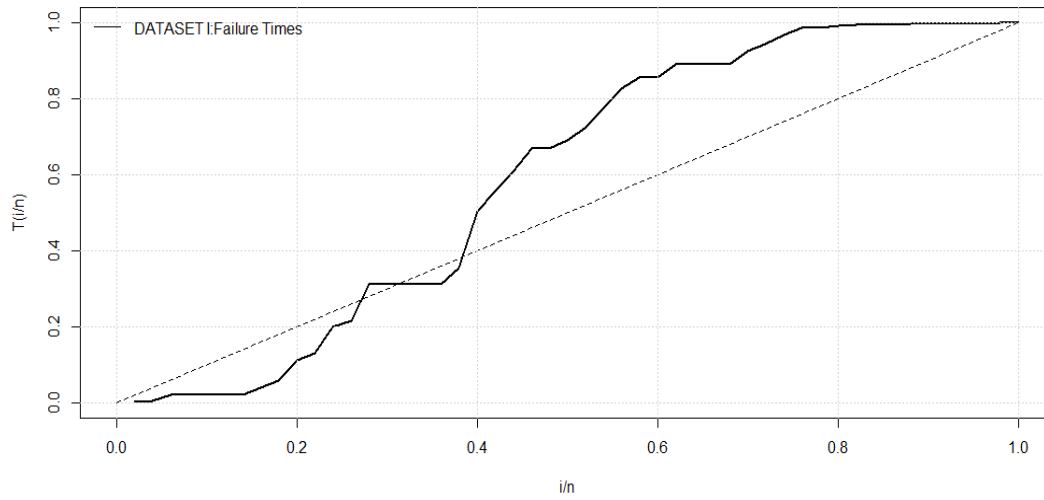
**Figure 5. 1: TTT transform plot of Failure times**

Six models were applied to fit the failure times data. These are: TLZNH, the generalisezd power generalized Weibull (GPGW) (Selim, 2017), exponentiated generalized Weibull (EPGW) (Fernando et al., 2017), power generalized Weibull (PGW) (Nikulin and Haghighi, 2009), Exponentiated Nadarajah Haghighi (ENH) (Lemonte et al., 2013) and generalized Nadarajah Haghighi (GNH) (Ortega et al., 2015).

Table 5.7 gives the maximum likelihood estimates, standard errors, z-values and the p-values of each of the six models. The parameters for many of the models were significant at 5% level of significance.

82

**Table 5. 7: Maximum likelihood estimates of failure times data**

| Model | Parameter | Estimate | Standard Error | z-value | p-value |
|-------|-----------|----------|----------------|---------|---------|
| **TLZNH** | $\hat{\alpha}$ | 6.9263 | $5.5990 \times 10^{-04}$ | $1.2371 \times 10^{4}$ | $< 2.2 \times 10^{-16}$ * |
| | $\hat{\beta}$ | 5.7913 | $1.8985 \times 10^{-05}$ | $3.0505 \times 10^{5}$ | $< 2.2 \times 10^{-16}$ * |
| | $\hat{\gamma}$ | $2.7978 \times 10^{-3}$ | $1.7994 \times 10^{-4}$ | $1.5548 \times 10^{1}$ | $< 2.2 \times 10^{-16}$ * |
| | $\hat{\lambda}$ | 2.0476e-01 | $3.0346 \times 10^{-02}$ | 6.7476 | $1.503 \times 10^{-11}$ * |
| GPGW | $\hat{\alpha}$ | $1.3707 \times 10^{-1}$ | $1.0484 \times 10^{-1}$ | 1.3074 | 0.1911 |
| | $\hat{\gamma}$ | $6.2574 \times 10^{-1}$ | $1.2253 \times 10^{-1}$ | 5.1067 | $3.278 \times 10^{-7}$ * |
| | $\hat{\lambda}$ | $1.2213 \times 10^{-2}$ | $9.2441 \times 10^{-3}$ | 1.3212 | 0.1864 |
| | $\hat{\omega}$ | $1.5476 \times 10^{1}$ | $6.9336 \times 10^{-4}$ | 22320.6634 | $< 2.2 \times 10^{-16}$ * |
| EPGW | $\hat{\beta}$ | 0.6613 | 0.3198 | 2.0679 | 0.03865 * |
| | $\hat{\gamma}$ | 1.0981 | 0.4533 | 2.4224 | 0.01542 * |
| | $\hat{\lambda}$ | 0.0022 | 0.0049 | 0.4532 | 0.6504 |
| | $\hat{\omega}$ | 3.9036 | 2.1414 | 1.8229 | 0.06831 |
| PGW | $\hat{\gamma}$ | 0.8294 | 0.1099 | 7.5438 | $4.566 \times 10^{-14}$ * |
| | $\hat{\lambda}$ | 0.01299 | 0.0084 | 1.5361 | 0.12451 |
| | $\hat{\omega}$ | 2.5884 | 1.1714 | 2.2098 | 0.02712 * |
| ENH | $\hat{\beta}$ | 0.7214 | 0.1144 | 6.3058 | $2.866 \times 10^{-10}$ * |
| | $\hat{\lambda}$ | 0.0029 | 0.0004 | 7.7513 | $9.098 \times 10^{-15}$ * |
| | $\hat{\omega}$ | 4.6046 | 0.0006 | 7332.2447 | $< 2.2 \times 10^{-16}$ * |
| GNH | $\hat{\alpha}$ | $4.9414 \times 10^{-1}$ | $3.2528 \times 10^{-01}$ | 1.5191 | 0.128725 |
| | $\hat{\lambda}$ | $2.1342 \times 10^{-3}$ | $7.7337 \times 10\text{-}04$ | 2.7596 | 0.005787 * |
| | $\hat{\omega}$ | $1.0101 \times 10^{1}$ | $3.8614 \times 10^{-4}$ | 26159.0273 | $< 2.2 \times 10^{-16}$ *** |

Significance at 5% is indicated as: *

Goodness-of-fit test of the failure times data are presented in Table 5.8 . The results of TLZNH gives smaller values of AIC, BIC, AICc, W*, A* and K-S than GPGW, EPGW, PGW and ENH. The implication is that, TLZNH is better in fitting the failure times.

**Table 5. 8: Goodness-of-fit for failure times**

| Model | AIC | BIC | AICc | $W^*$ | $A^*$ | K-S | P-Value |
|-------|-----|-----|------|-------|-------|-----|---------|
| **TLZNH** | **457.7414** | **465.3894** | **458.6302** | **0.1922** | **1.3654** | **0.1152** | **0.5211** |
| GPGW | 472.7656 | 480.4137 | 473.6545 | 0.3100 | 2.0034 | 0.1635 | 0.1380 |
| EPGW | 476.6777 | 484.3258 | 477.5666 | 0.3704 | 2.3346 | 0.2033 | 0.0321 |
| PGW | 480.9676 | 486.7036 | 481.4893 | 0.4289 | 2.6492 | 0.1968 | 0.0415 |
| ENH | 475.4455 | 481.1816 | 475.9672 | 0.3763 | 2.3662 | 0.2092 | 0.0252 |
| GNH | 477.6980 | 483.4340 | 478.2197 | 0.3108 | 2.0095 | 0.1600 | 0.1546 |

In Figure 5.2, the histogram plot also demonstrates that the TLZNH provides a better fit to the failure times than the existing competing models
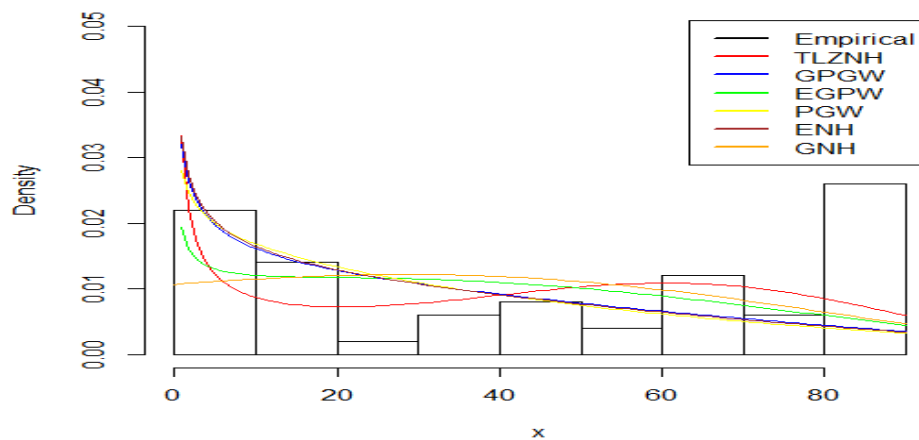


**Figure 5. 2:Histogram and estimated densities of failure times data**

84

The TLZNH was further applied to the second data known as the maximum stress data. Table 5.9 gives the descriptive statistics of the data. It shows average stress as 133.78 per 31,000 psi. with positive skewness of 0.3360 and kurtosis of 1.0379.

**Table 5. 9: Descriptive Statistics   of Maximum stress data**

| Dataset | Min | Max | Mean | Std. Dev. | Skewness | Kurtosis |
|---------|-----|-----|------|-----------|----------|----------|
| Maximum stress | 70.000 | 212.0000 | 133.7800 | 22.6134 | 0.3660 | 1.0379 |

The TTT transform plot of the maximum stress data shows increasing failure rate shape. The plot in Figure 5.3  is  concave above the 45 degrees line.
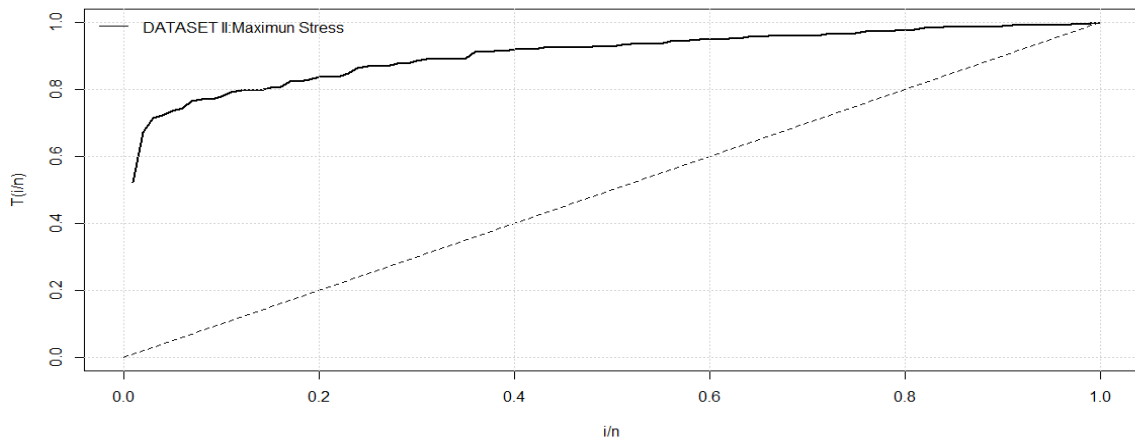


**Figure 5. 3: TTT Transform plot of Maximum stress**

Four models are applied to fit the maximum stress data. These are TL generalized exponential (TLGE) ( Sangsanit et al. 2016), generalized exponential (GE) and exponentiated generalized exponential (EGE) (Cordeiro et al. 2013).

The maximum likelihood estimates, standard errors, z-values and p-values of the maximum stress data are showed in Table 5.10. Many of the parameters show significance at 5%, with the exception of $\gamma$ and $\lambda$ for TLZNH and $\lambda$ for EGE.

**Table 5. 10: Maximum likelihood estimates of maximum stress data**

| Model | Parameter | Estimate | Standard Error | z-value | p-value |
|---|---|---|---|---|---|
| **TLZNH** | $\hat{\alpha}$ | 24.9548 | 0.0550 | 453.1038 | $< 2.2\times 10^{-16}$ * |
| | $\hat{\beta}$ | 1.0594 | 0.3878 | 2.7313 | 0.0063 * |
| | $\hat{\gamma}$ | 0.0277 | 0.0227 | 1.2201 | 0.2224 |
| | $\hat{\lambda}$ | 1.8191 | 1.2429 | 1.4636 | 0.1433 |
| **TLGE** | $\hat{\alpha}$ | 0.0288 | 0.0015 | 19.5518 | $2.2\times 10^{-16}$ * |
| | $\hat{\beta}$ | 22.3132 | 0.1871 | 119.2547 | $2.2\times 10^{-16}$ * |
| | $\hat{\lambda}$ | 3.8993 | 1.0539 | 3.6999 | 0.0002 * |
| **GE** | $\hat{\alpha}$ | $4.453\times 10^{-2}$ | $8.5789\times 10^{-4}$ | $5.1907\times 10^{1}$ | $< 2.2\times 10^{-16}$ * |
| | $\hat{\beta}$ | $2.3677\times 10^{+2}$ | $2.9804\times 10^{-8}$ | $7.9442\times 10^{9}$ | $< 2.2\times 10^{-16}$ * |
| **EGE** | $\hat{\alpha}$ | $8.8534\times 10^{-2}$ | $3.1427\times 10^{-1}$ | $2.8170\times 10^{-1}$ | 0.7782 |
| | $\hat{\beta}$ | $1.2187\times 10^{2}$ | $5.5783\times 10^{-4}$ | $2.1847\times 10^{5}$ | $<2\times 10^{-16}$ * |
| | $\hat{\lambda}$ | $4.4219\times 10^{-1}$ | 1.5696 | $2.8170\times 10^{-1}$ | 0.7782 |

Significance at 5% is indicated as: *

In Table 5.11, the goodness-of-fit results of TLZNH for the maximum stress data gives smaller values of AIC, BIC, AICc, W*, A*  and K-S than, TLGE, GE and EGE. The TLZNH is better in fitting maximum stress data than the competitive models.

**Table 5. 11: Goodness-of-fit of maximum stress data**

| Model | AIC | BIC | AICc | $W^*$ | $A^*$ | K-S | P-Value |
|-------|-----|-----|------|-----|-----|-----|---------|
| **TLZNH** | **915.8906** | **926.3113** | **916.3117** | **0.0955** | **0.5562** | **0.0862** | **0.4476** |
| TLGE | 916.7832 | 924.5987 | 917.0332 | 0.1266 | 0.7272 | 0.0949 | 0.3293 |
| GE | 921.4296 | 926.6399 | 921.5533 | 0.0527 | 0.3507 | 0.9718 | 0.0000 |
| EGE | 927.9154 | 935.7309 | 928.1654 | 0.0529 | 0.3516 | 0.9605 | 0.0000 |

The histogram plots and estimates, PDF of TLZNH and other fitted distribution for maximum stress data are presented in Figure 5.4. The plots show better fit for TLZNH.
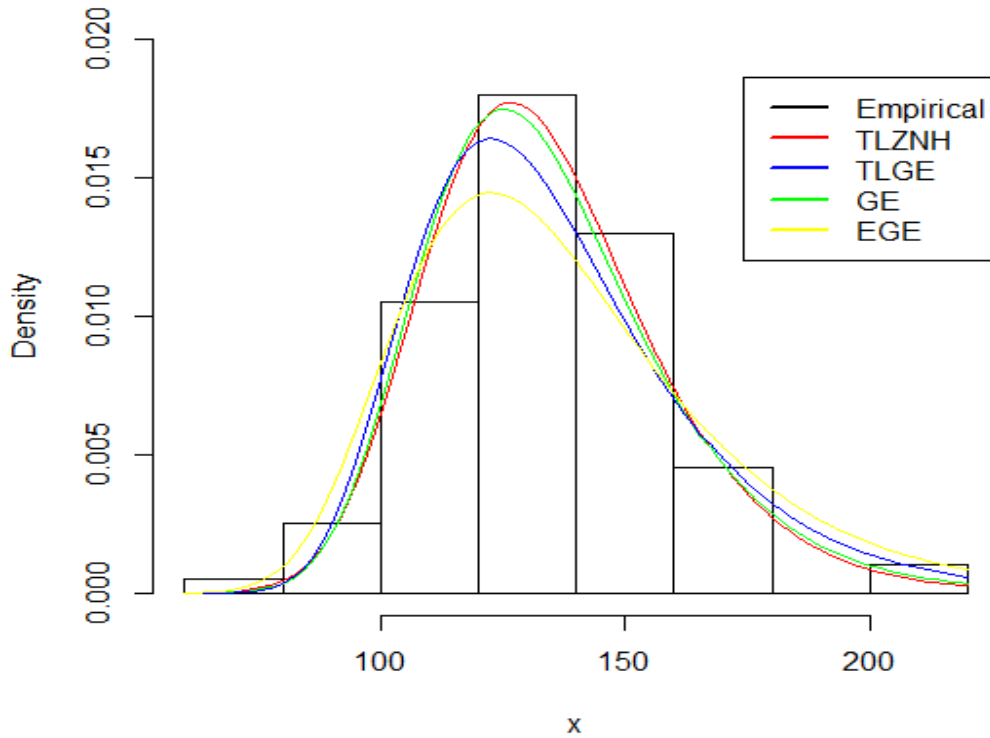
**Figure 5. 4: Histogram and estimated densities of maximum stress data**

## 5.2.2 Applications of TLZLx

The study applied five models to fit the survival times data, these models are TLZLx, TL Weibull Lomax (TLWLx) (Farrukh et al. 2019), TL Lomax (TLLx) (Sangsanit et al. 2016), Weibull Lomax (WLx) (Tahir et al. 2015) and Gomperz Lomax (GLx) (Oguntunde 2017).

The descriptive statistics of the survival data in Table 5.12 shows an average survival times of 1.8367 days with positive skewness 1.2156 and kurtosis of 3.9546.

**Table 5. 12: Descriptive Statistics   of Survival times data**

| Dataset | Min | Max | Mean | Std. Dev. | Skewness | Kurtosis |
|---|---|---|---|---|---|---|
| Survival  times | 0.0800 | 7.0000 | 1.8367 | 1.2156 | 1.7184 | 3.9546 |

The TTT plot of the survival times data in Figure 5.5 shows an increasing failure rate. The line is concave on the 45 degrees line.
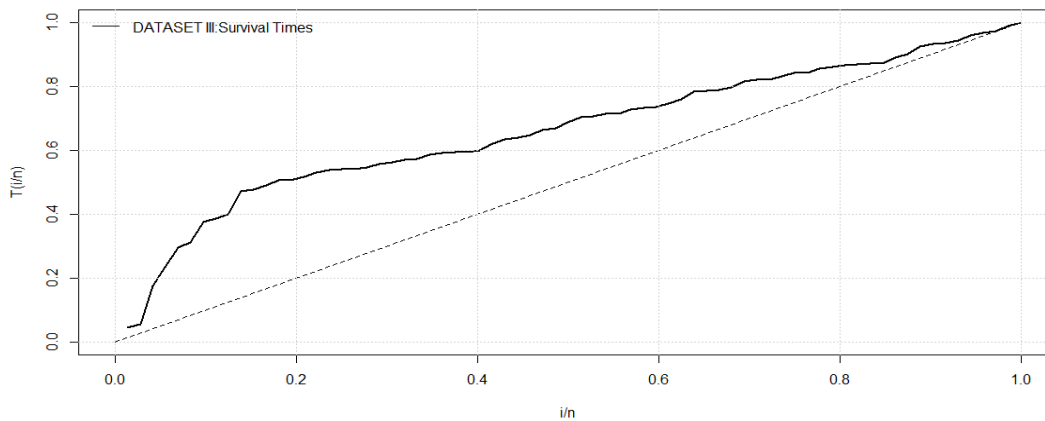


**Figure 5. 5: TTT Transform plot of Survival times data**

89

In Table 5.13 shows many of the parameter estimates not significant at 5% significant level, except for the parameter $\beta$ of the TLZNH and the $\lambda$ of TLLx.

**Table 5. 13: Maximum likelihood estimates of   survival times data**

| Model | Parameter | Estimate | Standard Error | z-value | p-value |
|-------|-----------|----------|----------------|---------|---------|
| **TLZLx** | $\hat{\alpha}$ | 9.3413 | 6.2803 | 1.4874 | 0.1369 |
| | $\hat{\beta}$ | 2.9434 | 0.9146 | 3.2183 | 0.0013 * |
| | $\hat{\gamma}$ | 1.4329 | 0.7799 | 1.8372 | 0.0662 |
| | $\hat{\lambda}$ | 0.5157 | 0.3372 | 1.5292 | 0.1262 |
| TLWLx | $\hat{\alpha}$ | 1.4266 | 0.9237 | 1.5446 | 0.1224 |
| | $\hat{\beta}$ | 0.6585 | 0.8895 | 0.7403 | 0.4591 |
| | $\hat{\gamma}$ | 0.6939 | 0.6793 | 1.0216 | 0.3070 |
| | $\hat{\lambda}$ | 1.6468 | 1.2001 | 1.3723 | 0.1700 |
| TLLx | $\hat{\beta}$ | 11.9226 | 14.3159 | 0.8328 | 0.4049 |
| | $\hat{\gamma}$ | 0.0426 | 0.0553 | 0.7714 | 0.4405 |
| | $\hat{\lambda}$ | 2.8291 | 0.5749 | 4.9209 | $8.616 \times 10^{-7}$ * |
| WLx | $\hat{\alpha}$ | 2.2232 | 0.6967 | 3.1913 | 0.0014 * |
| | $\hat{\beta}$ | 1.6563 | 1.7763 | 0.9325 | 0.3511 |
| | $\hat{\gamma}$ | 0.4735 | 0.2625 | 1.8040 | 0.0712 |
| GLx | $\hat{\alpha}$ | 0.7298 | 0.8167 | 0.8936 | 0.3716 |
| | $\hat{\beta}$ | 8.4117 | 9.0255 | 0.9320 | 0.3513 |
| | $\hat{\gamma}$ | 2.3277 | 2.6050 | 0.8935 | 0.3716 |
| | $\hat{\lambda}$ | 0.01660 | 0.03244 | 0.5116 | 0.6089 |

Significance at 5% is indicated as: *

In Table 5.14, the results present TLZLx to have smaller values for AICc, AIC, W*, BIC, A* and K-S than TLWLx, TLLx, WLx and GLx. This means that in the choice of fitting the survival times data, it is more appropriate to use TLZLx as it is better than the competing models.

**Table 5. 14: Goodness-of-fit for survival times data**

| Model | AIC | BIC | AICc | $W^*$ | $A^*$ | K-S | P-Value |
|-------|-----|-----|------|-------|-------|-----|---------|
| **TLZLx** | **208.4064** | **217.5131** | **209.0034** | **0.0534** | **0.3331** | **0.0713** | **0.8579** |
| TLWLx | 213.5021 | 222.6088 | 214.0991 | 0.1077 | 0.7144 | 0.1013 | 0.4510 |
| TLLx | 212.3250 | 219.1550 | 212.6780 | 0.1020 | 0.7175 | 0.1111 | 0.3365 |
| WLx | 212.3171 | 219.1471 | 212.6700 | 0.1250 | 0.8032 | 0.1077 | 0.3740 |
| GLx | 216.9100 | 226.0167 | 217.5070 | 0.1740 | 1.0373 | 0.1165 | 0.2828 |

The histogram plots and estimates PDF of TLZLx and other fitted distribution for survival data are presented in Figure 5.6. The data plots show better fit of TLZNH than TLLx, WLx and GLx.
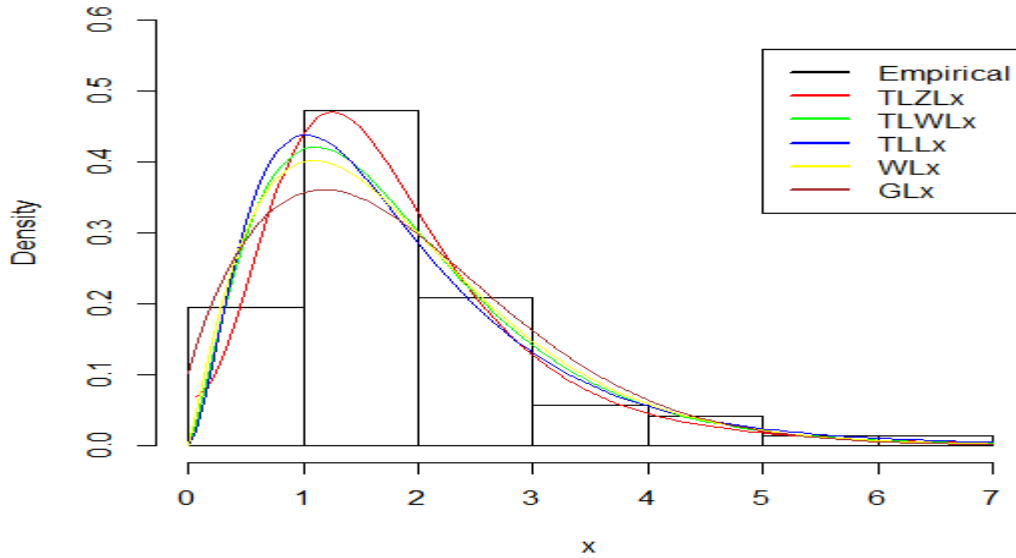


**Figure 5. 6: Histogram and estimated densities for survival times data**

### 5.2.3 Applications of TLZW

Two data sets: breaking stress and servicing times data are applied in the case of TLZW. In the breaking stress data, the models applied are TL generalized exponential (TLGE) (Sangsanit et al. 2016), generalized exponential (GE) and exponentiated generalised exponential (EGE) (Cordeiro et al. 2013). The models compared against servicing times data are TL Weibull Lomax (TLWLx), Topp-Leone Lomax (TLLx), Exponentiated Lomax (ELx), Gomperz Lomax (GLx). Table 5.15 shows the

92

descriptive statistics for the breaking stress data. The average breaking stress is 2.6214 Giga Pascal (GPa) , with positive  skewness of 1.0139 and kurtosis 0.0432.

**Table 5. 15: Descriptive Statistics   of Breaking stress data**

| Dataset | Min | Max | Mean | Std. Dev. | Skewness | Kurtosis |
| --- | --- | --- | --- | --- | --- | --- |
| Breaking stress | 0.3900 | 5.5600 | 2.6214 | 1.0139 | 0.3626 | 0.0432 |

The breaking stress data exhibits increasing failure rate for the fact that TTT transform plot in Figure 5.7 is concave on the 45 degrees line.
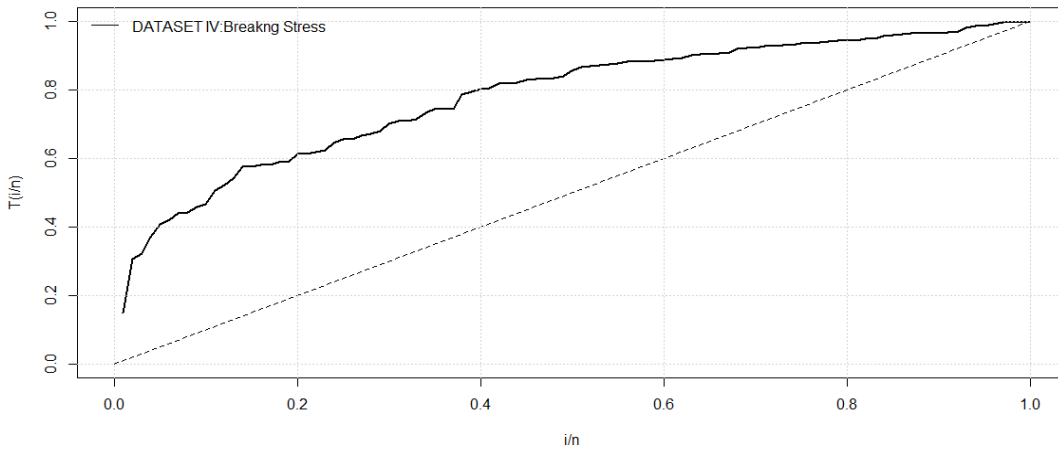


**Figure 5. 7: TTT Transform plot of Breaking stress data**

The results in Table 5.16 shows many of the parameter estimates based on the maximum likelihood estimator to be significant at 5% significance level, except for the parameters $\alpha$  and $\gamma$  for TLZNH and $\beta$  and $\lambda$  for TLGE.

93

**Table 5. 16: Maximum likelihood estimates of   breaking stress data**

| Model | Parameter | Estimate | Standard Error | z-value | p-value |
|-------|-----------|----------|----------------|---------|---------|
| **TLZW** | $\hat{\alpha}$ | 2.00848 | 2.45528 | 0.8180 | 0.41334 |
| | $\hat{\beta}$ | 1.47720 | 0.61208 | 2.4134 | 0.01580 * |
| | $\hat{\gamma}$ | 0.33383 | 0.39497 | 0.8452 | 0.39800 |
| | $\hat{\lambda}$ | 1.07494 | 0.44692 | 2.4052 | 0.01616 * |
| TLGE | $\hat{\alpha}$ | 0.8059 | 0.1275 | 6.3220 | $2.582 \times 10^{-10}$ * |
| | $\hat{\beta}$ | 20.2519 | 21.6437 | 0.9357 | 0.3494 |
| | $\hat{\lambda}$ | 0.3027 | 0.2947 | 1.0272 | 0.3043 |
| GE | $\hat{\alpha}$ | 1.0132 | 0.0874 | 11.5824 | $< 2.2 \times 10^{-16}$ * |
| | $\hat{\beta}$ | 7.7883 | 1.4962 | 5.2054 | $1.936 \times 10^{-07}$ * |
| EGE | $\hat{\alpha}$ | 0.3731 | 0.0316 | 11.8001 | $< 2.2 \times 10^{-16}$ * |
| | $\hat{\beta}$ | 7.7885 | 1.4962 | 5.2053 | $1.937 \times 10^{-07}$ * |
| | $\hat{\lambda}$ | 2.7154 | 0.0043 | 625.7944 | $< 2.2 \times 10^{-16}$ * |

Significance at 5% is indicated as: *

TLZW has smaller AICc, AIC, W*, BIC, A*   and K-S than TLGE, GE and EGE. It means that TLZW is better and more appropriate to use in modeling breaking stress, as shown in Table 5.17.

**Table 5. 17: Goodness-of-fit breaking stress data**

| Model | AIC | BIC | AICc | $W^*$ | $A^*$ | K-S | P-Value |
|-------|-----|-----|------|-------|-------|-----|---------|
| **TLZW** | **290.3853** | **300.8060** | **290.8063** | **0.0620** | **0.3730** | **0.0618** | **0.8403** |
| TLGE | 292.0938 | 299.9093 | 292.3438 | 0.1386 | 0.7116 | 0.0919 | 0.0618 |
| GE | 296.3646 | 301.5749 | 296.4883 | 0.2267 | 1.1860 | 0.1077 | 0.1962 |
| EGE | 298.3646 | 306.1801 | 298.6146 | 0.2267 | 1.1860 | 0.1077 | 0.1962 |

The histogram plot in Figure 5.8 shows TLZW as best fit model for analyzing the breaking stress data.
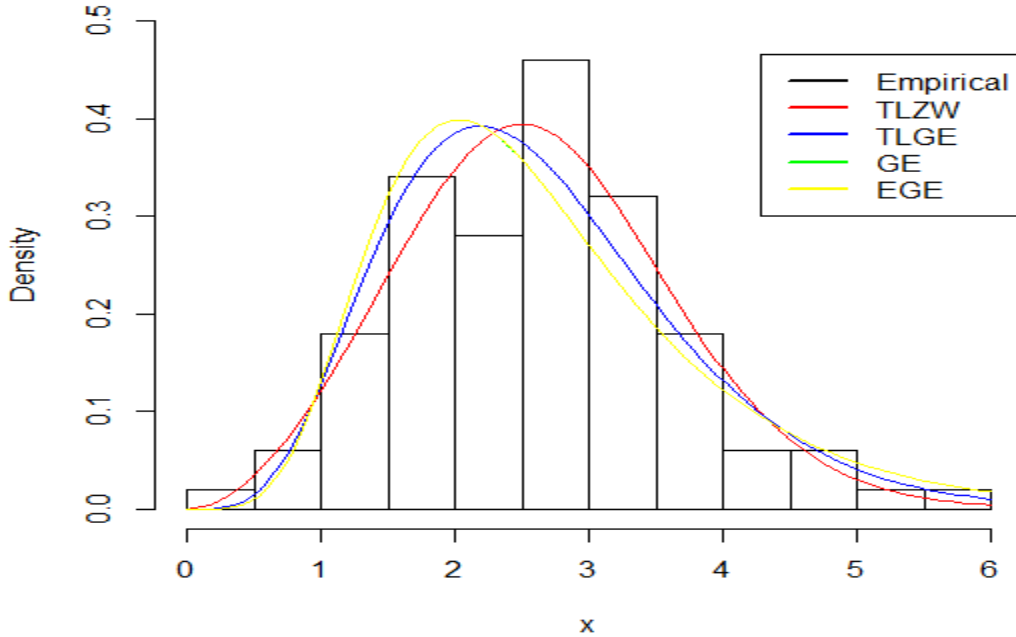


**Figure 5. 8: Histogram and estimated densities of breaking stress**

The second data applied on the TLZW is the windshield servicing times data: The descriptive statistics in Table 5.18 depicts an average servicing times of 2.0852 per 1000hour, with positive skewness of 0.4292 and kurtosis of -0.3535.

**Table 5. 18: Descriptive Statistics of windshield servicing times data**

| Dataset | Min | Max | Mean | Std. Dev. | Skewness | Kurtosis |
|---|---|---|---|---|---|---|
| Servicing time | 0.0460 | 5.1400 | 2.0852 | 1.2452 | 0.4292 | -0.3535 |

The windshield servicing times data exhibits an increasing failure rate as the TTT transform plot in Figure 5.9 shows concave on the 45 degrees line.
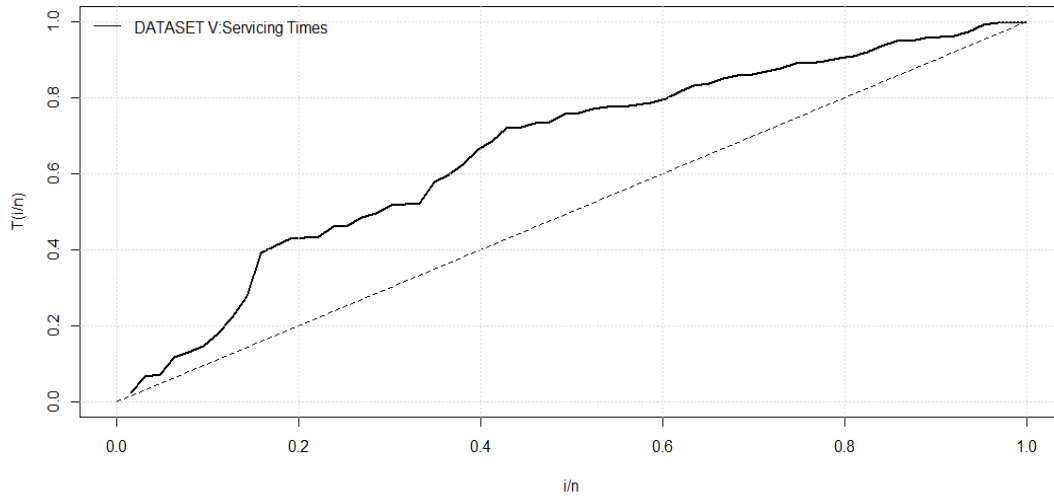


**Figure 5. 9: TTT Transform plot of Windshield Servicing Times data**

Table 5.19 depicts that only one of the estimated parameters of TLZW and GLx shows significance at 5% level of significance. However, for TLWLx , none of the estimated parameters shows significance. All the estimated parameters of TLLx and ELx shows significance.

**Table 5. 19: Maximum likelihood estimates of   windshield servicing times data**

| Model | Parameter | Estimate | Standard Error | z-value | p-value |
|---|---|---|---|---|---|
| **TLZW** | $\hat{\alpha}$ | 4.6291 | 2.4131 | 1.9183 | 0.0551 |
| | $\hat{\beta}$ | 1.1521 | 0.3231 | 3.5660 | 0.00036 |
| | $\hat{\gamma}$ | 0.5889 | 0.3332 | 1.7671 | 0.0772 |
| | $\hat{\lambda}$ | 0.4366 | 0.1522 | 2.8685 | 0.004 * |
| **TLWLx** | $\hat{\alpha}$ | 2.4337 | 2.3448 | 1.0379 | 0.2993 |
| | $\hat{\beta}$ | 0.0867 | 0.3914 | 0.2214 | 0.8247 |
| | $\hat{\gamma}$ | 2.2714 | 9.089 | 0.2499 | 0.8027 |
| | $\hat{\lambda}$ | 0.4652 | 0.4388 | 1.0602 | 0.2890 |
| **TLLx** | $\hat{\beta}$ | $2.6674\times 10^{1}$ | $2.8196\times 10^{4}$ | 94602.5448 | $< 2.2\times 10^{-16}$ * |
| | $\hat{\gamma}$ | $1.3254\times 10^{-2}$ | $1.8461\times 10^{-3}$ | 7.1793 | $7.005\times 10^{-13}$ * |
| | $\hat{\lambda}$ | 1.9174 | $3.4711\times 10^{-1}$ | 5.5239 | $3.316\times 10^{-8}$ * |
| **ELx** | $\hat{\alpha}$ | 1.8812 | $3.4031\times 10^{-1}$ | 5.5279 | $3.241\times 10^{-8}$ * |
| | $\hat{\beta}$ | $3.6789\times 10^{+01}$ | $2.1569\times 10^{-4}$ | $1.7056\times 10^{+05}$ | $< 2.2\times 10^{-16}$ * |
| | $\hat{\lambda}$ | $1.9123\times 10^{-2}$ | $2.7020\times 10^{-3}$ | 7.0773 | $1.470\times 10^{-12}$ * |
| **GLx** | $\hat{\alpha}$ | 1.2435 | 1.5708 | 0.7916 | 0.4286 |
| | $\hat{\beta}$ | 0.2330 | 0.6114 | 0.3811 | 0.7031 |
| | $\hat{\gamma}$ | 3.3278 | 0.4099 | 8.1189 | $4.703\times 10^{-16}$ * |
| | $\hat{\lambda}$ | 0.6045 | 1.0558 | 0.5726 | 0.5669 |

Significance at 5% is indicated as: *

In the Goodness-of-fit test results in Table 5.20, TLZW has smaller AICc, AIC, W*, BIC, A*  and K-S than TLWLx, TLLx, ELx and GLx. This shows that TLZW is better and more appropriate to use in modeling windshield servicing times data.

**Table 5. 20: Goodness-of-fit of windshield servicing times data**

| Model | AIC | BIC | AICc | W* | A* | K-S | P-Value |
|---|---|---|---|---|---|---|---|
| **TLZW** | **203.8196** | **212.3921** | **204.5092** | **0.0268** | **0.1875** | **0.0577** | **0.9768** |
| TLWLx | 204.5402 | 213.1128 | 205.2299 | 0.0470 | 0.3042 | 0.0734 | 0.8619 |
| TLLx | 213.7357 | 220.1651 | 214.1424 | 0.2123 | 1.2847 | 0.1449 | 0.1283 |
| ELx | 214.0420 | 220.4714 | 214.4488 | 0.2151 | 1.3022 | 0.1458 | 0.1242 |
| GLx | 204.2726 | 212.8451 | 204.9623 | 0.0384 | 0.2555 | 0.0676 | 0.9170 |

The histogram plot in Figure 5.10 shows TLZW as best fit model for analyzing windshield servicing times data.
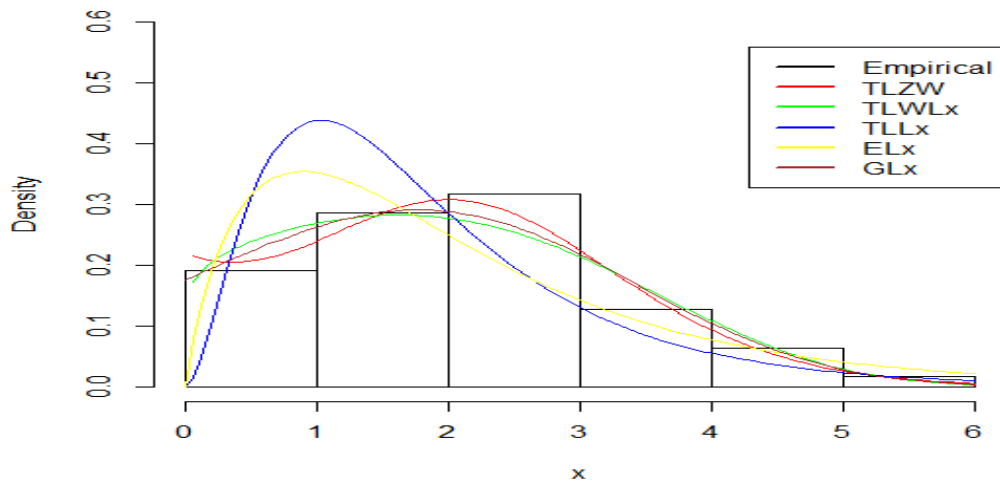


**Figure 5. 10: Histogram and estimated densities for windshield servicing times data**

### 5.2.4 Applications of TLZKw

Two data sets are used to assess fitness of TLZKw. These data sets presents as; milk production and cybercrime data. The competing models used are Topp-Leone Kumaraswamy (TLKw) (Sangsanit et al.2016) , Zubair Kumaraswamy (ZKw) (Zubair, 2018), Kumaraswamy(Kw), Weibull(W), Zubair Weibull(ZW), Topp-Leone generalized exponential(TLGE) and Topp-Leone Lomax (TLLx).

In the descriptive statistics of milk production data in Table 5.21, it shows average milk production rate of 0.4696 with negative skewness -0.3386 and kurtosis of -0.4053.

**Table 5. 21: Descriptive Statistics   of milk production data**

| Dataset | Min | Max | Mean | Std. Dev. | Skewness | Kurtosis |
|---------|-----|-----|------|-----------|----------|----------|
| Milk production | 0.0168 | 0.8781 | 0.4696 | 0.1938 | -0.3386 | -0.4053 |

The milk production data exhibits a bathtub failure rate. In the TTT transform plot in Figure 5.11, the data shows concave above the 45 degrees line, depicting as a lifetime data.
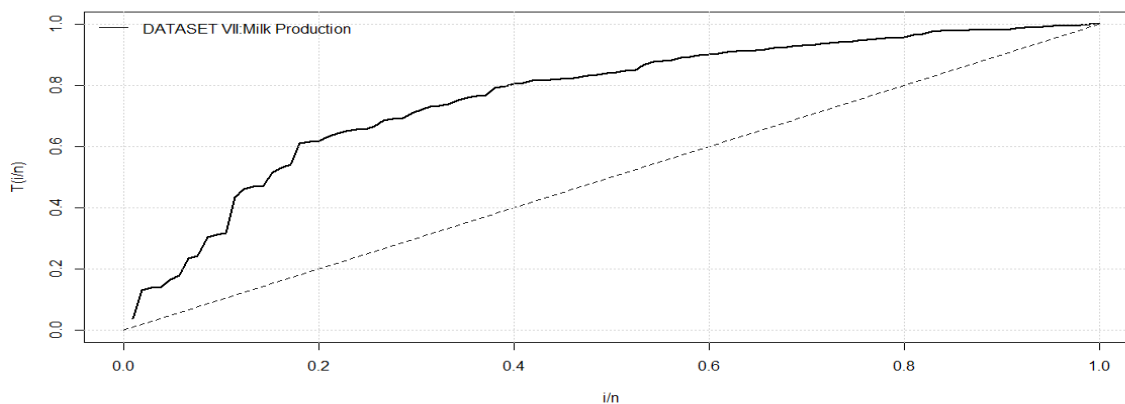
**Figure 5. 11: TTT Transform plot of Milk Production data**

Table 5.22 shows the estimated parameters, standard errors, z-value and the p-value. The result shows many of the estimated parameters for the models to be significant at 5% significant level, except for $\beta$ and $\lambda$ of TLGE.

**Table 5. 22: Maximum likelihood estimates milk production data**

| Model | Parameter | Estimate | Standard Error | z-value | p-value |
|---|---|---|---|---|---|
| **TLZKw** | $\hat{\alpha}$ | 4.6797 | 2.0135 | 2.3241 | 0.0201* |
| | $\hat{\beta}$ | 2.3134 | 0.4941 | 4.6820 | $2.841 \times 10^{-06}$ * |
| | $\hat{\gamma}$ | 0.9832 | 0.3845 | 2.5570 | 0.0106 * |
| | $\hat{\lambda}$ | 0.5929 | 0.2268 | 2.6139 | 0.0090 * |
| TLKw | $\hat{\beta}$ | 3.6621 | 1.7421 | 2.1021 | 0.035547 * |
| | $\hat{\gamma}$ | 5.5355 | 2.0861 | 2.6535 | 0.008 * |
| | $\hat{\lambda}$ | 0.3178 | 0.1446 | 2.1970 | 0.028022 * |
| ZKw | $\hat{\alpha}$ | 2.9365 | 1.10061 | 2.6681 | 0.0076 * |
| | $\hat{\beta}$ | 2.8317 | 0.3618 | 7.8263 | $5.024 \times 10^{-15}$ * |
| | $\hat{\gamma}$ | 0.8416 | 0.1911 | 4.4044 | $1.061 \times 10^{-05}$ * |
| Kw | $\hat{\beta}$ | 3.35618 | 0.57132 | 5.8744 | $4.244 \times 10^{-09}$ * |
| | $\hat{\gamma}$ | 2.1695 | 0.2229 | 9.7302 | $< 2.2 \times 10^{-16}$ * |
| W | $\hat{\beta}$ | 2.57856 | 0.21056 | 12.2465 | $< 2.2 \times 10^{-16}$ * |
| | $\hat{\gamma}$ | 5.2800 | 0.7680 | 6.875 | $6.213 \times 10^{-12}$ * |
| ZW | $\hat{\alpha}$ | 2.64338 | 0.80811 | 3.2711 | 0.001071 * |
| | $\hat{\beta}$ | 1.34763 | 0.14888 | 9.0519 | $< 2.2 \times 10^{-16}$ * |
| | $\hat{\gamma}$ | 5.9124 | 0.5314 | 11.1269 | $< 2.2 \times 10^{-16}$ * |
| TLGE | $\hat{\alpha}$ | 3.4157 | 0.4319 | 7.9069 | $2.638 \times 10^{-15}$ * |
| | $\hat{\beta}$ | 11.4094 | 7.1401 | 1.5979 | 0.11006 |
| | $\hat{\lambda}$ | 0.29385 | 0.17394 | 1.6894 | 0.09115 |
| TLLx | $\hat{\beta}$ | $7.1224 \times 10^{01}$ | $1.3265 \times 10^{-4}$ | $5.3695 \times 10^{5}$ | $< 2.2 \times 10^{-16}$ * |
| | $\hat{\gamma}$ | $2.9469 \times 10^{-2}$ | $2.6791 \times 10^{-3}$ | $1.1000 \times 10^{1}$ | $< 2.2 \times 10^{-16}$ * |
| | $\hat{\lambda}$ | 3.6609 | 5.6399 | 6.4911 | $8.524 \times 10^{-11}$ * |

Significance at 5% is indicated as: *

101

The results indicate in Table 5.23, that TLZKw achieves smaller values for AICc, AIC, W*, BIC, A*  and K-S. This means that,  TLZKw fits the data sets better than TLKw, ZKw, Kw, W, ZW, TLGE and TLLx.

**Table 5. 23**: **Goodness-of-fit for milk production**

| Model | AIC | BIC | AICc | $W^*$ | $A^*$ | K-S | P-Value |
|-------|-----|-----|------|-------|-------|-----|---------|
| **TLZKw** | **-48.6659** | **-38.0501** | **-48.2659** | **0.0271** | **0.1878** | **0.0441** | **0.9867** |
| TLKw | -47.0125 | -39.0506 | -46.7749 | 0.0853 | 0.5475 | 0.0728 | 0.6346 |
| ZKw | -46.3392 | -38.3773 | -46.1016 | 0.0891 | 0.6054 | 0.0533 | 0.9269 |
| Kw | -44.4216 | -39.1136 | -44.3039 | 0.1532 | 0.9902 | 0.0780 | 0.5461 |
| W | -35.9592 | -30.6513 | -35.8415 | 0.2349 | 1.5354 | 0.0875 | 0.3981 |
| ZW | -29.3116 | -21.3497 | -29.0740 | 0.2833 | 1.8457 | 0.0781 | 0.5445 |
| TLGE | -15.0561 | -7.0942 | -14.8185 | 0.5274 | 3.2613 | 0.1400 | 0.0326 |
| TLLx | -1.6198 | 6.3421 | -1.3821 | 0.7248 | 4.3705 | 0.1473 | 0.0210 |

The histogram plot in Figure 5.12 shows TLZKw as best fit model for analyzing milk production data.
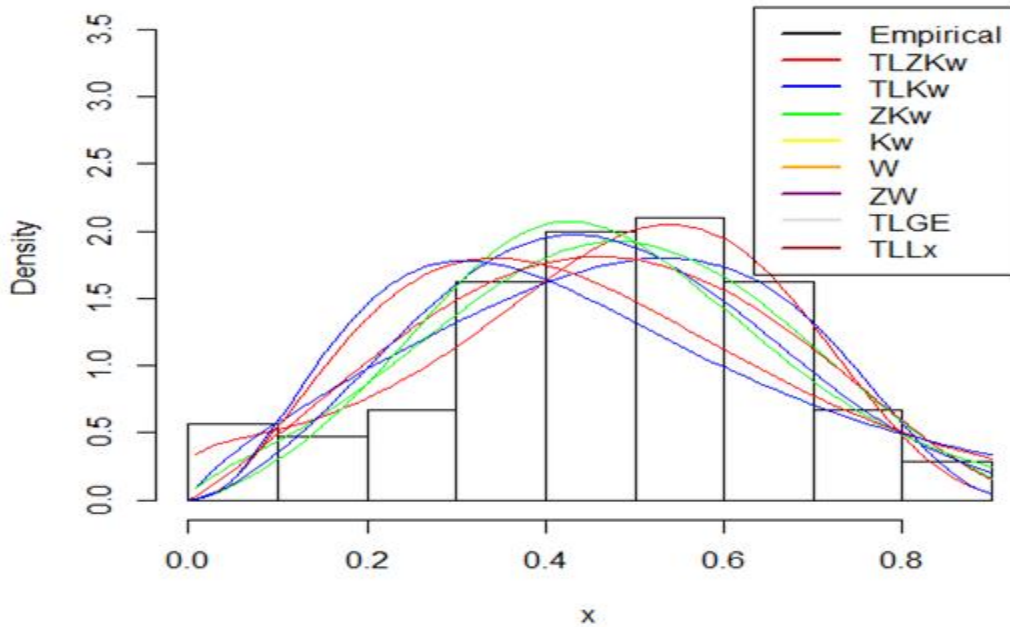


**Figure 5. 12: Histogram and estimated densities milk production**

The second data set applied to TLZKw is cyber security data. Table 5.24 shows average of 0.0027 rate of the cost of cybercrimes to GDP, positively skewed 2.7284 with kurtosis of 7.8497.

**Table 5. 24: Descriptive Statistics of Cyber security data**

| Dataset | | Min | Max | Mean | Std. Dev. | Skewness | Kurtosis |
|---|---|---|---|---|---|---|---|
| Cost of cybercrime to GDP | | 0.0004 | 0.0160 | 0.0027 | 0.0034 | 2.7284 | 7.8497 |

The cyber security data set exhibits an increasing failure rate in Figure 5.13. This is as the TTT transform plot is first concave above the 45 degrees line.
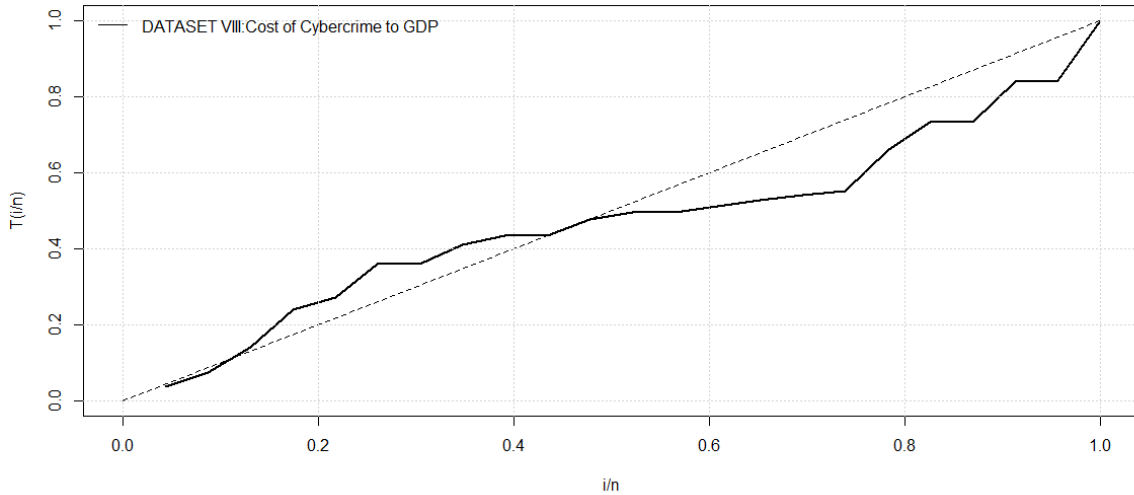


**Figure 5. 13: TTT Transform plot of Cost of cybercrimes to GDP**

Table 5.25 shows the majority of estimated parameters of the different models significant at 5% level of significance, except for, however three of the parameters of the TLZKw, one parameter of TLIW and TLGE that were not significant.

**Table 5. 25: Maximum likelihood estimates of cyber security data**

| Model | Parameter | Estimate | Standard Error | z-value | p-value |
|---|---|---|---|---|---|
| **TLZKw** | $\hat{\alpha}$ | 21.5059 | 0.2646 | 81.2796 | $<2\times10^{-16}$ * |
| | $\hat{\beta}$ | 11.4673 | 8.7150 | 1.3158 | 0.1882 |
| | $\hat{\gamma}$ | 0.2204 | 0.1387 | 1.5886 | 0.1122 |
| | $\hat{\lambda}$ | 0.6326 | 0.7526 | 0.8405 | 0.4007 |
| TLIW | $\hat{\beta}$ | 0.02134 | 0.0166 | 1.2898 | 0.1971 |
| | $\hat{\gamma}$ | 0.6865 | 0.1467 | 4.6785 | $2.89\times10^{-06}$ * |
| | $\hat{\lambda}$ | 0.5316 | 0.7433 | 0.7151 | 0.4746 |
| TLWLx | $\hat{\alpha}$ | $4.9212\times10^{-01}$ | $1.9786\times10^{-01}$ | 2.4872 | 0.01288 * |
| | $\hat{\beta}$ | $6.5502\times10^{-01}$ | $3.0368\times10^{-01}$ | 2.1570 | 0.03101 * |
| | $\hat{\gamma}$ | $2.5105\times10^{02}$ | $8.9214\times10^{-04}$ | $2.8140\times10^{05}$ | $<2\times10^{-16}$ * |
| | $\hat{\lambda}$ | 2.2139 | 1.4992 | 1.4768 | 0.13973 |
| TLKw | $\hat{\beta}$ | 96.5092 | 0.0011 | 89918.7070 | $<2.2\times10^{-16}$ * |
| | $\hat{\gamma}$ | 3.5771 | 0.6286 | 5.6905 | $1.267\times10^{-08}$ * |
| | $\hat{\lambda}$ | 0.0559 | 0.0173 | 3.2403 | 0.0012 * |
| TLGE | $\hat{\alpha}$ | 3.1433 | 1.6717 | 1.8803 | 0.0601 |
| | $\hat{\beta}$ | 23.1374 | 0.0016 | 14248.9174 | $<2.2\times10^{-16}$ * |
| | $\hat{\lambda}$ | 0.0082 | 0.0019 | 4.3231 | $1.538\times10^{-05}$ * |

Significance at 5% is indicated as: *

The results indicate in Table 5.26, that TLZKw also achieves smaller values for AICc, AIC, W*, BIC, A*  and K-S. This Indicates that TLZKw fits the data better than TLIW, TLKw, TLWLx, and TLGE.

**Table 5. 26**: **Goodness-of-fit for dataset   Cyber security**

| Model | AIC | BIC | AICc | $W^*$ | $A^*$ | K-S | P-Value |
|-------|-----|-----|------|-------|-------|-----|---------|
| **TLZKw** | **-220.8348** | **-216.2928** | **-218.6126** | **0.0863** | **0.4542** | **0.1517** | **0.6649** |
| TLIW | -218.4669 | -215.0605 | -218.4669 | 0.1598 | 0.9037 | 0.1981 | 0.3273 |
| TLWLx | -215.8569 | -211.3149 | -213.6347 | 0.1570 | 0.8699 | 0.2477 | 0.1190 |
| TLKw | -171.1297 | -167.7232 | -169.8666 | 0.0951 | 0.5007 | 0.4684 | 0.0001 |
| TLGE | -168.2346 | -164.8281 | -166.9715 | 0.0937 | 0.4934 | 0.4772 | 0.0001 |

The histogram plots and estimates PDF of TLZKw and other fitted distribution for Cyber security data are shown in Figure 5.14. The figure reveals that TLZKw fits the cyber security data better than the other competing models.
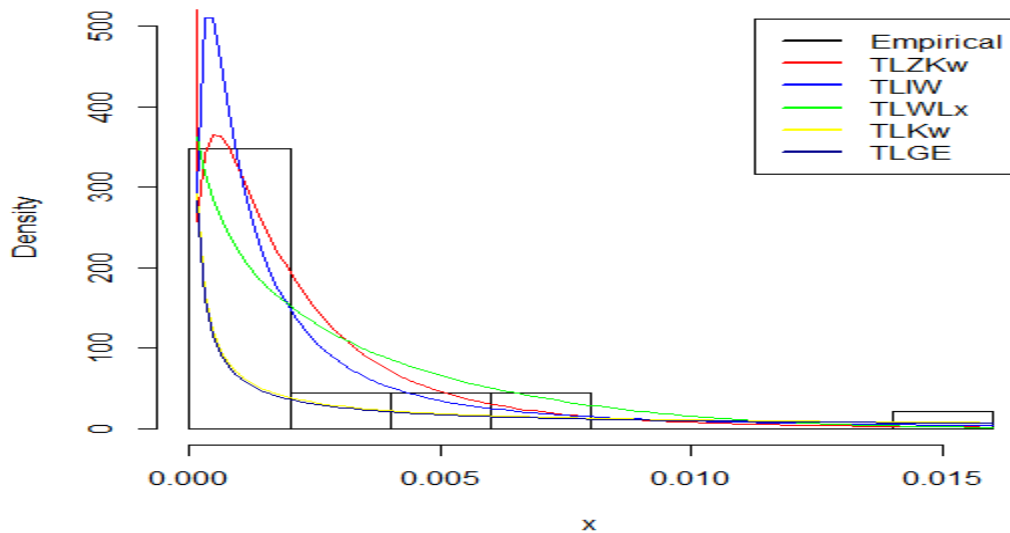


**Figure 5. 14: Histogram and estimated cyber security data**

**5.2.5 Applications of TLZIW**

The waiting times data is applied to TLZIW, the data set is modeled using these models : TLZIW, Topp-Leone inverse Weibull (TLIW) (Salman et al. 2017), Zubair Weibull (ZW), Inverse Weibull (IW) (Calabria and Pulcini 1994), Topp-Leone generalized exponential (TLGE), Topp-Leone Weibull Lomax (TLWLx), exponentiated generalized exponential (EGE) and Weibull (W).

In Table 5.27, it shows the average waiting times of the data as 39.8281 per second. The data is positively skewed with kurtosis of 2.5921.

**Table 5. 27: Descriptive Statistics of waiting times data**

| Dataset | Min | Max | Mean | Std. Dev. | Skewness | Kurtosis |
|---------|-----|-----|------|-----------|----------|----------|
| Waiting  times | 7.000 | 169.0000 | 39.8281 | 33.7505 | 1.5103 | 2.5921 |

The dataset shows   a bathtub failure rate. The TTT transform plot in Figure 5.15 is concave on the 45 degrees line.
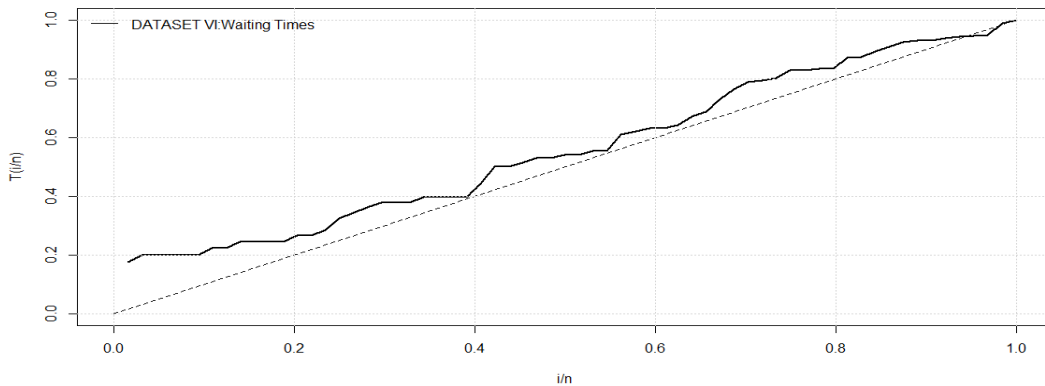


**Figure 5. 15: TTT Transform plot of Waiting Times data**

107

In Table 5.28, it shows that the estimated parameters on the waiting times data show significance at 5% level of significance, except for one of the parameters of TLZIW , two parameters of EGE and four of the TLWLx.

**Table 5. 28: Maximum likelihood estimates of waiting times data**

| Model | Parameter | Estimate | Standard Error | z-value | p-value |
|---|---|---|---|---|---|
| **TLZIW** | $\hat{\alpha}$ | 4.2984 | 1.9036 | 2.2581 | 0.02394 * |
| | $\hat{\beta}$ | 109.8955 | 81.1952 | 1.3535 | 0.17590 |
| | $\hat{\gamma}$ | 1.5393 | 0.1984 | 7.7604 | $8.465 \times 10^{-15}$ * |
| | $\hat{\lambda}$ | 0.2542 | 0.1088 | 2.3367 | 0.01946 * |
| TLIW | $\hat{\beta}$ | 142.0229 | 168.7576 | 0.8416 | 0.4000 |
| | $\hat{\gamma}$ | 1.1059 | 0.1492 | 7.4125 | $1.24 \times 10^{-13}$ * |
| | $\hat{\lambda}$ | 0.2177 | 0.2107 | 1.0331 | 0.3015 |
| ZW | $\hat{\alpha}$ | 57.0051 | 0.0024 | 24008.984 | $< 2.2 \times 10^{-16}$ * |
| | $\hat{\beta}$ | 0.2693 | 0.0242 | 11.105 | $< 2.2 \times 10^{-16}$ * |
| | $\hat{\gamma}$ | 2.1020 | 0.16667 | 12.611 | $< 2.2 \times 10^{-16}$ * |
| IW | $\hat{\beta}$ | 48.7580 | 17.4430 | 2.7953 | 0.0052 * |
| | $\hat{\gamma}$ | 1.3275 | 0.1293 | 10.2634 | $< 2.2 \times 10^{-16}$ * |
| TLGE | $\hat{\alpha}$ | $1.4017 \times 10^{-02}$ | $2.5750 \times 10^{-03}$ | 5.4435 | $5.225 \times 10^{-08}$ * |
| | $\hat{\beta}$ | $2.5749 \times 10^{-01}$ | $3.3861 \times 10^{-02}$ | 7.6043 | $2.865 \times 10^{-14}$ * |
| | $\hat{\lambda}$ | $1.1799 \times 10^{+01}$ | $4.6565 \times 10^{-04}$ | 25339.9044 | $< 2.2 \times 10^{-16}$ * |
| TLWLx | $\hat{\alpha}$ | 1.7447 | 1.6562 | 1.0534 | 0.2921 |
| | $\hat{\beta}$ | 1.4607 | 5.0759 | 0.2878 | 0.7735 |
| | $\hat{\gamma}$ | 0.1859 | 0.1581 | 1.1756 | 0.2397 |
| | $\hat{\lambda}$ | 4.7929 | 9.0878 | 0.5274 | 0.5979 |
| EGE | $\hat{\alpha}$ | 0.0569 | 0.3827 | 0.1487 | 0.8818 |
| | $\hat{\beta}$ | 1.7308 | 0.3197 | 5.4134 | $6.185 \times 10^{-08}$ * |
| | $\hat{\lambda}$ | 0.6146 | 4.1335 | 0.1487 | 0.8818 |
| W | $\hat{\beta}$ | 1.2620 | 0.1194 | 10.5657 | $< 2 \times 10^{-16}$ * |
| | $\hat{\gamma}$ | 0.0086 | 0.0044 | 1.9676 | 0.04911 * |

Significance at 5% is indicated as: *

In Table 5.29, the results of maximum likelihood estimates are presented. The goodness of fit shows that the TLZIW has smaller values of AIC, BIC, AICc, W*, A*  and K-S than TLIW, ZW, IW, TLGE, TLWLx, EGE and W. This implies that TLZIW is better and appropriate for modeling the waiting times.

**Table 5. 29**: **Goodness-of-fit for waiting times data**

| Model | AIC | BIC | AICc | $W^*$ | $A^*$ | K-S | P-Value |
|---|---|---|---|---|---|---|---|
| **TLZIW** | **589.8260** | **598.4615** | **590.5039** | **0.0785** | **0.5935** | **0.0750** | **0.8642** |
| TLIW | 593.6580 | 600.1347 | 594.0580 | 0.1331 | 0.9515 | 0.0956 | 0.6029 |
| ZW | 594.1804 | 600.6570 | 594.5804 | 0.1222 | 0.8892 | 0.0974 | 0.5777 |
| IW | 595.0162 | 599.3339 | 595.2129 | 0.1826 | 1.2501 | 0.1005 | 0.5380 |
| TLGE | 595.1706 | 601.6472 | 595.5706 | 0.1122 | 0.8080 | 0.1123 | 0.3953 |
| TLWLx | 595.6701 | 604.3056 | 596.3480 | 0.1106 | 0.8131 | 0.0924 | 0.6460 |
| EGE | 597.3321 | 603.8087 | 597.7321 | 0.1288 | 0.9010 | 0.1227 | 0.2905 |
| W | 597.8110 | 602.1287 | 598.0077 | 0.1464 | 1.0036 | 0.1077 | 0.4484 |

The histogram plots and estimates PDF of TLZIW and other fitted distribution for waiting times data is presented in Figure 5.16. The plot shows that the TLZIW provides better fit to the waiting times data.
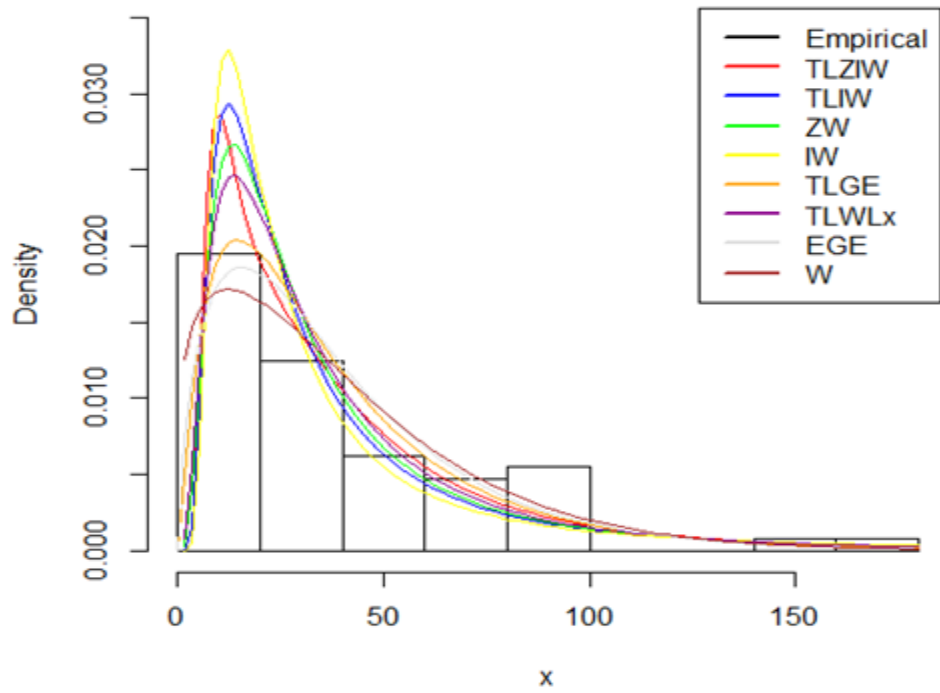
**Figure 5. 16: Histogram and estimated densities for waiting times data**

**5.2.6 Application of  TLZLx_R**

The transformer turn data were modeled using the TLZLx regression (TLZLX_R) model. The descriptive statistics in Table 5.30 shows the transformer data to have an average time of   135.6833 hours,   positive skewness of 2.4884, and kurtosis of 5.2136.

**Table 5. 30: Descriptive Statistics   of transformer turn data**

| Dataset | Min | Max | Mean | Std. Dev. | Skewness | Kurtosis |
|---|---|---|---|---|---|---|
| Transformer data | 0.6000 | 1002.3000 | 135.6833 | 261.8842 | 2.4884 | 5.2136 |

The transformer data shows a bathtub failure rate. This is seen in Figure 5.17 where the TTT transform plot shows convex below the 45 degrees line.
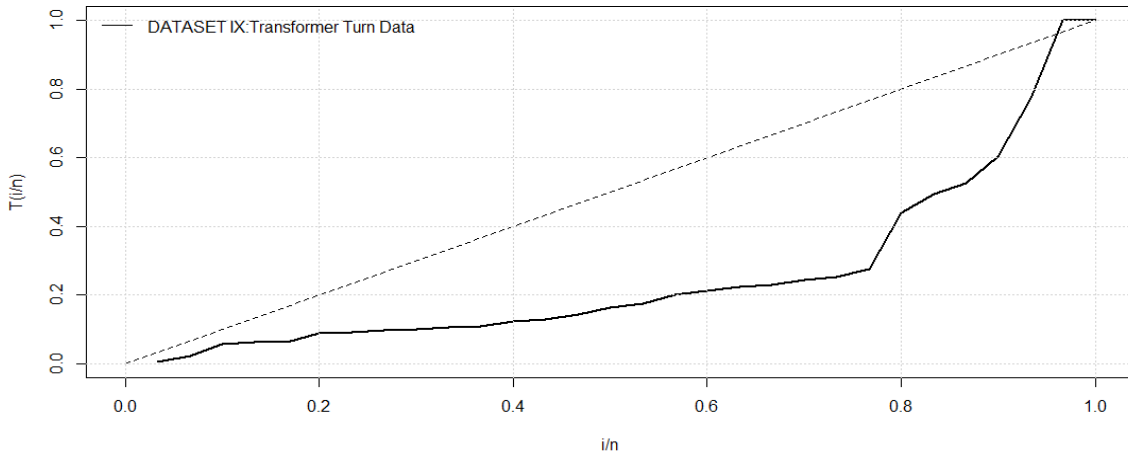


**Figure 5. 17: TTT transform plot of transformer turn data**

The study compares the following models: TL Zubair Lomax Regression (TLZLx_R), TL Gomperz Lomax Regression (TLGLx_R) (Sangsanit et al., 2016) and Gomperz Lomax Regression ( GLx_R) (Oguntunde 2017). Table 5.31 shows results of maximum likelihood estimates, standard errors and p-values. The results of the TLZ_R implies that, in subjecting the transformer to 35.4 Kv, there is a significant increase in the failure rate of the transformer by 2.8944. Also, at 42.4Kv, there is a significant increase of the transformer failure rate by 0.7414 with   insignificant constant increase of 1.0999. The result generally suggests that, subjecting the transformer to different voltage levels has different effects. Hence, the presence of the regressive parameters are in good place to estimate for these effective differences in the failure rates for 35.4 .Kv and 42.4 Kv independent voltage factor levels.

**Table 5. 31: Maximum likelihood estimates of Transformer Turn Censored Data**

| Model | Parameter | Estimate | Standard Error | z-value | p-value |
|---|---|---|---|---|---|
| **TLZLx_R** | $\hat{\alpha}$ | 9.6351 | 10.0557 | 0.9582 | 0.3379 |
| | $\hat{\beta}$ | 1.2519 | 0.4199 | 2.9815 | 0.0029* |
| | $\hat{\lambda}$ | 0.4301 | 0.4108 | 1.0470 | 0.2951 |
| | $\hat{\tau}0$ | 1.0999 | 0.9494 | 1.1584 | 0.2467 |
| | $\hat{\tau}1$ | 2.8944 | 0.4786 | 6.0482 | $1.465 \times 10^{-09}$* |
| | $\hat{\tau}2$ | 0.7414 | 0.4225 | 1.7548 | 0.0492* |
| TLGLx_R | $\hat{\alpha}$ | 0.2330 | 0.1449 | 1.6078 | 0.10789 |
| | $\hat{\beta}$ | 0.0817 | 0.0841 | 0.9713 | 0.33141 |
| | $\hat{\lambda}$ | 1.5650 | 0.7779 | 2.0117 | 0.04425 |
| | $\hat{\tau}0$ | -16.0651 | 0.9850 | -16.3096 | $< 2.0 \times 10^{-16}$* |
| | $\hat{\tau}1$ | -0.0104 | 0.8444 | -0.0124 | 0.99011 |
| | $\hat{\tau}2$ | -1.8744 | 24.1138 | -0.0777 | 0.93804 |
| GLx_R | $\hat{\alpha}$ | 0.8676 | 2.9644 | 0.2927 | 0.7697 |
| | $\hat{\beta}$ | 0.0377 | 0.0226 | 1.6709 | 0.09474 |
| | $\hat{\lambda}$ | 0.8805 | 3.0509 | 0.2886 | 0.7728 |
| | $\hat{\tau}0$ | -12.0952 | 28.2851 | -0.4276 | 0.6689 |
| | $\hat{\tau}1$ | -11.1954 | 23.8355 | -0.4697 | 0.6385 |
| | $\hat{\tau}2$ | -7.1001 | 0.05282 | -134.3983 | $< 2 \times 10^{-16}$* |

Significance at 5% is indicated as: *

The goodness of fit test in Table 5.32 shows the AIC and BIC results for TLZLx_R ,
TLGLx_R and GLx_R. It is seen that TLZLx_R is better for modeling transformer data.
This is because it has smaller values of AIC and BIC than the competitive models.

114

**Table 5.32: Goodness-of-fit for Transformer Turn Censored Data**

| Model | AIC | BIC |
|-------|-----|-----|
| **TLZLx_R** | **272.7620** | **281.1692** |
| TLGLx_R | 296.6745 | 305.0817 |
| GLx_R | 297.5820 | 305.9892 |

Cox-Snell residual analysis was conducted to see how the TLZLx_R model fits the Transformer Turn data against the other competitive models. In this case, if the model fits the data, the Cox-Snell residual is expected to follow a standard exponential distribution. The test results in Table 5.33 shows that the Cox-Snell residual of TLZLx_R follows the standard exponential better than TLGLx_R and GLx_R . The TLZLx_R has the smallest value of K-S and the highest P-value among the competitive models.

**Table 5.33: Standard exponential test results of Cox-Snell residual**

| Model | K-S | P-Value |
|-------|-----|---------|
| **TLZLx_R** | **0.1124** | **0.8433** |
| TLGLx_R | 0.1296 | 0.6950 |
| GLx_R | 0.1403 | 0.5960 |

Hence, using the standard exponential distribution to compute the CDF of the Cox-Snell residual  and plotting it against the empirical CDF of the Cox-Snell residuals is expected to cluster along the diagonal. The P-P plot of the Cox-Snell residual of TLZLx_R  is seen in Figure 5.18 to cluster along the diagonal more better than TLGLx_R and GLx_R. The TLZLx_R  shows a better fit to the Transformer Turn data.
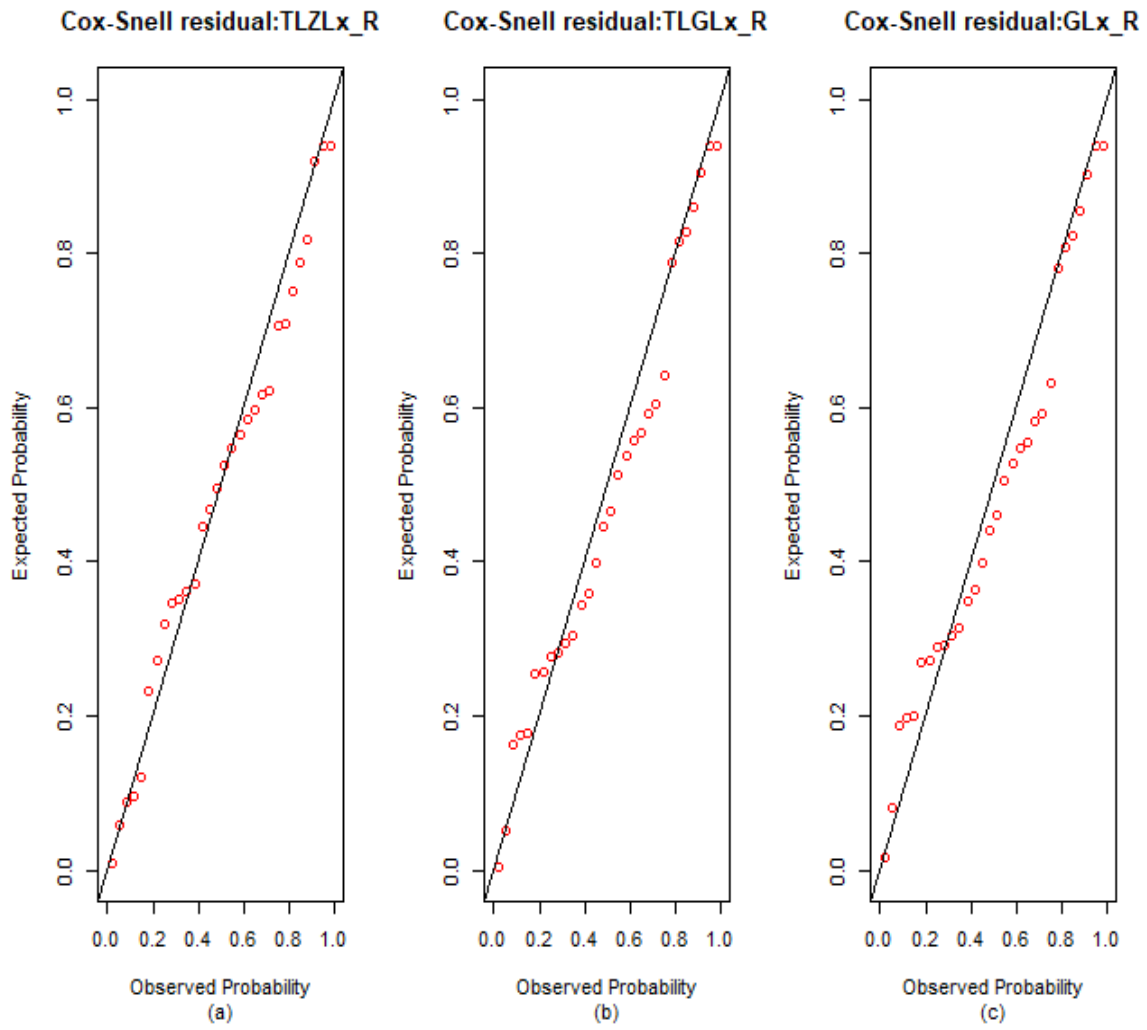
**Figure 5.18: Theoritical and empirical probabilities of Cox-Snell residual for: (a) TLZLx_R , (b) TLGLx_R and (c) GLx_R.**

### 5.3 Summary of Chapter Five

In this chapter, the simulation studies and empirical applications were presented. In the simulation study of the special distributions, when sample size was made to increase, there was responsive decrease of   average bias and that of root mean square error. The special distributions: TLZNH, TLZLx, TLZW, TLZKw, TLZIW and TLZLx_R, were subjected to data applications, all of them were better than their competitive distributions. The results show that the special models are appropriate for modeling several lifetime data from different application fields.

# CHAPTER SIX

# SUMMARY, CONCLUSIONS AND RECOMMENDATIONS

## 6.1 Introduction

This chapter presents the summary, conclusions and recommendations of the entire study.

## 6.2 Summary of Results

This section gives the summary of results based on the specific objectives. In all, there were five objectives.

**Objective one results:** The TLZ generator was developed. The new generator possessed at least one scale parameter and one shape parameter. The CDF, PDF and the hazard functions were primarily derived. Furthermore, six new models were derived from the TLZ generator. These new models were TLZNH, TLZLx, TLZW, TLZKw, TLZIW and the TLZLx_R. Each of the new models at least had a scale parameter and a shape that made them flexible enough to exhibit symmetrical, right skewed and left skewed illustrated by the PDF plots. The models also exhibited bathtub shape, upside down bathtub shapes by virtue of their hazard function plots.

**Objective two results:** The statistical properties of the TLZ generator were derived. These includes the moment generating function, quantile function, incomplete moments, moments, mean and median deviations, inequality measures, mean residual life, stochastic ordering, stress- strength reliability and order statistics.

UNIVERSITY FOR DEVELOPMENT STUDIES

**Objective three results:** The parameter estimators were derived. The maximum likelihood technique was used in this case. The score functions were derived from the total log likelihood function.

**Objective four results:** Simulation study was conducted to study the behavior of the parameter estimators. In the simulation study of the special distributions, whiles sample size was made to increase, there was responsive decrease of   average bias and that of root mean square error. This satisfied the consistency property of the maximum likelihood estimator.

**Objective five results:** In this last objective, the applications of the new models to real life data set. The special distributions: TLZNH, TLZLx, TLZW, TLZKw and TLZIW were subjected to data applications against some competitive models. The best model was however selected based on smaller AIC, BIC, Cramér-von and Mises test and Komogorov-smirnov values. The extent to which the models mimic density of the data was also illustrated through histogram plots. The TLZNH was subjected to the failure times data against competitive models: GPGW, EPGW, PGW, ENH and GNH. It was further subjected to the maximum stress data against competitive models: TLGE, GE and EGE. The TLZNH was better in both two data applications. The TLZLx was also applied to the survival times data against competitive models: TLWLx, TLLx, WLx and GLx. The TLZLx was better than the competing models.   The TLZW was applied to the breaking stress data against competitive models: TLGE, GE and EGE. It was again subjected to the windshield servicing times data against the competitive model: TLWLx, TLLx, ELx and GLx. All two data presented the TLZW to be better. The

TLZKw was also applied to the milk production data and the cyber security data respectively against the models: TLKw, ZKw, Kw, W, ZW,TLGE, TLLx and TLIW, TLWLx, TLKw, TLGE. Furthermore, the TLZIW was applied to the waiting times data against competitive models: TLIW, ZW, IW, TLGE, TLWLx, EGE and W . The model was better than the competitive models. In a similar way, the TLZLx_R, was applied to model the transformer turn censored data which had independent factors. The TLZLx_R, which is a parametric regression model, was better than its competitive model, thus TLGLx_R and GLx_R. The results show that the special models are appropriate for modeling several lifetime data from different application fields.

## 6.3 Conclusions

In this study, the TLZ-G family was developed with desirable statistical properties and well behaved parameter estimators. The special models, TLZNH, TLZW, TLZKw, TLZIW and TLZLx based on the family demonstrated well in modeling. This is due to the presence of both shape parameter and scale parameters inherited from the TLZ-G family. The models are capable of controlling skewness, kurtosis and variability, hence, permitting modeling of several lifetime data sets. Specifically:

- The special models were able to model right skewed, left skewed and symmetrical data sets.

- The hazard functions of the special models demonstrated bathtub and upside down bathtub characteristics. Hence they were able to model monotonic and non-monotonic data sets.

- The quantile function of the special models had closed forms, hence made generations of random numbers easier in simulation processes.

- The MLE of the special models exhibited consistency; thus, the average bias and root mean square error were decreasing when sample size was increasing.

- The special models fitted several data sets and they were all better than their competing models.

**6.4 Recommendations**

- Further studies may employ the TLZ-G generator to modify and study the properties of other existing distributions to model lifetime data.

- The bivariate extensions for the special distributions can be done to model bivariate data, for example studying some characteristic dependencies of age and employment.

- Also, further studies can look at the mixture distributions of the special models. In such case, different samples that come from the same population can be modeled. An example is modeling the failure rate of an aircraft that has right side and left side cooling systems.

- Further studies can also extent the special distributions to model extreme value events, for example, times of volcanic eruptions and river floods.

# REFERENCES

Aarset, M. (1987). How to identify a bathtub hazard rate. *IEEE Transactions on Reliabiliy*, 36(1):102-109.

Ahmed, A. O. M., Al-Kutubi, H.S., and Ibrahim, N. A. (2010). Comparison of the Bayesian and maximum likelihood estimation for Weibull distribution. Journal of Mathematics and Statistics , 2:100-104.

Akaike, A. (1973). Information theory aand an extension of the maximum likelihood principle. *International symposium on information theory, 2nd, Tsahkadsor,American SSR*: 239-290.

Akaike, A. (1974). A new look at the statistical model identifcation. IEEE Transactionson Automatic Control, 19(6):716-723.

Al-Fattah, A., El-Helbawy, A., Al-Dayian, G., (2017). Inverted Kumaraswamydistribution: properties and estimation. Pak. J. Stat. 33 (1)

Alizadeh,M. Emadi, M.Doostparast,M. Cordeiro,G. M. Ortega,E. Pescim, R. (2015b). A new family of distributions: The Kumaraswamy odd log-logistic,properties and applications. Hacettepe Journal of Mathematics and Statistics, 44, pp.1491–1512.

Alshawarbeh, E., Lee, C., and Famoye, F. (2012). The beta -Cauchy distribution. *Journal of Probability and Statistical Sciences*, 10(1):40-60.

Al-Zahrani, B. (2012). Goodness-of-fit for the Topp-Leone distribution with unknown parameters. *Applied Mathematical Science*, 6(128):4-9

Amal H., Elsayed E., Rokaya M., (2019). Odd Generalized Exponential Power Function Distribution: Properties and Applications. *Journal of Science.* 32(1): 351-370

Atkinson A. B.(1970) On the measurement of inequality, *Journal of Economics Theory* 2 (1970): 244–263.

Barlow, R. E.,  Doksum, K. A. (1972). Isotonic tests for convex orderings. *In proceedings of the 6th Berkeley symposium, volume 1*, pages 294-325.

Beno, I. (2018). Comparison of Parameter Estimation Methods to Determine the Frequency Data Magnitude of Aftershock in Nabire, Papua. *Journal of Science and Science Education*, 5: 2-4.

Birnbaum, Z. W.,  Saunders, S. C. (1969). Estimation for a family of life distributions with applications to fatique. *Journal of Applied Probability*, 6:321-350.

Bonferroni, C.E.(1930). Elementi di statistica general, Libereria Seber, Firenze, 1930. Page 5-9

Braga, A.S.; Cordeiro, G.M.; Ortega, E.M.M.; Silva, G.O.(2017). The Odd Log-Logistic Student t Distribution: Theory and Applications. J. Agricultural Biological Environmental  Statistics. 2017, 22, 615–639.

Bjerkedal , T . (1960) . Acquisition of resistance in guinea pigs infected with different doses of virulent tubercle bacilli. M. J. Hyg, 72:130-148.

Calabria, R. and Pulcini, G.(1994). Bayes 2-sample prediction for the Inverse Weibull distribution. *Communications in Statistics-theory and Methods*. 23(6):1811-1824, 1994.

Cordeiro, G.M., Castro, M. (2011). "A New Family of Generalized Distributions." *Journal of Statistical Computation and Simulation*, 81: 883–898.

Cordeiro, G.M., Ortega, E.M.M and Cunha D.C.C. (2013d). "The Exponentiated Generalized Class of Distributions." *Journal of Data Science,* 11: 1–27.

Cordeiro, GM, Ortega, E.M.M, Silva, G. (2012c). "The Beta Extended Weibull Family." *Journal of Probability and Statistical Science,* 10: 15–40.

Cordeiro, G. M., Ortega, E. M.,  Cunha, D. C. (2013). The expenentiated Generalized Class of Distribuion . ." *Journal of Data Science,* 3: 5–22.

Cordeiro, G. M., Ortega, E. M.,  Silva, G. O. (2012). The beta-extended Weibull family. *Journal of Probability and Statistical Science*, 10(10):15-40.

Cordeiro, G.M., Nadarajah, S. and Ortega, E.M. (2013). General Results for the Beta Weibull Distribution. *Journal of Statistical Computation and Simulation*, 83: 1082-1114.

Cordeiro, G.M., Ortega, E.M. and Nadarajah, S. (2010). The Kumaraswamy Weibull Distribution with Application to Failure Data. *Journal of the Franklin Institute*, 347: 1399-1429.

Cordeiro, G.M., Ortega, E.M. and Nadarajah, S., (2010). The Kumaraswamy Weibull distribution with application to failure data. *Journal of the Franklin Institute*, 347(8): 1399-1429.

Cordeiro, G.M.; Alizadeh, M.; Ozel, G.; Hosseini, B.; Ortega, E.M.M.; Altun, E.(2017). The generalized odd log-logistic family of distributions: Properties, regression models and applications. J. Statistical Computation Simulation.2017, 87, 908–932.

Cramér-Von and  Mises, R. (1928). On the composition of elementary errors. *Skand. Akt*, 11:141-180.

Cox, D. R. (1972). Regression models and life-tables.Journal of the Royal StatisticalSociety, series B, 34(2):187–220.

Cox, D. R. and Snell, E. J. (1968).  A general definition of residuals. Journal of theRoyal Statistical Society, series B, 30(2):248–275.

Da Cruz, J.N.; Ortega, E.M.M.; Cordeiro, G.M.(2016). The log-odd log-logisticWeibull regression model: Modelling, estimation, influence diagnostics and residual analysis.Journal of Statistical Computation and Simulation. 2016, 86, 1516–1538.

Da Cruz, J.N.; Ortega, E.M.M.; Cordeiro, G.M.; Suzuki, A.K.; Mialhe, F. L. (2017). Bivariate odd-log-logistic-Weibullregression model for oral health-related quality of life. Communication Statistical Applications and Methods 2017, 24, 271–290.

De Brito, E., Cordeiro, G. M., Yousof, H. M., Alizadeh, M. and Silva , G. O. (2017). Topp-Leone odd log-logistic family of distributions, Journal of Statistical Computation and Simulation, forthcoming. Page 9.

Dey, S., Ghosh, I., & Kumar, D. (2018). Alpha-Power Transformed Lindley Distribution: Properties and Associated Inference with Application to Earthquake Data. Annals of Data Science, 1-28.

Dey, S., Nassar, M., & Kumar, D. (2019). Alpha power transformed inverse Lindley distribution: A distribution with an upside-down bathtub-shaped hazard function. Journal of Computational and Applied Mathematics, 348, 130-145.

Eugene, N., Lee, C., Famoye, F. (2002). "Beta-normal distribution and its applications", Communication in Statistics – Theory and Methods 31: 497–512, (2002).

Famoye, F., Lee, C. and Olumolade, O. (2005). The Beta-Weibull Distribution. *Journal of Statistical Theory and Applications*, 4: 121-138.

Famoye, F., Olumolade, O.,  Lee, C. (2005). The beta-Weibull distribution. *Journal of statistical theory and applications*, 4(2):120-134.

Farrukh J., Hesham M. R., Arslan  N., Christophe  C.,  Akbar A.,(2019).  Topp-Leone Weibull-Lomax distribution: Properties, Regression Modeland Applications.02270561:3-15

Fernando A. Peña-Ramírez, Renata R. Guerra, Gauss M. Cordeiro And Pedro R.D. Marinho (2017). The Exponentiated Power Generalized Weibull: *Properties and Applications. Anais da Academia Brasileira de Ciências* . 90(3): 2553-2577

Freimer, M., Lin, C. T., Mudholkar, G. S., Kolha, G. (1988). A study of the generalized Tukey lambder family:*Communications in Statistics-theory and Methods*. Pages 3533-3551.

Ghitany, M. E. (2005). On some reliability measures and their stochastic ordering for the Topp-Loene distribution. *Journal of Applied Statistics*, 1:710-724.

Gleaton, J.U.; Lynch, J.D.(2006). Properties of generalized log-logistic families of lifetime distributions. Jounal of Probabability Statistical Science. 2006, 4, 51–64.

Gupta, RC, Gupta, PL, Gupta, R.D. (1998). "Modeling Failure Time Data by Lehman Alternatives." Communications in Statistics – *Theory and Methods*, 27: 887–904.

Gupta, R. D., Gupta, P. L., Gupta, R. C. (1998). Modeling failure time data by Lehman alternatives. *Communication statistics-Theory and Methods*, 27:(4): 888-910.

Gupta,R.D.,and Kundu,D.(1999). Generalized exponential distributions, Australian and New Zealand. *Journal of Statistics,* 41:173-188

Hadeel, S. (2019). The Weibull-Gamma Distribution: Properties and Applications. *MDPI*: 1-15.

Haitham, M. Y. Mustafa Ç. K. (2017). Topp-Leone Nadarajah-Haghighi distribution. *Journal of Statisticians: Statistics and Actuarial Sciences* IDIA , 10: 119-128

Hassan, A. S., Elgarhy, M., Mohamd, R. E., & Alrajhi, S. (2019). On the Alpha Power Transformed Power Lindley Distribution. Journal of Probability and Statistics, 2019.

Hogg, R. V. and Craig, A. T.(2012). Introduction to Mathematical Statistics, 7th ed. New York: Macmillan, 2012.

Hurvich, C. M.,  Tsai, C. (1989). Regression and time series model selection in small samples. *Biometrika*, 76(1-3):146-176.

Jones, M. (2009). Kumaruswamy's distribution: a beta-type distribution with tractability advantage. *statistical methodology*, 6(1):71-81.

Jones, M. C. (2004). The complementary beta distribution. *Journal of statistical planning and inference*, pages 329-338.

Jones, M.C. (2004). Families of distributions arising from the distributions of order statistics. Test 13:1–43.

Kaplan, E. L. Meier, P. (1958). Nonparametric estimation from incomplete observations. *Journal of the American Statistical Association*. 53 (282): 457–481.

Kareema, A., and Maysaa H., M., (2017). The General Formula of The Transmuted Distribution. *Journal of Babylon University/Pure and Applied S ciences*. No.(3) Vol.(25).

Keeping, E. and Kenney, J. (1962). Mathematics of Statistics. Volume 1, D. Van Nostrand Company, Princeton. Page 13-34

Kotz, S., Seier, E. (2007). Kurtosis of the Topp-Leone distributions with some tractability advantages. . *Interstat*. Pages 3-5

Kumaraswamy, P. (1980). A Generalized Probability Density Function for Double-Bounded Random Processes . *Journal of Hydrology*, 46: 79-88.

Lee, S., Alzaatreh, A., Famoye, F. (2013). Methods for generating famalies of univariate continuous distribution in recent decades. *WIREs Computationsl Statistics*, 5:217-248.

Lemonte, A. J.(2013). A new exponential-type distribution with constant, decreasing, increasing, upside down bathtub and bathtub-shaped failure rate function, Computational Statistics and Data Analysis, 62: 149-170.

Lemonte, A. J., Cordeiro G. M. , Moreno-Arenas G.(2016). A new useful three parameter extension of the exponential distribution, Statistics, 50: 312.337.

Lemonte, AJ, Barreto-Souza W, Cordeiro GM (2013). "The Exponentiated Kumaraswamy Distribution and Its Log-Transform." Brazilian Journal of Probability and Statistics, 27: 31–53.

Lemonte, A. J. (2013). A new exponential-type distribution with constant, decreasing, increasing, upside down bathtub and bathtub-shaped failure rate function, Computational Statistics & Data Analysis, 62, 149-170.

Lorenz M.O. (1905). Methods of measuring the concentration of wealth, *Publication of American Statistical Association*, pages 4-7.

Mahdavi, A., Kundu, D. (2017). A new method for generating distributions with an application to exponential distribution. Commun Stat Theory Methods 46(13):6543–6557

Marshall, A. W. and Olkin, I. (1997). A new methods for adding a parameter to a family of distributions with application to the exponential and Weibull families. Biometrika, 84, pp. 641–652.

McAfee Incorporation. (2014), Net losses: estimating the global cost of cybercrime report- economic impact of cybercrime II. *Center for Strategic and International Studies.* Page 22

Moors, J. J. A. (1987). A quantile alternative for kurtosis. (Ter discussie FEW; . 87.08): 3-7.

Morais, A. L., Cordeiro, G., A, C. A. (2013). The beta generalized logistic distribution. *Brazilian Journal of probability and statistics*, 27(2):187-200.

Nadarajah, S, Cancho V.G, Ortega E. M. M. (2013a). "The Geometric Exponential Poisson Distribution." *Statistical Methods and Applications*, 22: 355–380.

Nadarajah, S., Kotz, S. (2004). The beta Gumbel distribution. *Mathematical problems in engineering*, 4:320-333.

Nadarajah, S, Nassiri V, Mohammadpour A (2013b). "Truncated-Exponential SkewSymmetricDistributions."Statistics: *A Journal of Theoretical and AppliedStatistics*,48(4): 872–895.

Nadarajah, S., Teimouri M., Shih S.H. (2014). "Modified Beta Distributions." *Far East Journal of Theoritical Statistics*,76(1): 19–48.

Nadarajah, S., Gupta, A. K. (2004). The beta Fretchet distribution. *Far East Journal of Theoritical Statistics*, 14(1): 13-25.

Nadarajah, S., Kotz, S. (2003). Moments of some J-shaped distributions. *Journal of Applied Statistics*, 300-324.

Nadarajah, S., Kotz, S. (2005). The beta-exponential distribution. *Reliability Engineering and system safety*, 91(6):670-698.

Nadarajah, S., Kotz, S. (2006). The exponential type dstribution. *Acta Applicandae Mathematica*, 92:(2):99-121.

Nasir, A., Bakouch, H. S., and Jamal, F. (2018). Kumaraswamy odd Burr G family of distributions with applications to reliability data. Studia Scientiarum Mathematicarum Hungarica, 55(1), 94-114.

Nasiru, S. (2018). Extended Odd Frechet-G Family of Distributions. *Journal of Probability and Statistics*, 2018:1-2.

Nasiru, S., Mwita, P. N. and Ngesa, O. (2019). Alpha Power Transformed Frechet Distribution. Applied Mathematics & Information Sciences, 13(1):129-141.

Navarro, J., Hernandez P.J., (2008). Mean residual life functions of finite mixtures, order statistics and coherent systems. *Metrika* 67(3):277–298.

Nelson, Wayne , B. Accelerated testing: statistical models , test plans, and data analysis, John Wiley and Sons, 2004. Page 15.

Nichols, M. D., and Padgett, W.J. (2006). A bootstrap control chart for Weibull percentiles, Quality and Reliability Engineering International, 22, 141–151.

Nikulin, M., and F. Haghighi. (2009). On the power generalized Weibull family: model for cancer censored data. Metron 67 (1):75-86.

Oguntunde, P. E., Khaleel, M. A., Ahmed, M. T., Adejumo, A. O. and Odetunmibi, O. A. (2017). A New generalization of the Lomax distribution with increasing, decreasingand constant failure rate. *Modelling and Simulation in Engineering,* Article ID 6043169, 6 pages.

Ortega, E. M. M, Lemonte A. J. , Silva G. O. , Cordeiro G. M.(2015) New flexible models generated by gamma random variables for lifetime modelling, *Journal of Applied Statistics*, 42: 2159-2179.

Prataviera, F.; Ortega, E.M.M.; Cordeiro, G.M.; Braga, A.S.(2018) The heteroscedastic odd log-logistic generalized gamma regression model for censored data. Communications in Statistics - Simulation and Computation 2018, 48, 1–25.

Pinho, L.G.B.; Cordeiro, G.M.; Nobre, J.S.(2015) The Harris extended exponential distribution. *Communications in statistics-theory and methods*, 44, 3486–3502.

Rahman A, N. S. and El-Bassiouny, A.H. (2017). On the alpha-power exponential Weibull distribution, The 2nd National of Mathematics and Its Applications (NCMA17), 1-18.

Ramadan and Walaa (2018). On the Alpha-Power Inverse Weibull Distribution.International Journal of Computer Applications, 181(11) page 1-8

Salman, A., Syed, A. T., Fakhar M., Maryum,  M., Muhammad, Q. S. (2017). Topp-Leone Inverse Weibull Distribution: Theory and Application. *European Journal of Pure and Applied Mathematics* Vol. 10, No. 5, 2017, 1005-1022.

Sangsanit, Y.,  Bodhisuwam, W. (2016). The Topp-Leone generator of distributions:properties and inferences. *Songklanakarin Journal of Science and Technology*, 539.

Schwarz, G. (1978). Estimating the dimension of a model. *The Annals of statistics*, 460-461.

Selim, M. A (2017). The Generalized Power Gneralized Weibul Distribution: Properries and applications. *arXiv:*1807.10763

Shaw, W.T. and Buckley, I. R. C. (2009). The Alchemy of Probability Distributions: beyond Gram-Charlier Expansions, and a Skew-Kurtotic-Normal Distribution from a Rank Transmutation Map, pp:1-8, Submitted.

Stephens, M. A. (1974). EDF Statistics for Goodness of Fit and Some Comparisons, Journal of the American Statistical Association, 69, pp. 730-737.

Sugiura, G. (1978). Further analysis of data by Akaike's information criteria and the finite correction. *Communications in statistics-theory and methods*, 7(1):12-26.

Tahir, M. H., Cordeiro, G. M., Mansoor, M. and Zubair, M. (2015). The Weibull Lomax distribution: properties and applications. Hacettepe Journal of Mathematics and Statistics, 44(2): 461–480.

Tahir, M., Cordeiro, G.M., Alzaatreh, A., Mansoor, M., Zubair, M., (2016). The Logistic-X family of distributions and its applications. Commun. Stat. Theory Methods 45(24), 7326–7349.

Topp, C. W., Leone, F. (1955). A family of J-shaped frequency functions. *Journal of American Statistical Association*, 50(269),208-220.

Tukey, J. W. (1960). The practical relationship between the common transformations of percentages of counts and amounts. *Technical Report 36, Statistical Techniques Research Group, Princeton University, Princeton, NJ*, 12-19.

Tuner, M. E., Pruit, K. M. (1978). A common basis for survival, growth and autocatalysis. *Mathematical Biosciences*, 39(1): 112-127.

Unal, C., Cakmakyapan, S., and Ozel, G. (2018). Alpha Power InvertedExponential Distribution: Properties and Application. Gazi University Journal of Science, 31(3).

Vatto, V., A, D. N., Miranda, F., M.C.S Lima, P. L., G.M, a. C. (2016). Some Computational and Theoritical Aspects of the Exponentialed Generalized Nadarajah-Haghighi Distribution. *Chilean Journal of Statistics*, 3.

Vicaria, D. D. (2008). Two-sided generalized Topp and Leone distributions. *Journal of Applied Statistics*, 1025-1035.

Von Mises, R. E. (1928). Wahrscheinlichkeit, Statistik und Wahrheit. *Julius Springer, Vienna, Austria.* , 23-19.

Weibull, W. (1951). A Statistical Distribution Function of Wide Applicability. *Journal of Applied Mechanics,* 18, 293-297

Yazar O. M., (2015). An extension of the exponential distribution via Kumaraswamy-G family, Master's thesis, *Recep Tayyip Erdoğan University,* Rize, Turkey.

Yousof, H. M. Ahmed, Z. A. Saralees, N. (2018). The Marshall-Olkin Generalized-G Family Of Distributions With Applications, *Statistica,* anno LXXVIII, n. 3, 2018, page 1-13.

Zea, L. M., Silva, R. (2012). The beta exponentiated Pareto distribution with applications. *International Journal of stattitics and probability*, 1(2):8-20.

Zohdy, M, N., Gebaly, Y. M. (2017). The Generalized Transmuted Weibul Distribution for Lifetime Data. *Pakistan Journal of Statistics and Operation Research*, 356.

Zubair, A. (2018). The Zubair-G Family of Distributions: Properties and Applications. *Springer-Verlag GmbH, Part of Springer Nature 2018*, 3-5.

# APPENDIX A

## PDF AND CDF OF COMPETITIVE MODELS

### WLx_PDF

$$f(x) = \alpha\gamma\beta(1+\beta)^{\alpha\gamma-1}(1-(1+\beta x)^{-\gamma})^{\alpha-1}e^{\left(-\left(\frac{1-(1+\beta x)^{-\gamma}}{(1+\beta x)^{-\gamma}}\right)^{-\alpha}\right)}$$

### WLx_CDF

$$F(x) = 1 - e^{\left(-\left(\frac{1-(1+\beta x)^{-\gamma}}{(1+\beta x)^{-\gamma}}\right)^{-\alpha}\right)}$$

### TLWLx_PDF

$$f(x) = 2\lambda\left(\alpha\gamma\beta(1+\beta)^{\alpha\gamma-1}(1-(1+\beta x)^{-\gamma})^{\alpha-1}e^{\left(-\left(\frac{1-(1+\beta x)^{-\gamma}}{(1+\beta x)^{-\gamma}}\right)^{-\alpha}\right)}\right) \times$$

$$\left(1-e^{\left(-\left(\frac{1-(1+\beta x)^{-\gamma}}{(1+\beta x)^{-\gamma}}\right)^{-\alpha}\right)}\right)\left(1-\left(1-e^{\left(-\left(\frac{1-(1+\beta x)^{-\gamma}}{(1+\beta x)^{-\gamma}}\right)^{-\alpha}\right)}\right)^2\right)^{\lambda-1}$$

### TLWLx_CDF

$$F(x) = [1-(1-(1-\exp\left(-\left(\frac{1-(1+\beta x)^{-\gamma}}{(1+\beta x)^{-\gamma}}\right)^{-\alpha}\right)))^2]^\lambda$$

136

**TLIW_PDF**

$$f(x) = 2\lambda\beta \left( \frac{e^{\frac{-2\beta}{x^\gamma}}}{x^{\lambda+1}} \right) \left( 1 - \left( \frac{\beta}{x^{\lambda+1}} e^{-\frac{\beta}{x^\gamma}} \right)^2 \right)^{\lambda-1}$$

**TLIW_CDF**

$$F(x) = [1 - (1 - (\frac{\beta}{x^{\lambda+1}} e^{-\frac{\beta}{x^\gamma}}))^2]^\lambda$$

**TLLx_PDF**

$$f(x) = 2\lambda\beta\gamma(1+\gamma x)^{-\beta-1} \left( 1 - (1+\gamma x)^{-\beta} \right) \left( 1 - \left( 1 - (1+\gamma x)^{-\beta} \right)^2 \right)^{\lambda-1}$$

**TLLx_CDF**

$$F(x) = [1 - (1 - (1 - (1+\gamma x)^{-\beta}))^2]^\lambda$$

**GE_PDF**

$$f(x) = \beta\alpha(1 - e^{-\alpha x})^{\beta-1} e^{-\alpha x}$$

**GE_CDF**

$$F(x) = (1 - e^{-\alpha x})^\beta$$

**TLGE_PDF**

$$f(x) = 2\lambda\beta\alpha e^{-\alpha x}(1 - e^{-\alpha x})^{\beta(1+\lambda)-2}(1 - e^{-\alpha x}) \left( 1 - (1 - e^{-\alpha x})^\beta \right) \left( 2 - (1 - e^{-\alpha x})^\beta \right)^{\lambda-1}$$

**TLGE_CDF**

$$F(x) = [1 - (1 - (1 - e^{-\alpha x})^\beta)^2]^\lambda$$

137

**GLx_PDF**

$$F(x) = 1 - e^{\left(\frac{\lambda}{\gamma}\right)\left(1-(1+\beta x)^{\alpha\gamma}\right)}$$

**GLx_CDF**

$$f(x) = \lambda\alpha\beta(1+\beta x)^{\alpha\gamma-1}e^{\left(\frac{\lambda}{\gamma}\right)\left(1-(1+\beta x)^{\alpha\gamma}\right)}$$

**TLKw_PDF**

$$f(x) = 2\lambda\gamma\beta x^{\gamma-1}(1-x^\gamma)^{\beta-1}(1-(1-x^\gamma)^\beta)\left(1-\left(1-(1-x^\gamma)^\beta\right)^2\right)^{\lambda-1}$$

**TLKw_CDF**

$$F(x) = [1-(1-(1-(1-x^\gamma)^\beta))^2]^\lambda$$

**ZKw_PDF**

$$f(x) = \frac{2\alpha\gamma\beta x^{\gamma-1}(1-x^\gamma)^{\beta-1}(1-(1-x^\gamma)^\beta)e^{\alpha(1-(1-x^\gamma)^\beta)^2}}{e^\alpha - 1}$$

**ZKw_CDF**

$$F(x) = \frac{e^{\alpha(1-(1-x^\gamma)^\beta)^2} - 1}{e^\alpha - 1}$$

**ZW_PDF**

$$f(x) = \frac{2\alpha(\beta\gamma x^{\beta-1}e^{-\gamma x})(1-e^{-\gamma x^\beta})e^{\alpha(1-e^{-\gamma x^\beta})^2}}{e^\alpha - 1}$$

138

**ZW_CDF**

$$F(x) = \frac{e^{\alpha(1-e^{-\gamma x^\beta})^2} - 1}{e^\alpha - 1}$$

**PGW_PDF**

$$f(x) = \lambda\gamma\omega x^{\gamma-1}(1+\lambda x^\gamma)^{\omega-1} e^{(1-(1+\lambda x^\gamma)^\omega)}$$

**PGW_CDF**

$$F(x) = 1 - e^{(1-(1+\lambda x^\gamma)^\omega)}$$

**GPGW_PDF**

$$f(x) = \lambda\gamma\omega a x^{\gamma-1}(1+\lambda x^\gamma)^{\omega-1} e^{(a(1-(1+\lambda x^\gamma)^\omega))}$$

**GPGW_CDF**

$$F(x) = 1 - e^{(a(1-(1+\lambda x^\gamma)^\omega))}$$

**EGPW_PDF**

$$f(x) = \lambda\gamma\omega\beta x^{\gamma-1}(1+\lambda x^\gamma)^{\omega-1} \frac{e^{(1-(1+\lambda x^\gamma)^\omega)}}{1-e^{(1-(1+\lambda x^\gamma)^\omega)^{1-b}}}$$

**EGPW_CDF**

$$F(x) = (1 - \exp(1-(1+\lambda x^\gamma)^\omega))^b$$

**ENH_PDF**

$$f(x) = \omega\lambda\beta(1+\lambda x)^{\omega-1} e^{1-(1+\gamma x)^\omega}(1-e^{1-(1+\gamma x)^\omega})^{\beta-1}$$

139

**ENH_CDF**

$$G(x) = (1 - e^{1-(1+\lambda x)^{\omega}})^{\beta}$$

**EGE_PDF**

$$f(x) = \beta\alpha\lambda(1 - e^{-\alpha\lambda x})^{\beta-1}$$

**EGE_CDF**

$$F(x) = (1 - e^{-\alpha\lambda x})^{\beta}$$

# APPENDIX B

## DATA

**Appendix B1**: **Failure times of device components**

| 0.1 | 0.2 | 1.0 | 1.0 | 1.0 | 1.0 | 1.0 | 2.0 | 3.0 | 6.0 | 7.0 | 11.0 |
|---|---|---|---|---|---|---|---|---|---|---|---|
| 12.0 | 18.0 | 18.0 | 18.0 | 18.0 | 18.0 | 21.0 | 32.0 | 36.0 | 40.0 | 45.0 | 45.0 |
| 47.0 | 50.0 | 55.0 | 60.0 | 63.0 | 63.0 | 67.0 | 67.0 | 67.0 | 67.0 | 72.0 | 75.0 |
| 79.0 | 82.0 | 82.0 | 83.0 | 84.0 | 84.0 | 84.0 | 85.0 | 85.0 | 85.0 | 85.0 | 85.0 |
| 86.0 | 86.0 | | | | | | | | | | |

**Appendix B2: Maximum stress per 31,000psi**

| 70 | 90 | 96 | 97 | 99 | 100 | 103 | 104 | 104 | 105 | 107 | 108 |
|---|---|---|---|---|---|---|---|---|---|---|---|
| 108 | 108 | 109 | 109 | 112 | 112 | 113 | 114 | 114 | 114 | 116 | 119 |
| 120 | 120 | 120 | 121 | 121 | 123 | 124 | 124 | 124 | 124 | 124 | 128 |
| 128 | 129 | 129 | 130 | 130 | 130 | 131 | 131 | 131 | 131 | 131 | 132 |
| 132 | 132 | 133 | 134 | 134 | 134 | 134 | 136 | 136 | 137 | 138 | 138 |
| 138 | 139 | 139 | 141 | 141 | 142 | 142 | 142 | 142 | 142 | 142 | 144 |
| 144 | 145 | 146 | 148 | 148 | 149 | 151 | 151 | 152 | 155 | 156 | 157 |
| 157 | 157 | 157 | 158 | 159 | 162 | 163 | 163 | 164 | 166 | 166 | 168 |
| 170 | 174 | 201 | 212 | | | | | | | | |

**Appendix B3: Survival times of guinea pigs**

| | | | | | | | | | | | |
|---|---|---|---|---|---|---|---|---|---|---|---|
| 0.10 | 0.33 | 0.44 | 0.56 | 0.59 | 0.72 | 0.74 | 0.77 | 0.92 | 0.93 | 0.96 | 1.00 |
| 1.00 | 1.02 | 1.05 | 1.07 | 07 | 0.08 | 1.08 | 1.08 | 1.09 | 1.12 | 1.13 | 1.15 |
| 1.16 | 1.2 | 1.21 | 1.22 | 1.22 | 1.24 | 1.3 | 1.34 | 1.36 | 1.39 | 1.44 | 1.46 |
| 1.53 | 1.59 | 1.6 | 1.63 | 1.63 | 1.68 | 1.71 | 1.72 | 1.76 | 1.83 | 1.95 | 1.96 |
| 1.97 | 2.02 | 2.13 | 2.15 | 2.16 | 2.22 | 2.3 | 2.31 | 2.4 | 2.45 | 2.51 | 2.53 |
| 2.54 | 2.54 | 2.78 | 2.93 | 3.27 | 3.42 | 3.47 | 3.61 | 4.02 | 4.32 | 4.58 | 5.55 |

**Appendix B4: Breaking stress**

| | | | | | | | | | | | |
|---|---|---|---|---|---|---|---|---|---|---|---|
| 3.70 | 2.74 | 2.73 | 2.5 | 3.6 | 3.11 | 3.27 | 2.87 | 1.47 | 3.11 | 4.42 | 2.41 |
| 3.19 | 3.22 | 1.69 | 3.28 | 3.09 | 1.87 | 3.15 | 4.90 | 3.75 | 2.43 | 2.95 | 2.97 |
| 3.39 | 2.96 | 2.53 | 2.67 | 2.93 | 3.22 | 3.39 | 2.81 | 4.20 | 3.33 | 2.55 | 3.31 |
| 3.31 | 2.85 | 2.56 | 3.56 | 3.15 | 2.35 | 2.55 | 2.59 | 2.38 | 2.81 | 2.77 | 2.17 |
| 2.83 | 1.92 | 1.41 | 3.68 | 2.97 | 1.36 | 0.98 | 2.76 | 4.91 | 3.68 | 1.84 | 1.59 |
| 3.19 | 1.57 | 0.81 | 5.56 | 1.73 | 1.59 | 2.00 | 1.22 | 1.12 | 1.71 | 2.17 | 1.17 |
| 5.08 | 2.48 | 1.18 | 3.51 | 2.17 | 1.69 | 1.25 | 4.38 | 1.84 | 0.39 | 3.68 | 2.48 |
| 0.85 | 1.61 | 2.79 | 4.70 | 2.03 | 1.80 | 1.57 | 1.08 | 2.03 | 1.61 | 2.12 | 1.89 |
| 2.88 | 2.82 | 2.05 | 3.65 | | | | | | | | |

**Appendix B5:  Windshield Service Times**

| | | | | | | | | | | |
|---|---|---|---|---|---|---|---|---|---|---|
| 0.046 | 1.436 | 2.592 | 0.140 | 1.492 | 2.600 | 0.150 | 1.580 | 2.670 | 0.248 | 1.719 |
| 2.717 | 0.280 | 1.794 | 2.819 | 0.313 | 1.915 | 2.820 | 0.389 | 1.920 | 2.878 | 0.487 |
| 1.963 | 2.950 | 0.622 | 1.978 | 3.003 | 0.900 | 2.053 | 3.102 | 0.952 | 2.065 | 3.304 |
| 0.996 | 2.117 | 3.483 | 1.003 | 2.137 | 3.500 | 1.010 | 2.141 | 3.622 | 1.085 | 2.163 |
| 3.665 | 1.092 | 2.183 | 3.695 | 1.152 | 2.240 | 4.015 | 1.183 | 2.341 | 4.628 | 1.244 |
| 2.435 | 4.806 | 1.249 | 2.464 | 4.881 | 1.262 | 2.543 | 5.140 | | | |

**Appendix B6: Waiting Times of blowhole eruption**

| | | | | | | | | | | |
|---|---|---|---|---|---|---|---|---|---|---|
| 83 | 51 | 87 | 60 | 28 | 95 | 8 | 27 | 15 | 10 | 18 |
| 16 | 29 | 54 | 91 | 8 | 17 | 55 | 10 | 35 | 47 | 77 |
| 36 | 17 | 21 | 36 | 18 | 40 | 10 | 7 | 34 | 27 | 28 |
| 56 | 8 | 25 | 68 | 146 | 89 | 18 | 73 | 69 | 9 | 37 |
| 10 | 82 | 29 | 8 | 60 | 61 | 61 | 18 | 169 | 25 | 8 |
| 26 | 11 | 83 | 11 | 42 | 17 | 14 | 9 | 12 | | |

### Appendix B7: Milk Production

| | | | | | | | | | |
|---|---|---|---|---|---|---|---|---|---|
| 0.4365 | 0.4260 | 0.5140 | 0.6907 | 0.7471 | 0.2605 | 0.6196 | 0.8781 | 0.4990 | 0.6058 |
| 0.6891 | 0.5770 | 0.5394 | 0.1479 | 0.2356 | 0.6012 | 0.1525 | 0.5483 | 0.6927 | 0.7261 |
| 0.3323 | 0.0671 | 0.2361 | 0.4800 | 0.5707 | 0.7131 | 0.5853 | 0.6768 | 0.5350 | 0.4151 |
| 0.6789 | 0.4576 | 0.3259 | 0.2303 | 0.7687 | 0.4371 | 0.3383 | 0.6114 | 0.3480 | 0.4564 |
| 0.7804 | 0.3406 | 0.4823 | 0.5912 | 0.5744 | 0.5481 | 0.1131 | 0.7290 | 0.0168 | 0.5529 |
| 0.4530 | 0.3891 | 0.4752 | 0.3134 | 0.3175 | 0.1167 | 0.6750 | 0.5113 | 0.5447 | 0.4143 |
| 0.5627 | 0.5150 | 0.0776 | 0.3945 | 0.4553 | 0.4470 | 0.5285 | 0.5232 | 0.6465 | 0.0650 |
| 0.8492 | 0.8147 | 0.3627 | 0.3906 | 0.4438 | 0.4612 | 0.3188 | 0.2160 | 0.6707 | 0.6220 |
| 0.5629 | 0.4675 | 0.3635 | 0.4111 | 0.6844 | 0.3413 | 0.4332 | 0.0854 | 0.3821 | 0.4694 |
| 0.5349 | 0.3751 | 0.1546 | 0.4517 | 0.2681 | 0.4049 | 0.5553 | 0.5878 | 0.4741 | 0.3598 |
| 0.7629 | 0.5941 | 0.6174 | 0.6860 | 0.0609 | 0.6488 | 0.2747 | | | |

### Appendix B8: Cost of cybercrimes to GDP

| | | | | | | | | |
|---|---|---|---|---|---|---|---|---|
| 0.0008 | 0.0032 | 0.0017 | 0.0063 | 0.0014 | 0.0041 | 0.0011 | 0.0160 | 0.0021 |
| 0.0020 | 0.0004 | 0.0002 | 0.0001 | 0.0018 | 0.0017 | 0.0041 | 0.0014 | 0.0007 |
| 0.0011 | 0.0016 | 0.0064 | 0.0013 | 0.0019 | | | | |

### Appendix B9: Transformer Turn Data

| Voltage | Hours | | | | | | | | | |
|---|---|---|---|---|---|---|---|---|---|---|
| 35.4kV | 40.10 | 59.40 | 71.20 | 166.50 | 204.70 | 229.70 | 308.30 | 537.90 | 1002.30+ | 1002.30+ |
| 42.4kV | 0.60 | 13.40 | 15.20 | 19.90 | 25.00 | 30.20 | 32.80 | 44.40 | 50.20+ | 56.20 |
| 46.7kV | 3.10 | 8.30 | 8.90 | 9.00 | 13.60 | 14.90 | 16.10 | 16.90 | 21.30 | 48.10+ |